The Effect of Changes in Irradiance on the Growth, Biomass, Lipid Accumulation and pigment composition of *Botryococcus braunii*

Submitted by **Diane Louise Coppack**

to the University of Exeter as a Thesis for the Degree

of Masters by Research (MbyRes) in Biosciences in

September 2013

I certify that all material in this thesis which is not my own work has been identified and that no material has previously been submitted and approved for the award of a degree by this or any other University.

Signature: ……..

Abstract

Light is one of the strongest factors affecting the growth and accumulation products within algae. While low irradiance brings about a reduction in biomass and productivity, exposure to high irradiance causes oxidative damage to the photosynthetic machinery. The green, colonial alga *Botryococcus braunii* (*B. braunii*) is regarded as a potential source of renewable fuel because of its ability to produce and secrete large amounts of hydrocarbons. *B. braunii* was cultured under a range of illumination conditions to assess the effect increasing irradiance had on growth, biomass and lipid accumulation and composition of the photosynthetic apparatus. Cells were grown in successive photobioreactor runs and exposed to irradiances of 300, 450 and 600 $\mu mol_{photons}\ m^{-2}\ s^{-1}$ provided by an LED shroud. A fluorescent light shroud at 300 $\mu mol_{photons}\ m^{-2}\ s^{-1}$ was also used to investigate the effect of light quality. The maximum growth rate was achieved at an intensity of 450 $\mu mol_{photons}\ m^{-2}\ s^{-1}$. Production of botryococcene was found to be growth associated, while neutral lipid yield increased with irradiance. Extracts were compositionally identical for all illumination conditions investigated. *B. braunii* were shown to tolerate and acclimate to increasing light intensity by altering the composition of their photosynthetic apparatus. Although not statistically significant, growth at 450 and 600 $\mu mol_{photons}\ m^{-2}\ s^{-1}$ resulted in a decrease in the chlorophyll content per cell. Increased accumulation of zeaxanthin and β-carotene was observed in cells cultured at 450 $\mu mol_{photons}\ m^{-2}\ s^{-1}$ compared with those grown at 300 $\mu mol\ m^{-2}\ s^{-1}$ and is consistent with their role in non-photochemical quenching and the dissipation of excess energy as heat and light ($P > 0.05$). Photoinhibition was observed during the third run at 450 $\mu mol_{photons}\ m^{-2}\ s^{-1}$ and at all runs at 600 $\mu mol_{photons}\ m^{-2}\ s^{-1}$. Excessive irradiance did not cause cell necrosis, but resulted in decreased viability of *B. braunii* cells due to the progressive accumulation of irreparable photodamage over successive photobioreactor runs. This was confirmed by microscopic analysis and a significant reduction in growth rate. Illumination type had no effect on the growth of *B. braunii* when cultured at 300 $\mu mol_{photons}\ m^{-2}\ s^{-1}$, LED lighting did however prove to be a more reliable lighting source.

Acknowledgements

I would like to give special thanks to Dr. John Love, my research project supervisor for his patient guidance and valuable support, and to David Parker for his valuable and constructive recommendations on this project. Also a big thank you to Prof. Rob Lee and Shell for the opportunity of working towards my MbyRes degree and Karina Almeida-Lenero for guiding my research for the past several years.

I would also like to extend my thanks to the analytical department at Shell. Particularly to Carol Adams and Martin Selby for their unsurpassed knowledge of GC and HPLC, and Graham Smith, Damir Blazina and Martin Newman for all their help in microscopic analysis. Without their support this project would not have been possible.

Finally, I would like to thank my parents and friends who have given me their unequivocal support and encouragement throughout, as always, for which my mere expression of thanks likewise does not suffice.

Contents

Abstract 1

I. List of Figures 5

II. List of Tables 7

III. Abbreviations 8

1. Introduction 10

1.1 *Botryococcus braunii* 14

1.2 Photosynthetic efficiency 16

1.3 Photoinhibition 19

1.4 Photoprotective Mechanisms 22

1.4.1 Photoacclimation of the Photosynthetic Apparatus 22

1.4.2 Thermal Energy Dissipation 25

1.4.3 Mutation Research 29

1.5 Anti-oxidants 33

1.6 Hypothesis and Experimental Plan 35

2. Materials and Methods 37

2.1 Strains and medium 37

2.2 Modified Chu-13 medium 37

2.3 Growth Conditions 39

2.3.1 Measurement of Light Intensity (LED Shroud) 43

2.3.2 Washing Procedure 47

2.4 In process measurements 47

2.4.1 Optical Density 48

2.4.2 Biomass 48

2.4.3 Chlorophyll Measurement by Spectroscopy 48

2.4.4 Extraction of Photosynthetic Pigments 49

2.4.5 Identification and Quantification of Photosynthetic Pigments by HPLC 50

2.4.6 Microscopic examination 51

2.4.7 Total Hydrocarbon 52

2.4.8 Analysis of Total Oil Content 53

2.4.9 Inorganic Cation and Anion analysis 53

2.4.10 ASE Extraction of Total lipid 54

2.4.11 GC Analysis of Oil Extracts 57

3. Results 58
3.1 Growth Analysis 58
3.2 Growth and Terpene production 69
3.2.1 Total Extractable Lipid at Day 14 73
3.3 Ion and Nutrient Analysis 79
3.4 Microscopic Analysis of *B. braunii* 82
3.4.1 Morphology 82
3.4.2 Colony Size 88
3.5 Chlorophyll measured by Spectroscopy 92
3.5.1 Photosynthetic Pigments by HPLC 103
4. Discussion 114
4.1 Illumination Type 114
4.1.1 Growth Rate 114
4.1.2 Hydrocarbon Production 116
4.1.3 Nutritional Requirements 119
4.1.4 Increasing Productivity 119
4.1.5 Colony sizing 121
4.1.6 Photosynthetic Pigment Composition 122
5. Conclusion 130
6. Appendices 131
6.1 Raw Data Optical Density (680 nm) 131
6.2 Raw Data Biomass (DCW) (g l^{-1} d^{-1}) 131
6.3 Terpene Production (mg l^{-1}) 132
6.4 Terpene Production normalised to DCW (µg mg^{-1}) 132
6.5 ASE Extractions 133
6.6 Cation and Anion Analysis 138
6.7 Colony Size Analysis (All measurements in µm) 143
6.8 Chlorophyll UV-VIS Spectroscopy 144
6.9 Photosynthetic Pigments measured by HPLC 146
7. Bibliography 154

I. List of Figures

Figure 1 - *Botryococcus braunii* Guadeloupe at x 100 magnification.....15
Figure 2 - Summary of energy losses in photosynthesis. 17
Figure 3 - The light response curve of photosynthesis. 20
Figure 4 - The Xanthophyll Cycle 27
Figure 5 - Schematic Representation of the PBR for Microalgal Culture. 41
Figure 6 – Light ramping profile for LED shroud. 42
Figure 7 - Placement of light meter for the determination of irradiance for the LED shroud. 45
Figure 8 - Growth of *B*otryococcus *braunii* measured by absorbance at 680 nm (Panel A) and DCW (Panel B). 60
Figure 9 - Correlation between optical density and dry cell weight. 61
Figure 10 – Schematic showing successive PBR.....62
Figure 11 - Growth of *B. braunii* under four different lighting regimes. 63
Figure 12 – Spectra of emitted light from Fluorescent (FLU).....67
Figure 13 - Comparison of growth rate of *B. braunii* under four different lighting regimes 300 FLU, 300 LED, 450 LED and 600 LED. 68
Figure 14 – Terpene content of *B. braunii* over 14 day growth period with illumination provided by 300 FLU, 300 LED, 450 LED and 600 LED. 71
Figure 15 – Specific hydrocarbon production rates plotted as a function of the specific growth rate. 72
Figure 16 - Lipid yield of *B. braunii*. 77
Figure 17 – Neutral lipid and terpene composition of extracellular (A) and intracellular (B) material determined by GC. 78
Figure 18 – Concentration of Nitrate (solid line) and phosphate (dashed line) within the photobioreactor over the 14 day growth period of *B*otryococcus *braunii*. 81
Figure 19 - Microscopic images of a *B. braunii* colony. 83
Figure 20 - Microscopic images of a partial B. braunii colony.....87
Figure 21 - Frequency diagram showing the colony size distribution of *B. braunii* grown at 300 µmol m^{-2} s^{-1} with illumination provided by fluorescent lighting (300 FLU Run 1).....89

Figure 22 – Box plot to demonstrate the colony size distribution of *B. braunii* grown under each illumination condition. 90
Figure 23 - Absorbance spectra of Chlorophyll a and 94
Figure 24 - Changes in the total chlorophyll content of *B. braunii* as determined by UV-VIS spectroscopy, over a run time of 14 days. 95
Figure 25 - Changes in chlorophyll a and b content of *B. braunii* over a run time of 14 days shown in charts A and B respectively. 96
Figure 26 – HPLC Chromatogram of a pigment extract of *B. braunii*. 105
Figure 27 - Weight Ratio of Chlorophyll a to Chlorophyll b for *B. braunii* cultured under various illumination conditions. 106
Figure 28 - Changes in the zeaxanthin and β-carotene content of *B. braunii* over a run time of 14 days under three LED lighting systems. 109
Figure 29 - Weight ratio of β-carotene and zeaxanthin relative to Chlorophyll a for *B. braunii* cultured under various illumination conditions. 112

II. List of Tables

Table 1 - Formulation for 1 l Modified Chu-13 media.....38
Table 2 - Lighting configurations of high powered LED light shroud.....44
Table 3 – Experimental intensities investigated listing panel configurations and measured values.....46
Table 4 – ASE extraction parameters for *B. braunii*.....56
Table 5 - Average specific growth rates (SGR) and significance values (P values) for growth of *B. braunii* in different illumination conditions. 66
Table 6 – A two way ANOVA demonstrating the significance (P value) of changes in total chlorophyll, Chl a and Chl b content of *B. braunii* grown at four illumination conditions and at all time points investigated. 100
Table 7 - Weight ratio of chlorophyll a to chlorophyll b (a:b ratio) of *B. braunii* grown under various illumination conditions.....102
Table 8 - A two way ANOVA determining the significance of changes in the Chlorophyll a:b ratio of *B. braunii* grown under different illumination.....102
Table 9 - A two way ANOVA determining the significance of changes in Chl a:b ratios of *B. braunii* under various illumination conditions.....106
Table 10 - A two way ANOVA determining the significance of changes in pigment ratios of *B. braunii* grown under various illumination conditions. 113

III. Abbreviations

B. braunii	*Botryococcus braunii*
^{1}Chl	Singlet Chlorophyll
^{3}Chl	Triplet Chlorophyll
C. reinhardtii	*Chlamydomonas reinhardtii*
CHU-M	Modified Chu media
DI	Deionised
DIC	Differential Interference Contrast
DMSO	Dimethyl sulfoxide
DCW	Dry Cell Weight
FID	Flame Ionization Detector
GC	Gas Chromatography
HPLC	High Pressure Liquid Chromatography
LHC	Light Harvesting Complex
LL	Low Light
n.d.	No Date of Publication
NPQ	Non-Photochemical Quenching
OD	Optical Density
$^{1}O_2$	Singlet Oxygen
PI Curve	Photosynthesis Irradiance curve
P/N	Part Number
PBR	Photobioreactor
P_{max}	Light Saturation Point
qE	ΔpH dependant quenching
PSU	Photosynthetic Units

PSI	Photosystem I
PSII	Photosystem II
ROS	Reactive Oxygen Species
SGR	Specific Growth Rate
TAG	Triacylglycerides
µmol m^{-2} s^{-1}	$\mu mol_{photons}$ m^{-2} s^{-1}
UVL	Ultra Violet Light
VHL	Very High Light
ΔpH	Trans-membrane proton gradient

1. Introduction

Continued reliance on fossil fuel energy resources is unsustainable. Worldwide reserves of fossil hydrocarbons are rapidly diminishing due to overconsumption and increased demand, especially in developing countries such as India and China. Like many countries, those of the western hemisphere are already increasingly dependent upon imported sources of oil, with two thirds of supply coming from a just few countries around the World (Darzins *et al*, 2010). In addition, there is growing concern over the environmental impacts that accompany the continued burning of fossil fuels due to the release of greenhouse gasses and their role in global warming. These issues have driven research projects to develop an alternative renewable and carbon neutral biofuel and reduce our dependence on fossil fuels.

Currently first generation biodiesel and bioethanol derived from land crops such as *Saccharum officinarum* (sugarcane), *Beta vulgaris* (sugar beet), *Zea mays* (maize) and *Brassica napus* (rapeseed), are the most widely available forms of biofuel (Yuan *et al*, 2008). These biofuels can partially replace diesel and gasoline and can be used in cars today with little or no modifications to the vehicle engines (Mata *et al*, 2010). However, the potential market for biodiesel is greater than the availability of land for the growth of feedstocks. It is estimated that more than half of the total land area of the UK would be required in order to meet the UK demand for biodiesel from rapeseed oil (Scott *et al*, 2010). The main drawback for biofuels production is therefore the extensive pressure for land change use with the growth of feedstocks competing for valuable crop and virgin land (Williams and Laurens, 2010). This competition may lead to an increase in food commodity prices placing an enormous strain on World food markets (Brennan and Owende, 2010) and contribute to the destruction of the World's forests and areas of ecological importance, leading to loss of fragile habitats and their associated biological diversity (Mata *et al*, 2010).

Second generation biofuels such as bioethanol from lignocellulose can be produced from a large variety of feedstocks including whole plant matter or

agricultural residues, waste from forest harvesting or wood processing waste rather than food crops (Brennan and Owende, 2010). Around 30 % of the lignocellulosic feedstock for bioethanol production is already sustainably produced in the United States with large quantities also available in Scandinavia, New Zealand, Canada and South America (Zhu and Pan, 2010). However, there is still concern over competing or change in land use (Brennan and Owende, 2010) and the raw lignocellulosic materials require pre-treatment and saccharification to make sugar monomers available to the microorganisms that are typically used in the fermentation process (Mosier *et al*, 2005).

In the search for alternative fuels, interest has been shown in biochemical routes to hydrocarbons from photosynthetic microbes. Third generation biofuels derived from microalgae are without many of the major drawbacks associated with first and second generation biofuels. Microalgae are unicellular or simple multi-cellular photosynthetic microorganisms and include prokaryotes (*i.e.* cyanobacteria), and eukaryotes such as green algae, red algae and diatoms (Brennan and Owende, 2010). Their simple structure, which is predominantly aimed at energy conversion, and minimal growth requirements give microalgae both rapid growth potential and the ability to adapt and thrive in harsh aquatic environments, enduring temperature extremes and periods of low water availability (Darzins *et al*, 2010).

Microalgae are capable of all year round production and have higher growth rates and productivity than oil seed crops, thereby offering the potential for higher biomass yields per acre of cultivation (Ferrell and Sarisky-Reed, 2010). Algae with oil an content of 30 % dry weight require up to 40 times less land for growth compared to rapeseed or 132 times less than soybean crops (Mata *et al*, 2010). Higher productivity rates of microalgae in combination with their ability to grow in harsh conditions with limited nutrient requirements means they can be cultivated on non-arable land independently of the seasonal weather changes, without compromising food production and the pressure for change in land use (Mata *et al*, 2010).

Some algal species have been shown to have an oil content of 20 - 50 % dry weight of biomass (Brennan and Owende, 2010) with potential yields at least 60 times higher than *Glycine max* (soy bean), 15 times that of *Jatropha curcas* (jatropha) and 5 times more than *Elaeis guineensis* (African oil palm) on an oil-per-acre-of-land-per-year basis (Ferrell and Sarisky-Reed, 2010). Oil yields from microalgae may be significantly enhanced by varying growth conditions, but as oil synthesis is triggered by nutrient deficiencies, oil production usually comes at the expense of biomass yield (Darzins *et al*, 2010). Much of the lipid derived from microalgae includes free fatty acids (FFAs) and triacylglycerides (TAGs), both of which can be converted into biodiesel using conventional transesterfication technology (Darzins *et al*, 2010). Microalgal oils therefore would not require the expense of commissioning new conversion processes to a useable biofuel.

There is also the possibility of combining biofuel production from microalgae with pollution control. Wastewater can be used as culture medium where ammonia, nitrate and phosphate contaminants are used as nutrients for algal growth (Mata *et al*, 2010). In addition to providing treatment of organic effluent, these sources of wastewater cannot be used in conventional agriculture and algal culture and may consequently reduce the demand on freshwater resources (Darzins *et al*, 2010). The synergistic coupling of biofuel production with biological fixation of carbon dioxide from industrial flue gases can reduce the release of greenhouse gases into the atmosphere (Darzins *et al*, 2010). It is estimated that 1 Kg of dry algal biomass can fix approximately 1.83 Kg CO_2 (Brennan and Owende, 2010). As well as performing as well as petroleum diesel, biodiesel from microalgae contains no sulphur and benefits from reduced emissions of particulate matter, carbon monoxide, hydrocarbons, and sulphur dioxide. Emissions of nitrogen oxides maybe however be higher in some engine types (Mata *et al*, 2010).

An algal bio-refinery could potentially integrate several conversion technologies to produce different types of renewable fuels. Following oil extraction for biodiesel the residual biomass could provide feedstock for bioethanol production, methane from anaerobic digestion or simply burned for energy in the cogeneration of electricity and heat (Darzins *et al*, 2010; Mata *et al*, 2010). Biomass residues can

also be used as organic fertilizer due to its high nitrogen and phosphorus ratio or processed into valuable co-products with commercial applications including production of fine chemicals and bulk products, cosmetics, pharmaceuticals, nutraceuticals and food additives (Mata *et al*, 2010).

A key consideration in the production of algal biofuel is the choice of algal strain. Microalgae are present in terrestrial as well as in aquatic ecosystems, representing a large variety of species living in a wide range of environmental conditions. It is estimated that more than 50,000 microalgal species exist, but only around 3,000 have been studied and analysed (Mata *et al*, 2010). A large amount work has been carried out in the isolation and screening of novel algal species, which allows for the selection of strains adapted to a particular climate, water chemistry and other selective conditions such as extremes of pH, temperature, salinity, or which gives them the ability to grow in conditions where unscrubbed flue gas is to be used as a CO_2 source (Darinz *et al*, 2010). Much of the current research is focused on a small number of fast growing microalgal species which have been found to accumulate substantial quantities of lipid (Scott *et al*, 2010). Strains that have already shown some promise for lipid productivity may be further improved through the classical genetic techniques of mutagenesis and breeding (Darinz *et al*, 2010).

Previous work has shown that, without product secretion, yields relative to biomass are too low and product costs too high to be economically viable. With the ability to both produce and excrete a large amount of hydrocarbons *Botryococcus braunii* (*B. braunii*) fulfils these criteria and been actively investigated over past few years.

1.1 *Botryococcus braunii*

The green, colonial alga *Botryococcus braunii* belongs to the division *Chlorophyceae* (Banerjee *et al*, 2002) and is widespread in fresh and brackish waters, lakes, reservoirs and ponds (Dayananda *et al*, 2007). *B. braunii* colonies have three dimensional, amorphous structures and are formed from individual pyriform-shaped cells embedded in a thick extracellular matrix (Eroglu and Melis, 2010) (Figure 1).

The hydrocarbons accumulate in two distinct sites; internally in cytoplasmic inclusions and externally in successive outer walls and the extracellular matrix (Frenz *et al*, 1980). Although they may serve additional functions, these hydrocarbons allow *B. braunii* colonies to float, presumably to increase exposure to light for photosynthesis at the surfaces of ponds or lakes (Weiss *et al*, 2012).

B. braunii exists in three major races which can be differentiated by the structure of their oils. Race A is characterised by the production of C_{21} – C_{33} odd numbered alkadienes and alkatrienes which are derived from fatty acids (Dayananda *et al*, 2007). This race has been found to have the most variable hydrocarbon content from 0.4 to 60 % of dry cell weight (Eroglu and Melis, 2010). The L race has the lowest hydrocarbon content at 0.1 to 8 % of dry cell weight (Eroglu and Melis, 2010) and produces a single hydrocarbon called lycopodine ($C_{40}H_{78}$) that is not formed by any of the other strains of *B. braunii* (Banerjee *et al*, 2002).

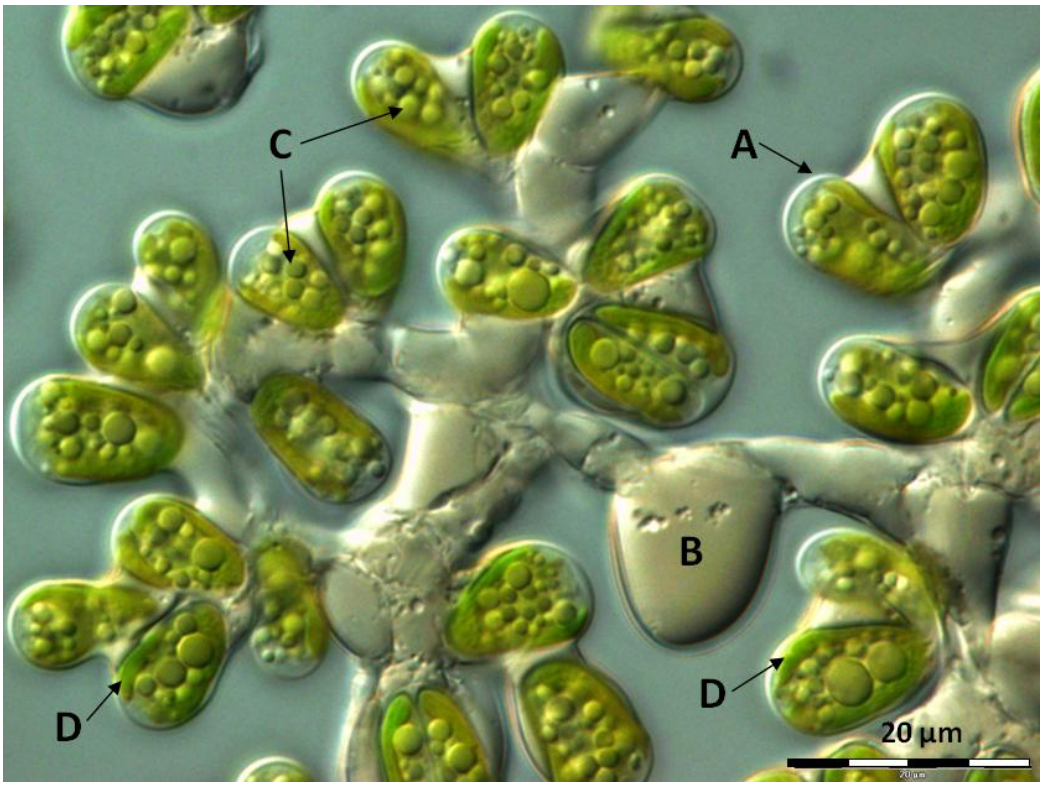

Figure 1 - *Botryococcus braunii* Guadeloupe at x 100 magnification.

Differential Interference Contrast (DIC) microscopy image of a partial *B. braunii* colony where the letter depict the following: (A) individual cell, (B) extracellular matrix, (C) cytoplasmic inclusions (D) chloroplast. NOTE: Not all cellular organelles can be seen in this image.

Products of the B Race include triterpenoid hydrocarbons known as botryococcenes of C_{30} – C_{37} (Eroglu and Melis, 2010) and small quantities of C_{31} – C_{34} methylated squalenes (Dayananda *et al*, 2007). With a reported botryococcene content of 27 to 86 % of dry cell weight (Banerjee *et al*, 2002) and the possibility of converting these oils into shorted length fuel-type hydrocarbons by catalytic cracking (Eroglu and Melis, 2010), indicates that B race *B. braunii* have enormous potential as a feedstock for biofuel production. The only drawback of *B. braunii* is that they are relatively slow growing with a doubling time of 72 hours. Work carried out at Shell Technology Centre Thornton over last year has shown this doubling time can be halved under optimum conditions. However, growth rates may not be as important as the method of hydrocarbon harvest; as the oils are secreted it makes 'milking' a possibility (Hejazi and Wijffels, 2004).

While key issues related to photosynthetic efficiencies and biomass production relative to production area remain a serious hurdle to the commercialisation of micro-algal biofuels, such biofuels may initially be produced alongside higher-value compounds or platform chemicals and, gradually, could substitute a significant proportion of the fossil fuels required to meet the growing energy demand.

1.2 Photosynthetic efficiency

More solar energy reaches the Earth's surface every hour (4.3×10^{20} J) than is used by the total of human activity in a year (4.1×10^{20} J) (Zhu *et al*, 2008). Despite the quantity of solar energy available, the maximum energy conversion efficiency of photosynthesis has been estimated at 8 - 10 % (Melis, 2009). In reality, photosynthetic energy conversion are much lower than that theoretical value; approximately 3 % for marine microalgae and 0.2 - 2 % for terrestrial plants (Stephenson *et al*, 2011). Figure 2 summarises the factors that contribute to this degree of inefficiency in microalgae.

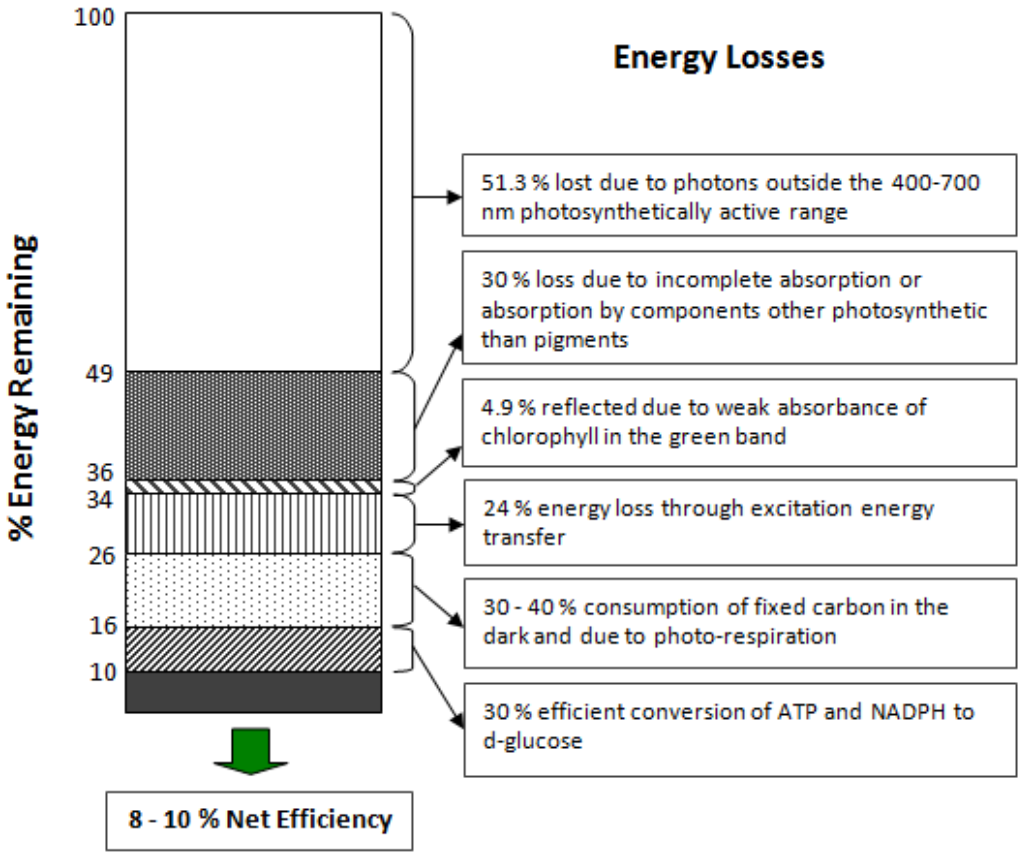

Figure 2 - Summary of energy losses in photosynthesis.

Adapted from Hall and Rao (1999).

Only a fraction of the incident solar radiation is converted into chemical energy during photosynthesis, resulting in a theoretical maximal photosynthetic efficiency of just 8 – 10 %. The arrows indicate the amount of energy losses at different processes.

A significant proportion of solar energy is lost simply because it is not of a useable wavelength. Photosynthetically Active Radiation or PAR (400-700 nm), represents only 48.7 % of the incident solar energy (Stephenson *et al*, 2011). Of PAR, a further 30 % is lost due to incomplete absorption by the photosynthetic apparatus or absorption by components other than pigments associated with photosynthesis (Hall and Rao, 1999) and 4.9 % is reflected due to the weak absorbance of chlorophyll in the green band (Zhu *et al*, 2008).

Energy losses also occur as part of photochemistry, with 24 % lost through excitation energy transfer from photons to pigment molecules (Hall and Rao, 1999). Shorter wavelength (blue) photons provide 75% more energy than longer wavelength (red) photons which can be used directly to drive Photosystem I (PSI) and Photosystem II (PSII) (Zhu *et al*, 2008). The excess energy in the blue band-width cannot be stored and is reemitted as heat (infra-red) and fluorescence (Beadle and Long, 1985).

The enzyme RUBISCO catalyses the carboxylation of ribulose-1,5-bisphosphate but has a low specific affinity for CO_2 and also catalyses the oxygenation of its substrate (Zhu *et al*, 2008). This duality in substrate specificity results in the light dependant consumption of oxygen, and increases the inefficiency of photosynthesis due to the consumption of ATP and of NADPH and the release of fixed carbon as CO_2 in a process known as photorespiration (Stephenson *et al*, 2011).

The consumption of fixed carbon through respiration (required for normal cell growth and bioenergetics) and photorespiration (due to the duality of RUBISCO) can account for incident energy losses up to 30 % (Zhu *et al*, 2008). Losses for microalgae are generally lower than plants as most used carbon concentrating mechanisms to increase CO_2 availability at the site of activity thus reducing the competition with O_2 (Stephenson *et al*, 2011). In the final stages of photosynthesis, 70 % of utilised energy is lost in the conversion of NADPH and ATP to *d*-glucose leaving a net efficiency of 8 - 10 % (Barber, 2008).

1.3 Photoinhibition

Sunlight powers the photochemical reactions of photosynthesis. The relationship between photosynthesis and light intensity is illustrated by the light response curve or Photosynthesis-Irradiance (PI) curve as shown in Figure 3.

The rate of photosynthesis increases linearly with increasing light intensity to a saturation point (P_{max}) (Stephenson *et al*, 2011). This corresponds to conditions when light absorption and the light reactions are limiting the overall process of photosynthesis (Hill, 1996) and when the solar energy conversion efficiency is at maximum (Melis, 2009). At higher light intensities the photosynthetic rate plateaus as photon absorption exceeds the rate at which they can be productively utilised by photosynthesis (Melis, 2009). At saturating light intensities, the limiting factor is set by the dark reactions of photosynthesis and the assimilation capacity of the Calvin cycle, primarily the activity RUBISCO (Hill, 1996). At very high light intensities some species show a decline in photosynthetic rate below P_{max} (Hill, 1996). Environmental factors that lower the photosynthetic rate such as salinity, nutrient deficiency and cold can increase the degree to which absorbed light is excessive and exacerbate high light stress (Demmig-Adams and Adams, 1996).

Absorption of excess photons causes accumulation of excitation energy in the light harvesting complex in the form of singlet excitation state of chlorophyll (^{1}Chl) (Niyogi, 1999 and 2000; Deming-Adams and Adams, 1996). This excitation energy would normally feed electron transport in the reaction centres, however at the light saturation point the system is running at full capacity and the bottle-neck at electron transport increases the lifetime of a ^{1}Chl. Singlet chlorophylls can be converted to triplet chlorophyll (^{3}Chl) through intersystem crossing, which although itself is not harmful can interact with molecular oxygen to form the highly reactive chemical species singlet oxygen ($^1O_2$) (Deming-Adams and Adams, 1996; Formaggio *et al*, 2001). If not quenched $^1O_2$ can act to directly damages proteins, pigments and lipid of the photosynthetic apparatus which leads to photoinhibition (Formaggio *et al*, 2001; Niyogi, 2000).

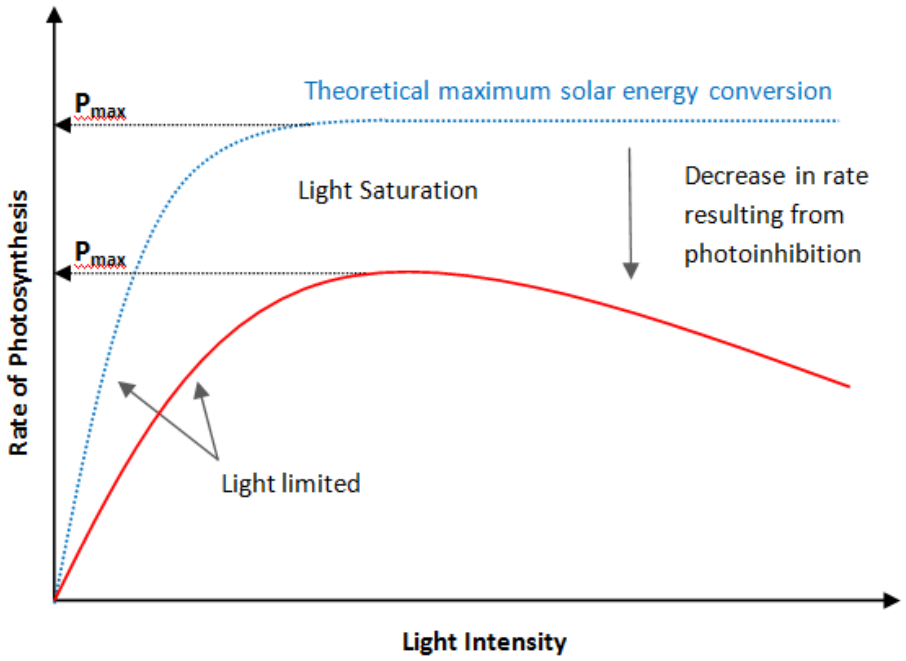

Figure 3 - The light response curve of photosynthesis.

Adapted from Stephenson *et al*, 2011.

Photosynthesis Irradiance (PI) curves characterise the relationship between changes in light intensity and the photosynthetic rate measured in terms of oxygen evolution or carbon fixation over time. The solid red line shows the PI curve of typical photosynthetic organism, compared with the theoretical maximum (blue dashed line) at a given irradiance. Note the reduction in P_{max} as a result of dynamic photoinhibition under moderate or excess light.

The D1 protein in photosystem II (PSII) is the target for photoinhibition resulting from Reactive Oxygen Species (ROS) (Förster *et al*, 2005). The high turnover rate of the D1 protein underlines continuous damage to the photosynthetic apparatus even under optimum conditions (Vasilikiotis and Melis, 1994). As the rate of D1 synthesis remains fairly constant on a per cell basis irrespective of irradiance, adverse affects on photosynthesis are only observed when the rate of damage exceeds the rate of repair (Vasilikiotis and Melis, 1994; Takahashi and Badger, 2010). Work performed by Vasilikiotis and Melis (1994) has shown that growth of *Dunaliella salina* under low light demonstrates damage, degradation and replacement of D1 protein every 7 hours, with a 21 fold increase in turnover rate under irradiance stress. A review by Takahashi and Badger (2010) has shown that primary photodamage is in fact caused by light absorption of the manganese cluster in the oxygen-evolving complex of PSII. The generation of ROS as above, acts to accelerate photoinhibition by impeding PSII repair processes, rather than causing photodamage directly.

Regardless of the cause, photoinhibition results in reduced photosynthetic efficiency (PE), lowered rates of algal growth and productivity, and a lower light-saturated rate of photosynthesis (Vasilikiotis and Melis, 1994).

Photoinhibition of algal photosynthesis may be a significant consideration for algal cultures, as sunlight can reach intensities of around 2500 $\mu mol_{photons}\ m^{-2}\ s^{-1}$ (Carnicas *et al*, 1999) and the light-saturation of typical algae has been reported at irradiances of 100 - 500 $\mu mol_{photons}\ m^{-2}\ s^{-1}$ (Carnicas *et al*, 1999; Hill, 1996) ($\mu mol_{photons}\ m^{-2}\ s^{-1}$ is abbreviated to $\mu mol\ m^{-2}\ s^{-1}$ throughout this report). Under such circumstances it is estimated that more than 80 % of the absorbed solar irradiance would be wasted in the photosynthetic apparatus during the course of a day (Melis, 2009).

1.4 Photoprotective Mechanisms

If PE is to be maintained, the photosynthetic apparatus must be continuously repaired by re-synthesis of damaged components (Simionato *et al*, 2011). Repair of photodamage is energetically very demanding and may strongly influence the biomass productivity (Simionato *et al*, 2011). Photosynthetic organisms can use several photoprotective systems in order to minimise the effects of photoinhibition or cellular damage in response to increasing irradiance. These mechanisms either modify the composition of the photosynthetic apparatus thus preventing the over absorption of photons; increase the repair of damaged D1 proteins in PSII reaction centres; reduce the life time of harmful ROS through scavenging antioxidant molecules; or dissipate excess absorbed energy as heat through non-photochemical quenching and the action of xanthophyll pigments (Niyogi, 1999).

1.4.1 Photoacclimation of the Photosynthetic Apparatus

The successful survival of a photosynthetic organism depends upon the extent to which the species can tolerate changes in illumination condition. Many photosynthetic organisms have developed mechanisms to alter the composition of their photosynthetic apparatus (Carnicas *et al*, 1999) allowing them to achieve and maintain optimal rates of photosynthesis under limited or excess light (Beneragama and Goto, 2010). This phenotypic response of algae to changes in irradiance is described as photoacclimation and is usually initiated by a stress response to a sudden change in environmental conditions (Falkowski and LaRoche, 1991; Huner *et al*, 1998). “Photoacclimation” is not to be confused with “photoadaptation” which is a stable, long-term adjustment in the genotype of algae to irradiance that has risen during evolution (Moore *et al*, 2006).

The major photosynthetic pigments can be divided into two groups, the chlorophylls and the carotenoids. Both groups of pigments are present in chloroplasts bound to light-harvesting complex (LHC)-proteins of the thylakoid membranes (Boyer, 1990; Takahashi and Badger, 2010). Collectively these

proteins form photosynthetic units (PSU) or “antennae” which typically consist of 300 - 400 chlorophyll molecules associated with a single reaction centre (Dring, 1998). The main function of the antenna is to transfer excitation energy to the photosynthetic reaction centres which leads to photochemistry.

Most of the light harvesting is performed by the chlorophylls. Although several chlorophyll molecules exist, the most abundant are Chlorophylls a and b, which occur in the approximate ratio of 3:1 (Lichtenthaler, 1987). The carotenoids play two important roles; some function as accessory light harvesting pigments, although with relatively low efficiencies of 30 – 40 % (Schagerl and Müller, 2006), their major role is in photoprotection (Carnicas *et al*, 1999).

Under high light, more photons are absorbed by photosynthetic pigments which leads to a build up of excitation pressure in PSII (Huner *et al*, 1998). Some taxa acclimate to increasing irradiance by reducing the size of the light harvesting antenna associated with each reaction centre (a change in PSU size) (Moore *et al*, 2006). Consequently, there are less chlorophyll molecules available to harvest and transfer excitation energy to the reaction centres is, thereby limiting an organism’s capacity for light absorption (Förster *et al*, 2005; Melis and Harvey, 1981). This is a short term acclimation mechanisms which takes place over a period of hours to days (Lichtenthaler and Burkart, 1999).

Other algae and plant species prevent over excitation by reducing the number of reaction centres whilst the size of the antenna remains relatively constant (a change in PSU number) (Moore *et al*, 2006). The algae *Chattonella subsalsa* maintains photochemical activity under high irradiance by down-regulating the number of reaction centres, thus preventing photoinhibition through lowered electron transport (Warner and Madden, 2006).

Both acclimation responses have characteristic effects on the PI curve and relate to the number of reaction centres available (Jodłowska and Latała, 2012; Moore *et al*, 2006). A decrease in antenna size reduces the number of photons absorbed, but as there is no change in the number of reaction centres the rate of electron

transport remains unchanged. Organisms with different antenna configurations but the same number of reaction centres will have different photosynthetic rates under light limiting conditions, but the same P_{max}. If the number of reaction centres decrease, organisms will show a lower photosynthetic rate when light is limited and become saturated at lower intensities.

Irradiant stress can bring about adjustments in the photosystem ratio of the thykaloid membranes (Kim *et al*, 1993). *Dunaliella salina* increases the ratio of PSII to PSI from 1.4:1 under low-light conditions to 15:1 under irradiance stress (Vasilikiotis and Melis, 1994). A large pool of PSII allows more than 80 % of the photosystems to be photochemically inactive due to a damaged D1 protein, while a balance in electron transport is maintained between PSII and PSI (Melis, 1990; Vasilikiotis and Melis, 1994). When the PSII / PSI ratio is optimised, it allows an organism resume photosynthesis and growth under adverse irradiance (Kim *et al*, 1993).

Modifications in the proportion of chlorophyll a to chlorophyll b in the antenna, which is normally in the approximate ratio of 3:1, is an essential adaptation mechanism of an photosynthetic organism to a change in lighting conditions (Kitajima and Hogan, 2003; Lichtenthaler, 1987). Chlorophyll a is the most abundant pigment but can only utilise energy from a limited part of the visible light spectrum (Roberts *et al*, 2000). Accessory pigments are able to utilise light from other parts of the spectrum, and by incorporating them into the LHC a photosynthetic organisms can effectively increase the range of wavelengths from which it can obtain energy (Roberts *et al*, 2000). For example, chlorophyll b enhances the efficiency of blue light absorption (Beneragama and Goto, 2010). *Euglena gracilis* and other shade tolerant species acclimate to low light environments by producing a higher proportion of chlorophyll b to chlorophyll a (*i.e.* a lower Chl a/b ratio) which aims to capture as much of the prevailing light energy as possible allowing them to thrive in conditions where light is limited. On the other hand, photosynthetic organisms exposed to excessive irradiance may exhibit higher Chl a/b ratios (Kitajima and Hogan, 2003; Lichtenthaler, 1987). This effect has been reported in many organisms including *Dunaliella salina* where a 5-

fold increase in the chlorophyll a/b ratio was observed under exposure to high light (Harrison *et al*, 1992).

Adaptation mechanisms to high irradiance may simply involve the avoidance of light. Chloroplasts are able to alter their position in the cell, gathering at cell walls parallel to the direction of light which prevents the excessive absorption of photons and maximise uptake of CO_2 from the intracellular air space (Lichtenthaler *et al*, 2007;Takahashi and Badger, 2011). In the short term, some species can use alternative electron transport systems to removed excess absorbed energy (Niyogi, 1999) such as the transfer of energy from PSII to PSI through state transitions (Huner *et al*, 1998).

1.4.2 Thermal Energy Dissipation

The dissipation of excess energy from pigment molecules through non-photochemical quenching of chlorophyll fluorescence (NPQ) plays a central role in decreasing the excitation pressure on PSII, thus protecting against photoinhibition (Niyogi, 1999; Stephenson *et al*, 2011; Zigman *et al*, 2012). NPQ is composed of three components; qI due to photoinhibition; qT which is quenching resulting from the transfer of excess excitation energy from PSII to PSI via state-transitions (Niyogi, 1999); and qE which is energy dependant quenching regulated by the build up of a trans-thykaloid proton gradient (ΔpH) (Zigman *et al*, 2012).

Under high light, ΔpH dependant quenching (qE) is triggered in the light-harvesting complex of PSII (Johnson and Ruban, 2011). It is a rapid, inducible mechanism for the harmless conversion and dissipation of excess excitation energy as heat and fluorescence (Zigman *et al*, 2012; Niyogi*,* 2000). Under both laboratory conditions and in the field, qE has shown to be activated and deactivated within 1 - 2 minutes in response to rapidly changing irradiance (Jahns and Holzwarth, 2012; Niyogi, 1999) and is accountable for the thermal dissipation of more than 75 % of excess excitation energy in light saturated conditions (Niyogi, 1999). Energy

dependant quenching (qE) is related to the operation of the xanthophyll cycle (Figure 4).

There are two independent pathways for the synthesis of carotenoids in green plants and algae, those derived from α-carotene and those from β-carotene. The xanthophyll cycle operates in the *β*-carotene branch of the pathway and involves zeaxanthin, antheraxanthin and violaxanthin (Niyogi ,1999; Zigman *et al*, 2012). While much work has been carried out on the characterisation of xanthophyll pigments in higher plants, green algae such as *Chlamydomonas*, *Dunaliella* and cyanobacteria (Pisal and Lele, 2004; Demmig-Adams and Adams, 1996) much less work has been carried out on other algal taxa such as *B. braunii*. The second branch, α-Carotene serves as the precursor for lutein, the most abundant xanthophyll where it is bound to LHC-proteins (Niyogi, 1999) and aids in structural stabilisation of the antenna proteins, light harvesting and the quenching of ^{3}Chl (Jahns and Holzwarth, 2012). The core carotenoid pathway is conserved in most plant species although some plants accumulate special and rare carotenoids via unique biosynthetic routes (Hannoufa and Hossain, 2011).

The qE mechanism is regulated on a feedback loop that is controlled by the magnitude of the trans-thykaloid proton gradient (ΔpH), formed as a result of photosynthetic electron transport (Johnson and Ruban, 2011; Niyogi, 2000). Under conditions of high irradiance, increased photon absorption causes the build-up of a high ΔpH and a resultant decrease in lumen pH (Niyogi, 2000). This decrease in pH induces the enzyme violaxanthin de-epoxidase, a lumenal enzyme that catalyses the conversion of violaxanthin to zeaxanthin via the xanthophyll cycle (Figure 4) (Demmig-Adams and Adams, 1996; Niyogi, 1999).

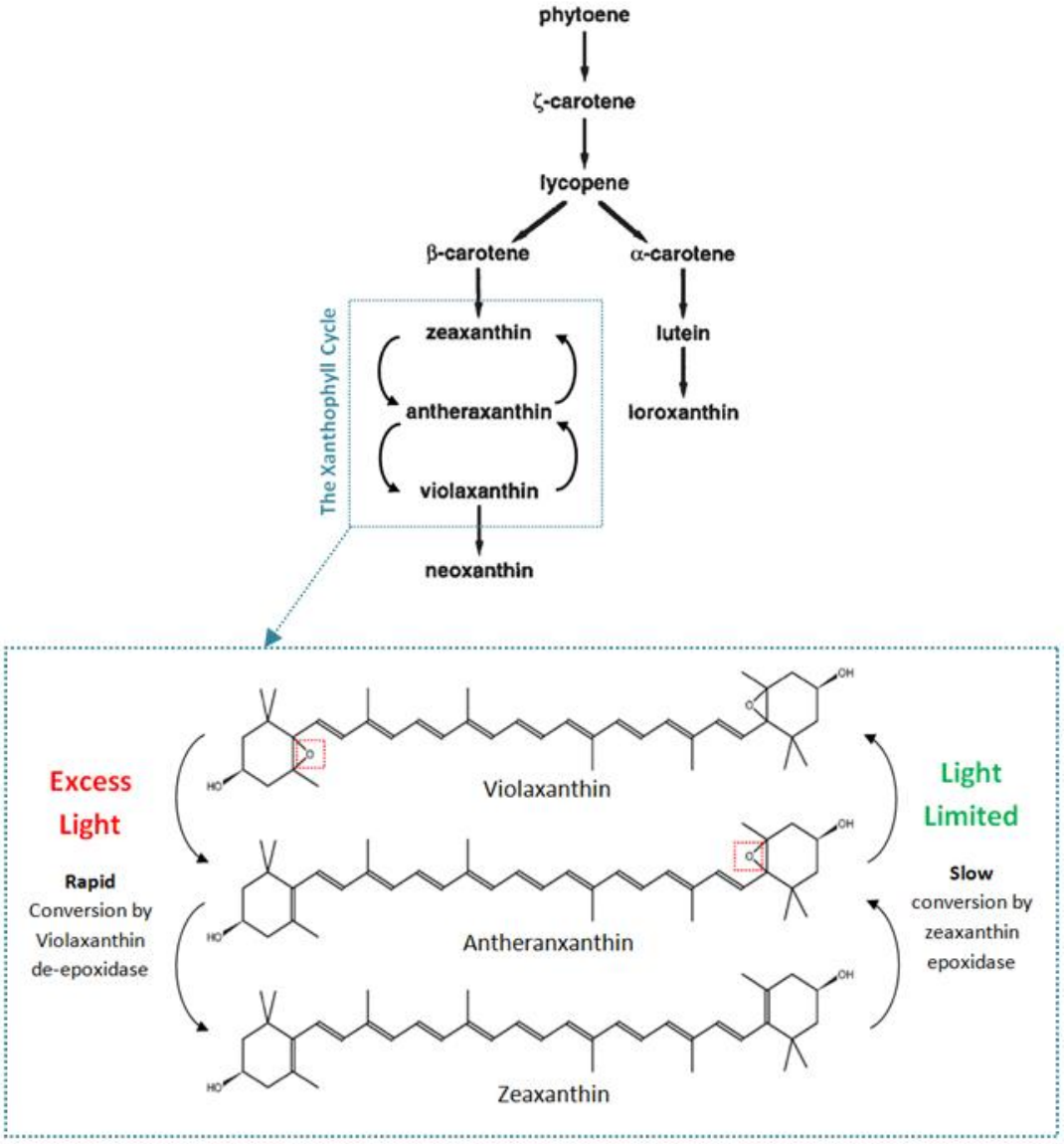

Figure 4 - The Xanthophyll Cycle

(Adapted from Dreuw *et al*, 2003; Niyogi *et al*, 1997b).

Scheme of the xanthophyll cycle and its regulation under excess of limiting light. Under high light there is a two-step de-epoxidation of violaxanthin to zeaxanthin (Dreuw *et al*, 2003). The oxygen functions removed are illustrated by the red dashed boxes. De-epoxidation occurs within minutes to hours and is catalysed by the enzyme violaxanthin de-epoxidase (Demmig-Adams and Adams, 1996). The reaction is reversible under conditions of low light.

The enzymatic conversion of violaxanthin to zeaxanthin is only part of the NPQ process. An increase in the thykaloid ∆pH is thought to result in the protonation of acidic amino acid on the chlorophyll a/b binding polypeptides in PSII (Niyogi, 1999; Niyogi *et al*, 1998). The pH sensing proteins LHCSR or PsbS detect a low lumen pH and transfer the signal to specific antenna proteins in PSII (Jahns and Holzwarth, 2012). The PsbS protein is probably associated with the kinetic modulation of qE, but not the mechanism of qE (Takahashi and Badger, 2011). The combination of a high ∆pH, low lumen pH, together with production of zeaxanthin, is assumed to cause a conformational change in the LHC proteins of PSII (Jahns and Holzwarth, 2012; Zigman *et al*, 2012), switching them to a state in which efficient de-excitation of ^{1}Chl can occur (Niyogi, 2000).

NPQ is a complex process and the molecular mechanism for de-excitation of ^{1}Chl in qE is still unknown (Dreuw *et al*, 2003). Estimates of excited state energy levels suggest that the lowest singlet state of zeaxanthin can accept excitation energy directly from ^{1}Chl, the excited xanthophyll returning to ground state by non-radioactive decay (heat dissipation) (Demmig-Adams and Adams, 1996; Dreuw *et al*, 2003; Niyogi *et al*, 1997b). Alternatively, quenching may be achieved through the formation of a chlorophyll-zeaxanthin dimer, which acts to increase the efficiency of the energy transfer processes through the creation of new channels for heat dissipation (Dreuw *et al*, 2003). To date, there is no experimental evidence for the existence of a chlorophyll-zeaxanthin dimer during NPQ.

Strict regulation of NPQ by ∆pH ensures that the zeaxanthin only accumulates under conditions where electron transport is saturated at high irradiance (Jahns and Holzwarth, 2012). When light is no longer in excess, a decreases in ∆pH reverses the conformational changes to the LHC, avoiding the undesirable dissipation of excitation energy under light limiting conditions (Niyogi, 2000; Jahns and Holzwarth, 2012).

The xanthophylls have essential photoprotective roles as quenchers of ^{1}Chl and ^{3}Chl in the light harvesting antenna proteins (Jahns and Holzwarth, 2012; Niyogi *et*

al, 1998). In addition to NPQ, zeaxanthin provides enhanced protection against lipid peroxidation (Förster *et al*, 2005; Zigman *et al*, 2012) and *β*-carotene, the precursor of xanthophylls pigments, can act to deactivate $^1O_2$ (Jahns and Holzwarth, 2012). Persistent high light stress can bring about an increase in pool size of carotenoid and xanthophyll pigments within a cell (Jin *et al,* 2001). Pisal and Lele (2004) reported a 2-fold increase in the accumulation of β-carotene in *Dunaliella salina* grown under high irradiance. Similarly, carotenoid accumulation was linked with high light stress in *Nanochloropsis gaditana*, but was enhanced further when in combination with nutrient deficiency (Simionato *et al*, 2011). In addition to high irradiance, the synthesis of xanthophylls is up regulated in response to environmental stresses that act to lower the photosynthetic rate and increase the degree to which absorbed light is excessive (Zhu *et al*, 2010).

Although cyanobacteria do not possess the xanthophyll cycle, elevated zeaxanthin concentrations could be seen as an adaptive strategy against irradiance stress (Schagerl and Müller, 2006). *Synechocystis* PCC 6603 and *Synechococcus* PCC 7942 showed a significant increase in carotenoid biosynthesis when grown under excessive irradiance (2 and 3.9 fold increase respectively) with a shift in composition towards zeaxanthin compared to those grown under low irradiance (Steiger *et al*, 1999; Masamoto and Furukawa, 1996). Cyanobacteria favour other photoprotective processes such as state transitions and the rapid repair of the D1 protein of the PS II reaction centre (Zigman *et al*, 2012).

1.4.3 Mutation Research

The role of xanthophylls in photoprotection has been confirmed by mutation analysis studies using genetically strains defective in xanthophyll metabolism. The *npq1* mutants of *Chlamydomonas reinhardtii* and *Arabidopsis thaliana* are defective in the gene encoding violaxanthin epoxidase and therefore unable to convert violaxanthin to zeaxanthin (Niyogi *et al*, 1998). While the *Arabidopsis npq1* mutant showed a significant drop in qE, the *npq1 mutant of C. reinhardtii* was

only partially defective in NPQ and still had substantial pH-dependant NPQ in excessive light (Niyogi *et al*, 1997a; Niyogi *et al*, 1998).

A second mutant, *C. reinhardtii lor1* defective in xanthophylls derived from the α-carotene pathway, and thus unable to make lutein was also used in this study (Figure 4) (Niyogi *et al*, 1997a). In high light the *npq1* and *lor1* single mutants sustained relatively normal growth compared to the wild type. However, the *C. reinhardtii npq1 lor1* double mutant blocking the synthesis of xanthophyll derived from both the α- and β-carotene pathway grew slower than wild-type cells under high light, showed no pH-dependant NPQ and were rapidly bleached (Niyogi, 1999). Similarly, the *A. thaliana* mutants lacking the production of lutein (*lut2*) demonstrated a reduction in qE compared to the wild type and double mutants lacking both *npq1* and *lut2* were completely deficient in qE (Niyogi *et al*, 2000).

Growth of *A. thaliana* is almost completely inhibited in high light suggesting that the xanthophyll cycle performs an essential photoprotective function in this species. Conversely, the xanthophyll cycle is not required for survival of *C. reinhardtii* in excessive light and other processes compensate for the defective *npq1* gene. Characterisation of the *C. reinhardtii lor1* mutant and *npq1 lor1* double mutant, together with the reduction in qE in *lut2* deficient strains of *A. thaliana* suggests the involvement of lutein in the thermal dissipation of excess excitation energy (Niyogi *et al*, 1997b; Niyogi *et al*, 2000). Taken together, these studies confirm the photoprotective role of xanthophyll pigments and their involvement in NPQ (Niyogi, 1999).

There are few reports of mutations that provide improved, rather than impaired, resistance to high light without compromising on productivity. Förster *et al*, 1999 isolated 34 Very High Light (VHL) resistant mutants from a cross of wild type strain of *Chlamydomonas reinhardtii* (CC-125) and the chloroplast *psbA* mutant *A251L** which has a Ala to Leu substitution in the D1 protein. The *A251L** mutation confers herbicide resistance but results in more than 10-fold slower electron transfer in PSII, elevated rates of D1 degradation and synthesis and poor photoautotrophic growth (Chlamydomonas Resource Centre, n. d.). Spontaneous

nuclear gene mutants were evolved by transferring cultures of wild type and *A251L**cells from low light (LL - 70 µmol photons m^{-2} s^{-1}) to VHL (1500-2000 µmol m^{-2} s^{-1}) for a period of 7 – 21 days. Initially exposure to VHL resulted in photo bleaching, but the VHL resistant mutants became green again. Four of these mutants have been characterised; two derived from the wild type (*S4* and *S9*) and two from *psbA* mutant *A251L** (*L5* and *L30*). All mutants showed comparable growth to the parental strains under High Light (HL - 600 µmol m^{-2} s^{-1}) and maintained growth rates under VHL which proved lethal to the wild type and *A251L**.

In response to an increase in irradiance, mutant strains exhibited changes in the composition of the photosynthetic apparatus that limited their capacity for light absorption. All mutants had a lower chlorophyll content on a per-biomass basis than the parental strains at each lighting condition investigated (Förster *et al*,1999) and an increase in the chlorophyll a/b ratio was observed in mutant strains grown under VHL (Förster *et al*, 2001).

Mutant strains also demonstrated lower saturated rates of photosynthesis (P_{max}) and a reduced efficiency of light utilisation at a given irradiance compared to the wild type (Förster *et al*, 1999), indicating that acclimation to high light may be through down-regulation of the number of reaction centres. This was confirmed by Förster *et al* (2001) where VHL resistance in the *S4* and *S9* mutants was accompanied by slower PSII electron transfer and an overall decrease in PSII efficiency. These inadequacies in PSII function are already present in the herbicide resistant mutants *A251L**, *L5* and *L30* and show that optimal PSII function is not critical for survival in VHL.

The VHL mutants *S4* and *S9* showed greater NPQ than the wild type under high light and VHL. In contrast, *A251L**, *L5* and *L30* exhibited low levels of NPQ under all conditions. Despite the occurrence of NPQ, none of the strains showed elevated levels of xanthophyll pigments which suggest photoprotection via the xanthophyll cycle is not involved in these VHL mutants (Förster *et al*, 1999). As well as being capable of growth under VHL, the *S4*, *S9*, *L5* and *L30* mutants were

able to maintain growth in concentrations of ROS that were lethal to the wild type (Förster *et al*, 2005). Detailed investigations into 30 other VHL resistant isolates of *C. reinhardtii* showed the VHL resistance phonotype to be primary through the enhanced tolerance of ROS, while photosynthetic activity remained unaffected.

Comparative proteomic analysis of wild-type *C. reinhardtii* and two VHL-resistant mutants *S4* and *S9* performed by Förster *et al* (2006) substantiate the changes in phenotype observed by both Förster *et al* (1999) and Förster *et al* (2001). The *S9* mutant showed reduced levels of the NAB1 protein which plays an important role in controlling the expression of the light-harvesting antenna of photosystem II (Mussgnug *et al*, 2005) and decreased expression of the RB38 protein which is a chloroplast encoded mRNA binding protein shown to be an essential part of chloroplast gene expression (Barnes *et al*, 2004). Proteomic analysis also revealed decreased expression of DEAD box RNA helicase in the *S4* mutant, a family of proteins whose purpose is to unwind nucleic acids and is involved in various aspects of RNA metabolism (Jarmoskaite and Russell, 2011) and increased levels of oxygen evolving enhancer 1 (OEE1). OEE1 is part of the oxygen evolving complex of PSII and is critical for maintaining normal photosynthetic oxygen evolution (Mayfield *et al*, 1987). Changes from increased levels in HL to decreased levels in excess light, included OEE1 in the *S9* mutant. The reverse change for NAB1, RB38, beta-carbonic anhydrase and an ABC transporter-like protein in the VHL mutant *S4*. The identification of some of these proteins in non-light stressed *Chlamydomonas* cells may contribute to "pre-adaptation" of the mutants to VHL (Förster *et al*, 2001).

Overall, photoprotection in *C. reinhardtii* is complex; the increase in resistance to VHL results from a ‘nested series of photoacclimatory responses’ which are different for each genotype (Förster *et al*, 2001; Förster *et al*, 2006) and may involve an increased tolerance of ROS, regulation of photosystem stoichiometry and changes in the size and function of the antenna. The Xanthophyll cycle is not involved in photoprotection in these mutants.

1.5 Anti-oxidants

Additional chemical protection from photo-oxidative damage is conferred by different anti-oxidant metabolites. Within the chloroplast, there are several antioxidant defence systems comprising of a variety of molecules and enzymes that act to scavenge and destroy reactive oxygen species and thus limit photo-oxidative damage (Foyer *et al*, 1994; Niyogi, 1999). Ascorbate (vitamin C) and glutathione are the major, soluble antioxidants present in the chloroplast and are primarily responsible for the quenching of $^1O_2$, O_2^- and OH^* (Niyogi *et al*, 1999; Noctor and Foyer, 1998). In addition to its function as an antioxidant, ascorbate has a second role in photoprotection where it is cofactor for the enzyme violaxanthin de-epoxidase of the xanthophyll cycle (Smirnoff, 1996). Vitamin E (α –tocopherol) is a lipid soluble antioxidant that can quench $^1O_2$, O_2^- and OH^* in the thylakoid membrane thus preventing fatty acid peroxidation (Foyer *et al*, 1994). Reactive oxygen species can also be scavenged by enzymes such as superoxide dismutase and ascorbate peroxidase (Niyogi *et al*, 1999), which are either directly involved in the processing of ROS or function by catalyzing redox reactions (Noctor and Foyer, 1998).

The concentration of many antioxidants has been shown to increase during acclimation to high light (Niyogi, 1999). Activity of enzymes in the ascorbate-glutathione cycle were found to increased under stress conditions (*i.e.* high irradiance, drought) which act to lower the rate of CO_2 fixation and increases the degree to which absorbed light is excessive (Smirnoff, 1996). These observations suggest a requirement for ascorbate in photoprotection. Studies using mutant and transgenic organisms are required to understand the specific roles of these antioxidant molecules and the metabolic pathways controlling their production (Niyogi, 1999). Once established the pathway can be manipulated, allowing for it's over expression within a cell (Ishikawa *et al*, 2006). Recent studies conducted using the ascorbate-deficient (*vtc*) mutants of the model plant *Arabidopsis thaliana* are providing evidence for a key role for the ascorbate-glutathione cycle in protecting plants against oxidative stress (Page *et al*, 2012).

Not all ROS are damaging, however low levels of ROS are always present within the cell and play an important role in signal transduction and metabolism (Foyer *et al*, 1994; Jahns and Holzwarth, 2012).

1.6 Hypothesis and Experimental Plan

The continued use of hydrocarbon based fossil fuels is unsustainable because of overconsumption and depleting supplies. Additionally, the associated release of CO_2 and other greenhouse gasses, primarily as the result of the combustion of petroleum products has lead to a steady increase in atmospheric levels and raised concerns over global warming. The short fall in demand combined with growing evidence that links the greenhouse gas emissions and global climate change highlights the need to develop cost effective 'carbon neutral' fuels.

Much current recent research has focused around photosynthetic routes to hydrocarbons and the growth of microalgae. In principle, microalgae can utilise free energy from sunlight to convert CO_2 and water, both of which are in abundant supply from waste streams of many industrial processes, into energy rich biomass and ultimately valuable fuel components. These minimal growth requirements, accompanied by rapid growth rates, their ability to thrive in harsh conditions and growth which does not compete for land with food production, makes microalgae an ideal candidate for biofuel feedstocks.

Botryococcus braunii has reported hydrocarbon concentrations of up to 60 % of the dry cell weight (Eroglu and Melis, 2010). To date many studies into *B. braunii* have been centred around maximising growth and oil production rates, but relatively little is known about the effect high irradiance has on the physiology of these cells. While preliminary studies under laboratory conditions have confirmed the high oil yield in a strain of *B. braunii* isolated in Guadeloupe, they are unable to sustain growth under HL (300 µmol m^{-2} s^{-1}) or VHL (> 600 µmol m^{-2} s^{-1}) intensities.

Algal cultivation depends upon a set of climatic conditions which spreads across most of the equatorial region; water temperatures remains a constant 20 - 30 °C and the minimal fluctuations in day length make it suitable for all year round cultivation (Meisinger, 2009). However, light intensities at the equator can reach up to 2500 µm m^{-2} s^{-1} (Carnicas *et al*, 1999) and the light-saturation of typical

algae has been reported at irradiances of 100 - 500 µm m^{-2} s^{-1} (Carnicas *et al*, 1999; Hill, 1996).

Although microalgae are a unique source of high-value compounds, their commercial application is still limited. One of the major limitations with microalgal culture is a relatively slow growth rate and low productivity, both in terms of biomass and product formation owing to the inefficient use of strong light. This investigation aims to address the effect irradiance has on the growth, biomass and hydrocarbon accumulation of *B. braunii* and the acclimative mechanisms to high irradiance. Acclimative mechanisms may be the key to increasing photosynthetic productivities and exploiting this organism for large scale biofuel production, thereby allowing algal culture facilities to be deployed at suitable locations around the equator.

B. braunii was cultured in custom built split column airlift photobioreactors (PBR) (Electrolab). The effect of irradiance on the growth, physiology and photosynthetic pigment composition of *B. braunii* was examined by comparing the cultures growth under four illumination conditions; fluorescent lighting at 300 µm m^{-2} s^{-1}, LED lighting at 300 µm m^{-2} s^{-1}, LED at 450 µm m^{-2} s^{-1} and LED at 600 µm m^{-2} s^{-1}. The gradual acclimation of the cells was observed between repeat runs at the same irradiance. Photoacclimation was assessed by measuring changes in the photosynthetic physiology or biochemistry of a given genotype in response to grown under a range of light intensities (Moore *et al*, 2006).

The distribution of photosynthetic pigments was be monitored throughout each photobioreactor run to see how their production changes with increasing light intensity. Some play an important role in protecting the organism from excess light in the xanthophyll cycle and therefore would expect their amounts to increase with light intensity.

2. Materials and Methods

2.1 Strains and medium

The algal strain used in this study was the green microalga *Botryococcus braunii* Guadeloupe (B-race) obtained from the University of Exeter. Cells were cultivated in modified Chu-13 medium (CHU-M). Unless otherwise stated, all chemicals were Analytical Grade purity and purchased from Sigma-Aldrich, UK.

2.2 Modified Chu-13 medium

Modified Chu-13 medium (CHU-M) is supplemented with essential minerals and trace elements required for the normal growth of algae (Table 1). CHU-M was made up in deionised (DI) water and pH adjusted to 7.2 ± 0.1 with 1M KCl. Media up to 2 l in volume was autoclaved at 121 ºC for 15 minutes. For larger volumes the sterilisation time was increased to 20 minutes. Stock concentrates of inorganic macronutrients and trace metals were prepared and added to a large proportion of the final volume of water in order to avoid precipitation.

Compound	Concentration in 1 l media (mg l^{-1})
$MgSO_4 \cdot 7H_2O$	200
K_2HPO_4	108.8
KNO_3	400
Na_2O_4Se	0.00152
FeNaEDTA	20
Citric acid	200
$CaCl_2 \cdot 2H_2O$	108
$CuSO_4 \cdot 5H_2O$	0.08
$ZnSO_4 \cdot 7H_2O$	0.22
$CoSO_4 \cdot 7H_2O$ Stock Solution	0.09
$MnSO_4 \cdot 4H_2O$	1.77
$Na_2MoO_4 \cdot 2H_2O$ Stock Solution	0.06
H_3BO_3	2.86
Conc. H_2SO_4	1 drop

Table 1 - Formulation for 1 l Modified Chu-13 media

CHU-M was prepared according to the method described by the University of Exeter. CHU-M is supplemented with essential minerals and trace elements that are required for the algal growth, but does not include a carbon source so is only suitable for the growth of phototrophs.

2.3 Growth Conditions

B. braunii was acclimated to high light by exposing cells to an increasing intensity on consecutive photobioreactor (PBR) runs. Triplicate runs were performed at each light intensity which allowed changes to be observed within a set of replicates under the same lighting condition and over increasing levels.

Due to the successive nature of the PBR runs it was important that cells were in good condition and actively growing before re-inoculation. Cells were washed between runs according to the procedure described in section 2.3.2. Each new PBR run was inoculated to an initial OD of 0.2 (Ab_{680}) and grown for a period of 14 days. Previous work demonstrated linear growth up to day 18 with no decrease in total chlorophyll content observed until day 14. The lag period was reduced (1 - 2 days) or eliminated completely when successive runs were inoculated with washed cells, grown over a period of 14 days (illumination provided by fluorescent lamps at 300 µmol m^{-2} s^{-1}).

B. braunii was cultured in custom built split column airlift PBRs (Electrolab). Airlift are characterised by high volumetric transfer coefficients where the bubbling of gas from the bottom of the column enables efficient CO_2 utilisation and O_2 removal (Wang *et al*, 2012). Also, as gas bubbles mix the culture gently, there very little cell damage associated with shear stress compared to mixing with impellers and pumps (Wang *et al*, 2012).

A schematic representation of the PBR used for microalgal culture is shown in **Figure 5**. The PBR was a borosilicate glass cylinder (internal diameter 13 cm, height 52.7 cm) providing a total illuminated area of 1805.16 cm^2 (excludes surface area of the top and base sections); working volume of 6.5 to 7 l due to placement of the baffle. The base, top plate and internal baffle were of stainless steel construction. Mixing was by sparging gas into the bottom of the reactor through a perforated pipe attached to the air duct outlet. The head plate configuration incorporated air in and air out with condenser, one harvest/ sample port with long dip tube, two cold fingers and two addition ports. The temperature was maintained at 23 °C by two cold fingers within the reactor connected to a

refrigerated/ heating circulator (Julabo, FP40-HE) with external Pt100 probe. Constant airflow with a CO_2 concentration of 5 % was prepared by mixing air with pure CO_2 and aerated into the PBR at a rate of 7 l min^{-1}. To ensure sterility of sparged gas, a filtration capsule (0.2 µm) was fitted before the air inlet. A condenser on the outlet gas at -2 °C prevented evaporation during the run which can lead to an increase in nutrient concentration and decrease in volume. A second water trap (bubble bottle) was fitted before the exhaust gas vent. Vented gasses were passed through a filtration capsule (0.2 µm) to ensure no microbial release into the atmosphere.

Cells were grown in a 12 h light:dark photoperiod. Illumination was provided by fluorescent lamps with a fixed irradiance of 300 µmol m^{-2} s^{-1} (Sanyo MLR-351 Plant Growth Chamber) or a warm white LED shroud comprising four LED panels (Growlights, 600 W). Each panel on the LED shroud had three settings: 1 - low; 2 - medium; 3 - high which allowed variable quantum output depending on their on/off configuration. Lighting configurations for the LED shroud and their associated irradiance are listed in Table 3.

The LED shroud was programmable allowing light ramping which significantly reduces the stress associated with sudden changes in light intensity that is seen with on / off type lighting. Light stress was observed in previous experiments where the culture turned yellow-brown after 4 days; the *B. braunii* culture did not recover when irradiance was reduced or cells were re-inoculated into fresh media under optimum conditions. For effective light ramping each 12 hour light period was divided into three equal segments (Figure 6). Noon was set at the target or highest light intensity for a period of 4 hours, keeping the maximum exposure time consistent for each run.

During ‘sunrise’, the increase in light intensity was split evenly over the 4 hour period from 300 µmol m^{-2} s^{-1}(the lowest achievable intensity) to the highest intensity (noon) over the available range. For sunset the decrease in light intensity was the reverse. Sampling was performed at ‘NOON’ when light exposure is at a maximum.

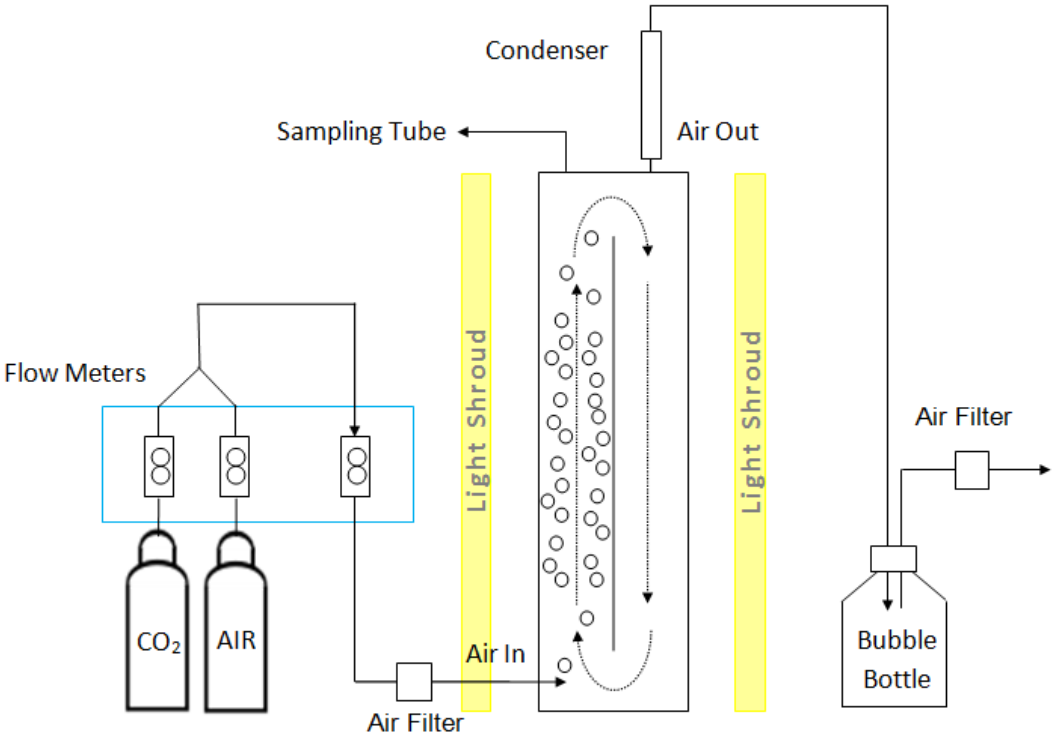

Figure 5 - Schematic Representation of the PBR for Microalgal Culture.

Botryococcus braunii was cultured in a closed PBR with an internal volume of 7 l. Mixing was by bubble-lift with 5% CO_2 enriched compressed air. Illumination was by fluorescent lamps provided by a Sanyo MLR-351 Plant Growth Chamber or warm-white LED shroud with variable quantum output. A central baffle generated turbulent flow within the reactor vessel.

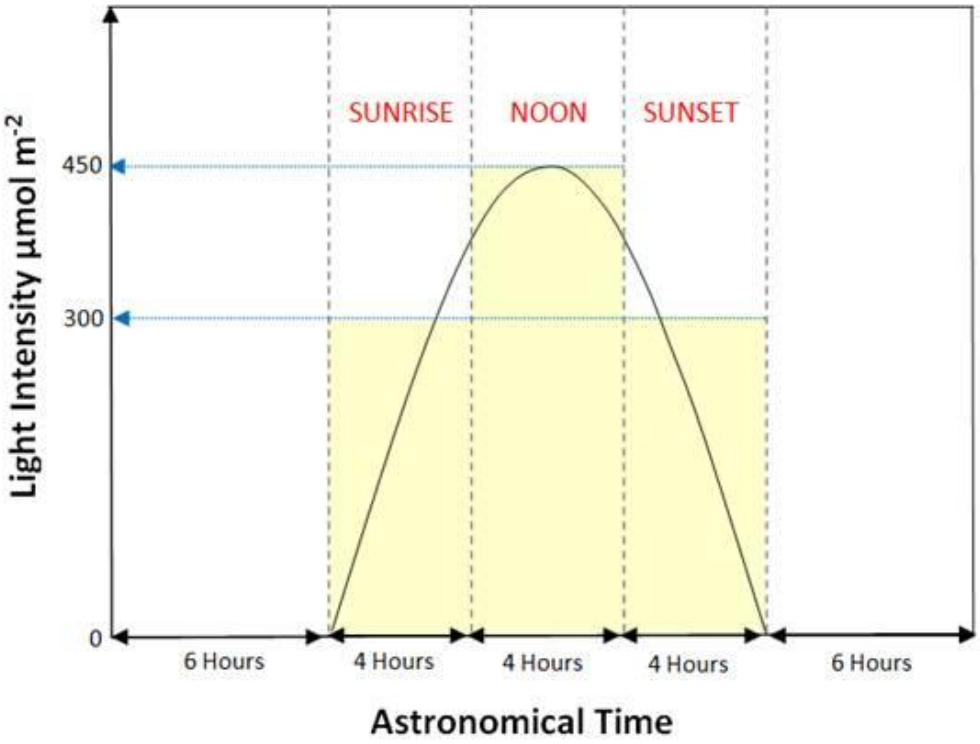

Figure 6 – Light ramping profile for LED shroud.

Cells were grown in a 12 h light:dark photoperiod. The light period was divided into 3 equal segments; sunrise (ramping up of irradiance), noon (target or maximum light intensity) and sunset (ramping up of irradiance). Ramping of irradiance during sunrise allowed time for the organisms to adjust to the lighting regime and minimised the effect of light stress. The yellow shaded areas in the diagram shows an example of how light intensity is ramped to a maximum intensity of 450 µmol m^{-2} s^{-1}; sunrise consists of 4 hours at 300 µmol m^{-2} s^{-1}, noon is 4 hours at 450 µmol m^{-2} s^{-1} dropping back to an intensity of 300 µmol m^{-2} s^{-1} for 4 hours during sunset.

2.3.1 Measurement of Light Intensity (LED Shroud)

Illumination provided by fluorescent lamps had a fixed irradiance of 300 µmol m^{-2} s^{-1}, no further light measurements were required. Table 2 lists all possible lighting configurations and associated irradiance of the LED light shroud; 4 panels each of which had 3 settings.

The PBR was positioned within the LED shroud and light measurements taken through the glass (Figure 7). For even illumination it was important to keep the PBR central within the shroud, ensuring the baffle was aligned with opposite corners to minimise the effect of shading. The average irradiance for each panel configuration was determined by taking duplicate readings at 10 locations (Figure 7). Light measurements were taken using a light meter (LI-COR, LI-250A). The sensor head pointed in the direction shown by arrows at each of position. Slight movements in placement of the probe resulted in significant fluctuations in the measured value, to improve reliability the probe was held in position using a stand and clamp.

The final list of experimental intensities and associated panel configurations are listed in Table 3. Where irradiance was obtained by more than one panel configuration, the arrangement with the best distribution of light was chosen. For example, an intensity of approximately 1150 µmol m^{-2} s^{-1} was achieved by configurations of 3, 2, 3, 0 and 2, 2, 2, 2 (Table 2). The second was the preferred option. Continuing from this the lowest achievable intensity is 300 µmol m^{-2} s^{-1} with both panel 1 and 3 set at level 1. This was the starting point for all experimental work.

Measured Light Intensity (μmol m^{-2} s^{-1})	LED Panel Configuration
308	1, 0, 1, 0
462	1, 0, 1, 1
585	2, 0, 2, 0
655	1, 1, 1, 1
748	2, 1, 2, 0
865	3, 0, 3, 0
894	2, 1, 2, 1
1022	3, 1, 3, 0
1029	2, 2, 2, 1
1149	3, 2, 3, 0
1150	2, 2, 2, 2
1180	3, 1, 3, 1
1307	3, 2, 3, 1
1428	3, 2, 3, 2
1546	3, 3, 3, 2
1674	3, 3, 3, 3

Table 2 - Lighting configurations of high powered LED light shroud

The 4 numbers represents each of the 4 panels so a configuration of 2, 1, 2, 1 would be panel 1 and 3 at level 2 and panels 2 and 3 at level 1. It is assumed that mixing is effective and the average value gives an accurate measure of light intensity allowing for the various panel configurations and orientation of the internal baffle within the LED shroud.

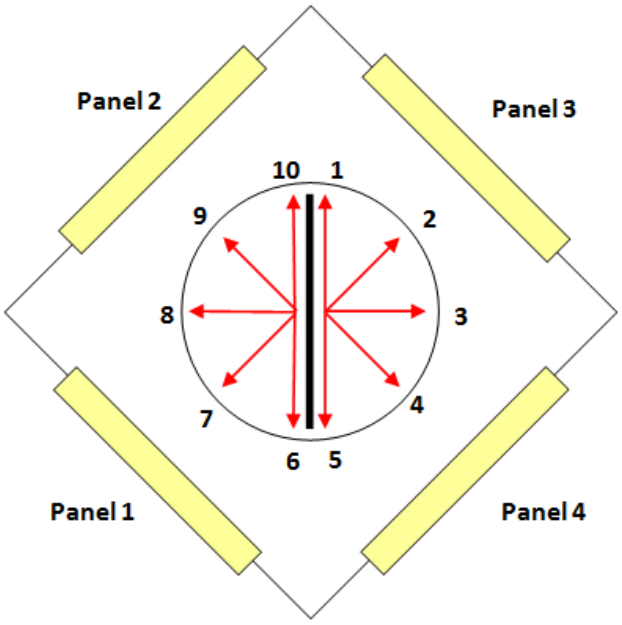

Figure 7 - Placement of light meter for the determination of irradiance for the LED shroud.

For even illumination, the PBR was centrally located with the LED shroud, the baffle aligned with opposite corners. Duplicate readings were taken at the 10 locations highlighted above, the arrow indicating the direction of the sensor head (sensor: LI-COR, LI-250A). All light measurements taken through the glass of the PBR.

Required Light Intensity (μmol m^{-2} s^{-1})	Measured Light Intensity (μmol m^{-2} s^{-1})	LED Panel Configuration
300	308	1, 0, 1, 0
450	462	1, 0, 1, 1
600	585	2, 0, 2, 0
750	748	2, 1, 2, 0
900	894	2, 1, 2, 1
1050	1029	2, 2, 2, 1
1200	1180	3, 1, 3, 1

Table 3 – Experimental intensities investigated listing panel configurations and measured values.

2.3.2 Washing Procedure

Harvested material was centrifuged at 10,000 x *g* for 10 minutes to pellet the majority of bacterial cells and dead material. Healthy *B. braunii* cells remain in suspension or float due to a high oil content. All material except the pellet was transferred to a 20 µm sieve (VWR, P/N 510-0700) and rocked gently to remove traces of old media and remaining bacterial cells. Up to 2 l CHU-M was passed through the sieve to further wash cells. Colonies of *B. braunii* are large enough to be retained. All steps were carried out using good aseptic technique in a Class II cabinet. Washing has been shown to produce a cleaner inoculum by reducing the level of bacterial contamination which would otherwise compete with the growth of *B. braunii* and removing debris and dead cellular material. Method validated by Blazina (2011).

CHU-M was used in place of DI water to prevent osmotic shock which resulted in an increase in lag time and slower initial growth rate. Over washing of *B. braunii* cells produces similar effects, possibly from the excessive removal of commensal bacterial associated with the matrix or embedded in the cells walls which provide a growth advantage to *B. braunii*, or through disruption of the colony and extracellular matrix.

2.4 In process measurements

In process measurements for the growth of *B. braunii* included optical density (OD), dry cell weight (DCW) and chlorophyll content. OD gives an instant result but the reading does not take levels of commensal bacterial growth into account. DCW determined by filtration is a better measure of growth as it allows bacterial populations not attached to algal colonies to be removed by washing. However, as proportion of DCW is extracellular material made up of water soluble polysaccharides and free floating droplets of hydrocarbons that have broken free of the colonies, they are not retained on the filter and results in an underestimation of DCW (Casadeval *et al*, 1985). Samples were mixed thoroughly prior to taking a

reading as the high oil content causes cells float to the surface over time. Cation and anion levels of the media, oil content and microscopic analysis were also performed to assess how levels change throughout the growth period.

2.4.1 Optical Density

The OD of the culture was measured using a spectrophotometer (GeneSys 10S Bio, Thermo Scientific) at a wavelength of 680 nm (Li and Qin, 2005). Measurements were performed in duplicate.

2.4.2 Biomass

DCW was performed by filtering 5 ml of culture under a low vacuum using a 47 mm Whatman glass filtration unit and pre-weighed Whatman 47mm GF/D glass fibre filters. Filters were washed with 15 - 20 ml DI water to remove media salts from the recovered cells which could otherwise lead to overestimation of DCW. Excess moisture was removed by ventilation. Filters were dried overnight at 70 ^{0}C, reweighed and the mass of recovered cells calculated. DCW was expressed per volume of liquid culture (g l^{-1}). Measurements were performed in duplicate.

2.4.3 Chlorophyll Measurement by Spectroscopy

Chlorophyll content was measured spectrophotometrically. As with dry weight, 5 ml of culture was filtered through a 47 mm Whatman GF/D glass fibre filters and recovered cells washed with 15 - 20 ml DI water. The filter was transferred to a vial, submerged in 10 ml methanol and sonicated at 4 °C, in dim light for 30 minutes. It was important to avoid heat and light exposure throughout sample preparation to prevent degradation of chlorophyll and the possible formation of

artefacts (Pocock *et al*, 2004). Full extraction of intracellular pigments is indicated by cells on the filter becoming white. Where this had not occurred sonication time was increased. Extracts were centrifuged at 1,000 x *g* to pellet fragments of filter paper (GeneVac, EZ-2 personnel evaporator). Samples were transferred to a quartz cuvette and the absorbance read at 650 and 665 nm. Methanol was used as a blank. Chlorophyll a, b and total chlorophyll were calculated using the following formulas (Becker, 1994):

$$\text{Chlorophyll A (mg l}^{-1}) = (16.5 \times A665) - (8.3 \times A650)$$
$$\text{Chlorophyll B (mg l}^{-1}) = (33.8 \times A650) - (12.5 \times A665)$$
$$\text{Total Chlorophyll (mg l}^{-1}) = (25.8 \times A650) + (4 \times A665)$$

NOTE: A dilution factor of 2 was used as 5 ml culture was extracted with 10 ml methanol. Results were multiplied accordingly to give chlorophyll measurements in mg l^{-1}.

2.4.4 Extraction of Photosynthetic Pigments

Chlorophyll and some carotenoids are lipophilic and occur as pigment-protein complexes within the thylakoid membrane of chloroplasts. Carotenoids also occur within of the chloroplast envelope (Pocock *et al*, 2004). A full extraction therefore requires external and internal membranes to be disrupted to separate pigments from their associated proteins.

Pigments are susceptible to degradation by heat, light and oxygen. All procedures throughout sample preparation and extraction were therefore were carried out rapidly, in dim light and at a temperature of 4 °C. This also prevented the possible formation of artefacts (Pocock *et al*, 2004).

Documented methods include disruption with a mini-beadbeater, French press (Pocock *et al*, 2004) or freezing drying followed by multiple solvent extractions

(Dunn *et al*, 2004). In this study cells were freeze dried and ball-milled as previous experience shows it gives a more complete extraction.

Harvested culture (5 ml) was transferred into 15 ml Falcon tubes, snap frozen in liquid nitrogen; freeze dried and stored at -80 °C. Two replicates were prepared. Freeze dried samples were weighed into 2 ml Eppendorf tube containing a stainless steel bearing (2 mm) and snap froze in liquid nitrogen. Samples were then milled using a Retsch MM 400 mini-ball mill (20 sec at 30 Hz) to maximise pigments extraction. Following disruption, samples were immediately transferred to crushed ice, opened and resuspended in 1 ml of pre-chilled HPLC grade acetone. Eppendorf vials were placed on a Stuart SSL2 reciprocating shaker for 15 minutes (250 strokes min^{-1} in the dark). Sample vials were placed in a container with ice in order to maintain a low temperature during this period. The supernatant was clarified by centrifugation at 10'000 x *g* for 5 minutes and bubbled with N_2. Samples were stored at -20 °C while awaiting analysis.

2.4.5 Identification and Quantification of Photosynthetic Pigments by HPLC

Pigment extracts were analysed at the Analytical Department, Shell Technology Centre Thornton using modifications to a method described by Val *et al* (1994). An Agilent 1200 HPLC was used equipped with a Phenomenex synergi Hydro-RP, Polar Endcapped C_{18} column (Length 15 cm, 4 µm particle diameter) with a flow rate of 1.2 ml min^{-1}, 50 µl sample injection. This column has strong hydrophobic interactions and slight polar interactions for extreme retention of non-polar and extremely polar alkyl compounds. Pigments were detected at 440 nm with a diode array detector (Agilent 1200 DAD) and peak areas integrated with EZChrom.

The mobile phase was based on a duel isocratic step. The staring phase was a mixture of 1.75 % methanol, 1.75 % dichloromethane, 1.75 % water and 94.75 % acetonitrile. The second was 50 % acetonitrile and 50 % ethyl acetate. The second phase entered the system 5 minutes after beginning the chromatography.

2.4.6 Microscopic examination

Microscopical imaging was performed using an Olympus BX51 microscope with Olympus DP71 camera in differential interference contrast (DIC) mode. DIC mode was used as it gives the appearance of 3D physical relief that corresponds to the variation of optical density in the sample and allows a greater depth of focus thereby allowing thicker specimens to be observed under higher magnifications.

BODIPY 505/515 staining was used to assess the oil content of cells, both intracellular and secreted. For these studies, a 5 mM solution of the dye was prepared in dimethyl sulfoxide (DMSO) and mixed with the diluted algal samples in a 20:1 algae: dye ratio. Each sample was allowed to stand for 10 min to allow time for the dye to permeate the cells. Micrographs were obtained using UV illumination and the WIB filter cube. This cube gives excitation of 460-495 nm (blue light), emission >510 nm and was expected to show green fluorescence in lipid-rich regions, with possible red fluorescence due to non-lipid components in the cytoplasm. In those cases where x100 objectives were used for imaging, the above techniques were combined with oil immersion.

From these it was possible to assess the general health of the culture including colouring, cluster size, matrix composition and levels of oil secretion, damaged or disrupted cells, debris and contamination. It also allowed the culture to be examined at cellular level with presence of organelles including chloroplasts, size and number of oil vacuoles and membrane integrity.

Particle size analysis was also conducted on *B. braunii* cultures to assess the effect increasing irradiance had on colony size. Images were captured using Olympus Cell-F software, thresholded and subject to automated particle size analysis to determine equivalent circle diameter particle (cluster) sizes. A minimum particle size of 16 pixels in adjacent contact was used.

2.4.7 Total Hydrocarbon

Hydrocarbons were extracted directly from the culture by liquid-liquid extraction using solvents with varying degrees of polarity. Heptane was selected as the solvent because it only recovers extracellular lipophilic molecules including those which has been secreted into the media or can easily be extracted from the biofilm matrix without undue adverse effect on the cells (Eroglu and Melis, 2010). Oil extracted by the solvent phase in this method is extracellular. It is more relevant to refer to this as easily extractable oil as it does not recover oil that trapped deep within the colony matrix.

Ethyl acetate is more polar and able to penetrate the layer of water on the surface of the cells. It can breakdown the extra cellular matrix, disrupt cell membranes and aids in cellular disruption which releases the oil making it available for extraction. This provides a measure of total oil concentration. Measurements were not performed in duplicate as to limited the sample size for in-process measurements and minimise the effect of sampling on reactor volume.

For both extractions 5 ml solvent was added to an equal volume of culture. The culture was diluted with DI water where required. It was important that the sample OD was less than or equal to 0.5 to maintain a favourable extraction gradient and prevent solvent saturation. The sample was transferred to a 28 ml vial (LSL group, squat form trident vial) and placed on a reciprocating shaker at room temperature for 30 minutes, 250 strokes per minutes (Stuart, SSL2 reciprocating shaker). Extracts were centrifuged for 5 minutes at 1000 x *g* in a GeneVac for rapid phase separation. 1 ml of the heptane layer was remove and placed in a vial for GC analysis (squalene standard). Results were expressed as terpene per mg l^{-1} of culture and multiplied where applicable to dilution factors into account.

2.4.8 Analysis of Total Oil Content

Terpene analysis was performed by the Analytical Department, Shell Global Solutions. 1 µl of the sample was injected into an Agilent 7890 GC system equipped with an on-column injector, a 30 m HP5 column (30 m x 320 µ x 0.25 µ) and Flame Ionization Detector (FID). Helium was used as carrier gas at 2.25 ml min^{-1}. The oven temperature was programmed as follows: 65 °C raised to 320 °C (8 °C min^{-1}) and held for 7 minutes. The on-column injector tracked the oven temperature plus 3 °C and the Flame ionization detector was held at 345 °C. Terpenes were quantified against external Squalene standards and peaks were integrated using an EZChrome data system.

2.4.9 Inorganic Cation and Anion analysis

Concentration of inorganic cations and anions were measured using a Dionex ICS-3000 Reagent-Free Ion Chromatography (RFIC) system. This required a sample of cell free media obtained by collecting the filtrate from DCW or chlorophyll analysis before washes of the filter had been performed. Samples were stored at -20 ºC.

Samples were injected into a stream of potassium hydroxide eluent, passed through an ion exchange column and measured by a conductivity detector. The first column, a guard column, protects the analytical column by removing particulate and organic matter. The analytical column separates anions/ cations by their relative affinities for a low-capacity, strongly basic anion exchanger. The suppressor (between the analytical column and the conductivity detector) provides continuous suppression of background conductivity of the eluent and enhances response of the target analytes by acidification. The separated anions/cations in their acidified form are measured by conductivity. The anions/cations are identified based on retention times and quantified by conductivity relative to standard response. Testing performed by the Analytical Department, Shell Global Solutions.

2.4.10 ASE Extraction of Total lipid

The total lipid content of *B. braunii* was determined using a Dionex ASE 300 Accelerated Solvent System with a 100 ml volume sample cell and a 250 ml collection bottle. Extracts were cleaned-up by liquid-liquid phase separation which removes non-lipid material from the organic phase to the aqueous phase. Extractions were performed in duplicate.

Cells were recovered by vacuum filtration using a 90 mm Whatman 3 piece funnel and GF/D glass fibre filter (Whatman). The volume of culture required was calculated from the DCW to give between 0.08 and 0.1 g biomass. This gave sufficient material to send for GC analysis without forming a filter cake where cells were so tightly packed it was impenetrable to solvents during extraction resulting in a lower in yield. It also prevented overloading of the filter causing it to block. Traces of media salts in the recovered biomass would not give rise to errors in oil concentrations so washes were not performed. A small volume of DI water was used to rinse the inside of the Buchner funnel to recover cells stuck to the sides. Excess moisture was removed by ventilation. Filters were removed from the funnel assembly and the edge of the filter paper clear of cells used to wipe the rim of the filter reservoir. For accurate calculation of recovered solid DCW was performed in duplicate (See section 2.4.2).

Two extractions were performed on each cell; heptane for recovery of extracellular oil followed by chloroform:methanol (1:2) for residual extracellular oil and intracellular oil. Extraction parameters were the same for both solvent systems as listed in Table 4.

Filters were rolled (cells to the inside) and placed in an extraction cell with no surfaces touching thereby maximising the surface. Using tweezers, the filter was held in place and empty spaces filled with Ottawa sand. Cells were run on the appropriate Dionex method. Extracts for each solvent systems was collected in a separate bottle.

Solvent from heptane extractions were evaporated directly. Chloroform: methanol extractions contained significant quantities of water soluble constituents and required clean-up prior to solvent evaporation.

Extract volume was determined and transferred to a separating funnel. Based on the extract volume and ratio of chloroform and methanol within the extract (35:65), the volume of chloroform and water required to achieve Bligh and Dyer phase separation of chloroform: methanol: water (1:1:0.9) (Bligh and Dyer, 1959) was calculated using the following equations. Losses to glassware were reduced by using rinsing the extraction bottle and measuring cylinder with the extra chloroform.

$$\text{Chloroform (ml)} = 0.35 \times \text{Extract Volume (ml)}$$

$$\text{Water (ml)} = 0.9 \times 0.65 \times \text{Extract Volume (ml)}$$

The separation funnel was gently shaken for 1 minute to homogenize the solvent mixture and left for 2 hours for phase separation to occur or until a biphasic layer was observed. Once separated the organic phase was run-off into a suitable pre-weighed vial and solvent evaporated using the GeneVac. Settings: low boiling point mixture at 30 ^{0}C. Samples were purged under nitrogen for 1 hour before the weight was determined to remove residual solvent. Heptane extracts were treated in the same way.

Parameter	Setting
Cell Size	100 ml
Oven Temperature	60 °C
Heat Up Time	5 min
Pressure	1500 psi
Static Time	5 min
Number of Static Phases	2
Flush Volume	60 % of cell volume
Purge Time	100 seconds

Table 4 – ASE extraction parameters for *B. braunii*.

NOTE: On the ASE solvent mixtures go up in steps of 5 %. An exact 2:1 solvent ratio is not possible so 35 % chloroform and 65 % methanol was used.

Where an emulsion had formed samples were centrifuged to accelerate phase separation. The emulsified layer or the whole aqueous layer if no clear line was observed was collected into a suitable vial and centrifuged for 5 minutes in the GeneVac or until a biphasic layer had formed. The organic layer was removed using a Pasteur pipette and added to the collection vial. To minimise losses the Pasteur pipette was rinsed with chloroform and transferred into the collection vial.

To verify the cleanliness of the dispersing agent a cell containing Ottawa sand was extracted with chloroform: methanol, the worse case solvent following the same Dionex method. This was run before each set of ASE samples.

2.4.11 GC Analysis of Oil Extracts

Oil extracts analysis was performed by the Analytical Department, Shell Global Solutions. 1 µl of the sample was injected into an Agilent 6890 GC system equipped with an on-column injector, a 10 m Varian Biodiesel column for glycerides (10 m x 320 µ x 0.1 µ) and FID. Helium was used as carrier gas at 3.0 ml min^{-1}. The oven temperature was programmed as follows: 50 °C hold for 1 minute, raised to 180 °C at a rate of 15 °C min^{-1} and held for 0 minutes, raised to 230 °C (7 °C min^{-1}) and finally to 385 °C (10 °C min^{-1}) and held for 5 minutes. The on-column injector tracked the oven temperature plus 3 °C and the FID was held at 400 °C. TAGs quantified using relative response factors, C36 alkane is the internal standard, (TAG response factors relative to C36). Peaks were integrated using an EZChrome data system.

3. Results

Botryococcus braunii was grown in airlift batch culture, for approximately 14 days, in a 12 h light – 12 h dark photoperiod. Algae were cultured in different irradiances and with different light sources; fluorescent strips emitting 300 $\mu mol_{photons}$ m^{-2} s^{-1} (μmol m^{-2} s^{-1}) and warm white LEDs, emitting 300, 450 and 600 μmol m^{-2} s^{-1} (referred to 300 FLU, 300 LED, 450 LED and 600 LED throughout). Biomass accumulation (growth), hydrocarbon production and photosynthetic pigment concentration were monitored to more fully understand the response of *B. braunii* to light intensity.

3.1 Growth Analysis

Biomass was measured at equal time intervals over the culture period by Optical Density (OD) at an absorbance of 680 nm ($Abs_{680\ nm}$) and Dry Cell Weight (DCW). The experiments were run in triplicate. OD and DCW were plotted against time for the four lighting conditions (Figure 8).

B. braunii showed linear growth with no lag phase in all illumination regimes. Cells did not reach stationary phase over the 14 day growth period. In 600 μm m^{-2} s^{-1} LED illumination, (600 LED) *B. braunii* growth was reduced compared to the other light regimes. The cultures reached a maximum cell density of 1.333, 1.082, 1.230 and 0.602 when measured at an absorbance of 680 nm for 300 FLU, 300 LED, 450 LED and 600 LED after inoculating with the same amount of cells. When taking DCW into consideration the maximum cell density in the respective cultures were 2.284 g l^{-1}, 2.443 g l^{-1}, 2.497 g l^{-1} and 1.545 g l^{-1}.

All four illumination conditions had an initial OD (Abs_{680}) of 0.2 and DCW of 0.45 g l^{-1}. The exception was 600 LED which had an OD of 0.2 but a measured DCW of 0.695 g l^{-1}. For OD the maximum algal biomass was achieved under 300 FLU reaching an OD of 1.333 after 14 days. Taking DCW into account, 450 LED gave the highest yield at almost 2.5 g l^{-1}. Algal cells grown under the 600 LED yielded

the least biomass reaching an OD of just 0.602 and a DCW of 1.545 g l^{-1} on day 14.

When OD and DCW were plotted against each other, a positive linear relationship was observed (Figure 9) with an r^2 value of 0.8919. This indicates that the regression line fits the data well and there is a good correlation between the two methods used for quantifying growth. During experimentation, variations in Abs_{680} were observed and were ascribed to the colonial phenotype of *B. braunii*. This variance was observed in the repeat measurements for all experimental samples. Conversely, biomass measured by DCW was less variable but took significantly longer to acquire (24 h for DCW as opposed to 5 min for Abs_{680}); despite this difference in time, DCW was adopted as the preferred method for biomass determination. As well as giving a more representative measure of growth, the exclusive use of DCW facilitated future analyses.

In this series of experiments *B. braunii* were acclimated to a given light intensity in successive PBR batch cultures, before being exposed (and acclimated) to higher irradiance from further, successive batch cultures (Figure 10).

In this scenario, “replicates” might not be considered as true technical replicates, as the experiments were not performed simultaneously (due to a lack of the required equipment) and the inoculum for each batch was derived from the previous one, not from a master stock. However, in practise, it is not possible to maintain a consistent master stock without sub-culturing the algae, and cryo-preservation of *B. braunii*, the preferred method for maintaining consistent stock cultures, is not possible. However, replicate cultures, *i.e.* cultures performed under identical conditions, were inoculated consistently at the same starting density which allowed for a sustained period of growth. When analysed as independent runs of culture, there is generally no different in growth for cultures exposed to identical light intensities (Figure 11). Consequently, while the experiments described here may not represent true technical replicates, these data suggest that is appropriate to consider them to represent acceptable biological replicates.

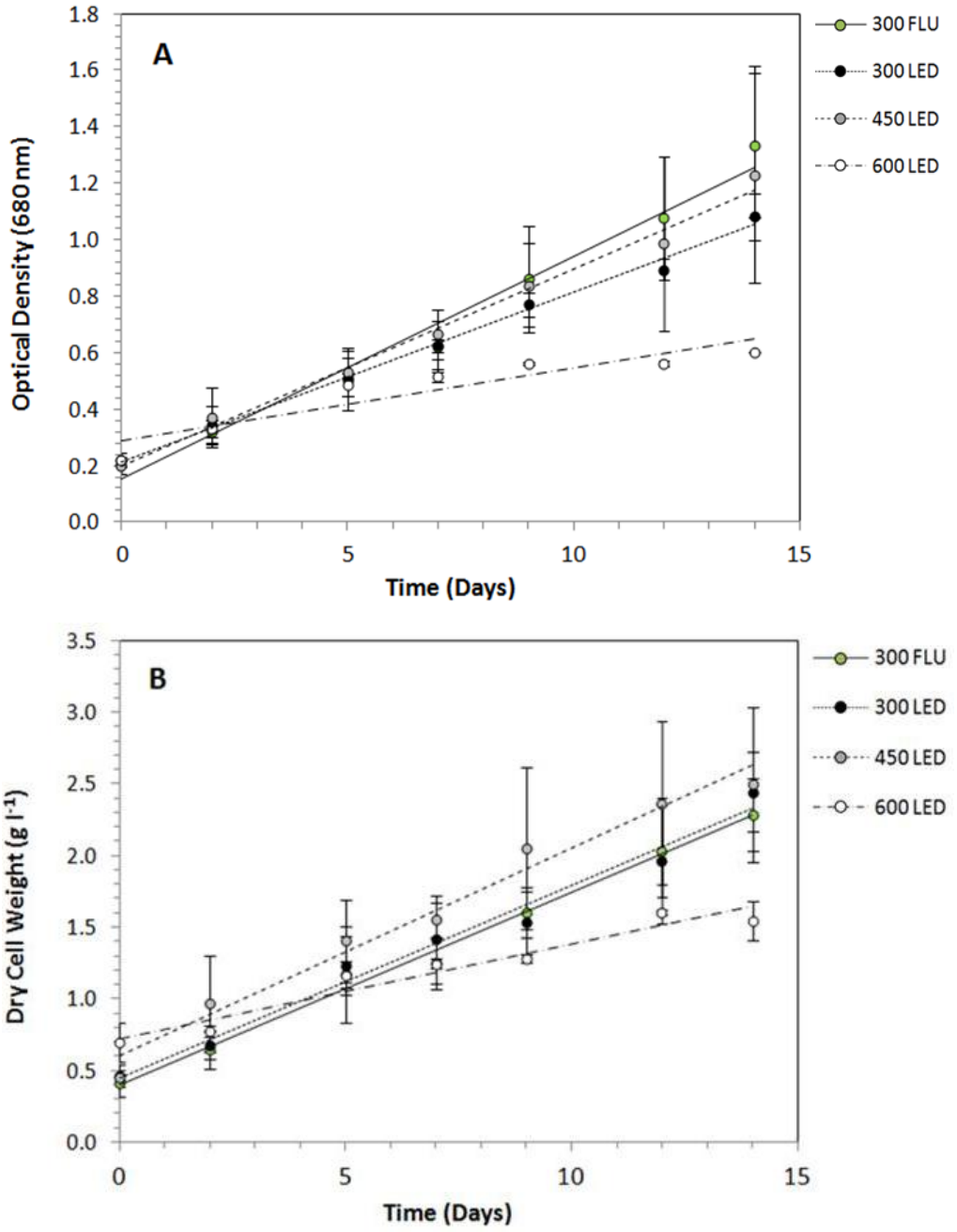

Figure 8 - Growth of *B*otryococcus *braunii* measured by absorbance at 680 nm (Panel A) and DCW (Panel B).

B. braunii was grown for 14 days with illumination provided by fluorescent shrouds at 300 µmol m^{-2} s^{-1} and LED shrouds at 300, 450 and 600 µmol m^{-2} s^{-1} for comparison of light quality. Each data point represents the average of 5, 3, 3 and 2 replicates for 300 FLU, 300 LED, 450 LED and 600 LED respectively, with standard error bars shown. When error bars are not seen, they are masked by the symbol. Trend lines show the linear relationship for each series. All light intensities are expressed in µmol m^{-2} s^{-1}.

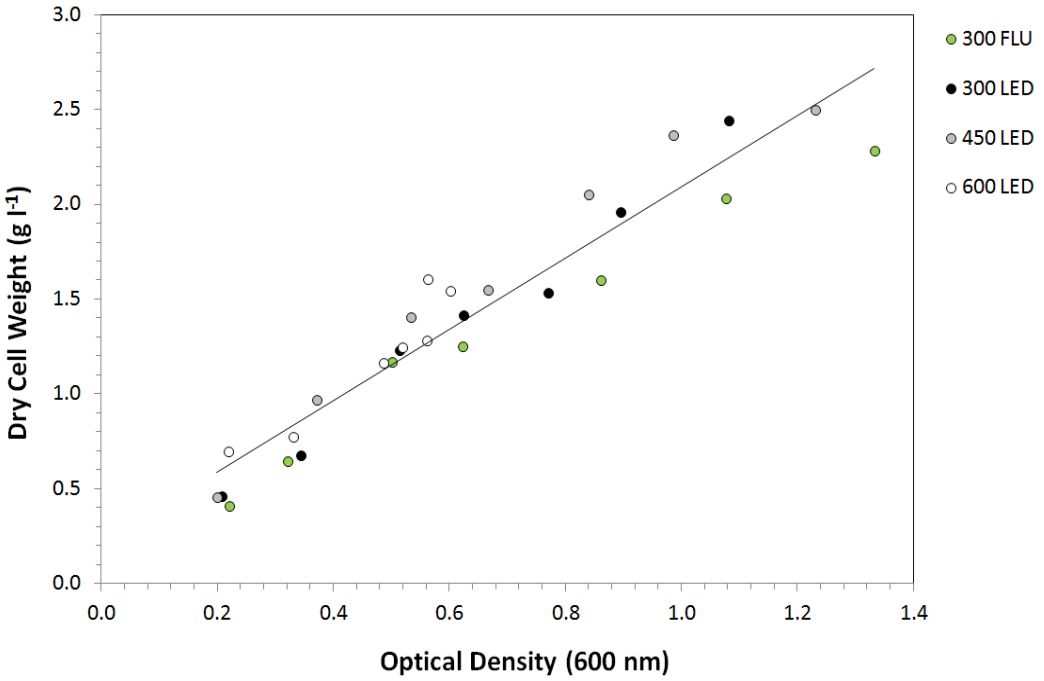

Figure 9 - Correlation between optical density and dry cell weight.

Correlation between methods of biomass determination in cultures of *B. braunii*. The average OD data was plotted against the average DCW data for each run. A positive linear relationship is apparent demonstrating a fairy good fit with an r^2 value of 0.8919. The coloured markers represent the light regime from which each point was dertermined.

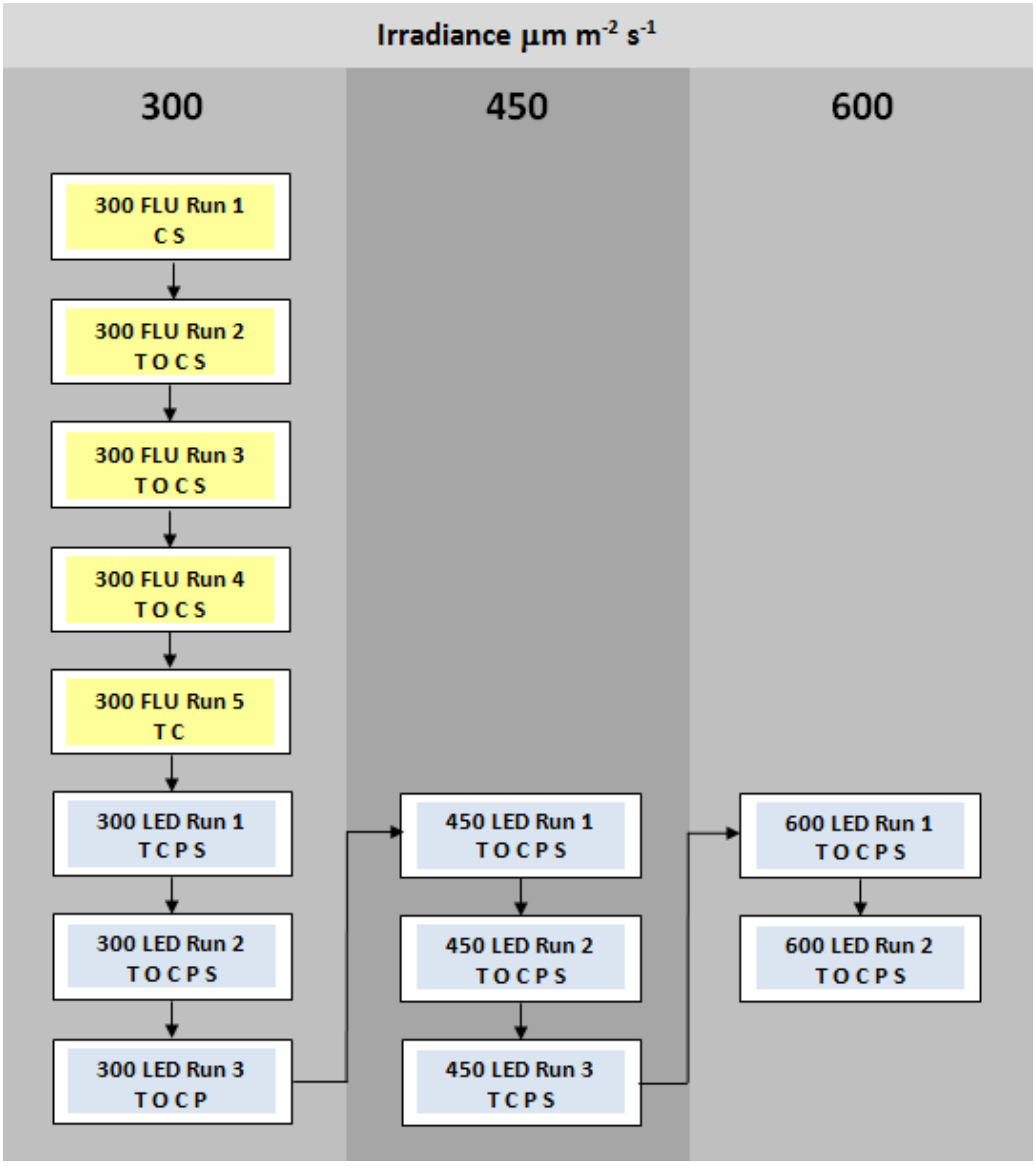

Figure 10 – Schematic showing successive PBR batch cultures of *B. braunii*.

Successive photobioreactor runs of *B. braunii* showing cell lineage and associated analysis. Growth measurements and microscopy were performed on all runs; other analyses are indicated on the flow chart as follows: T – Terpene analysis, O - End oil analysis by ASE, C - Chlorophyll content by UV-VIS, P - Pigment content by HPLC and S - Colony size.

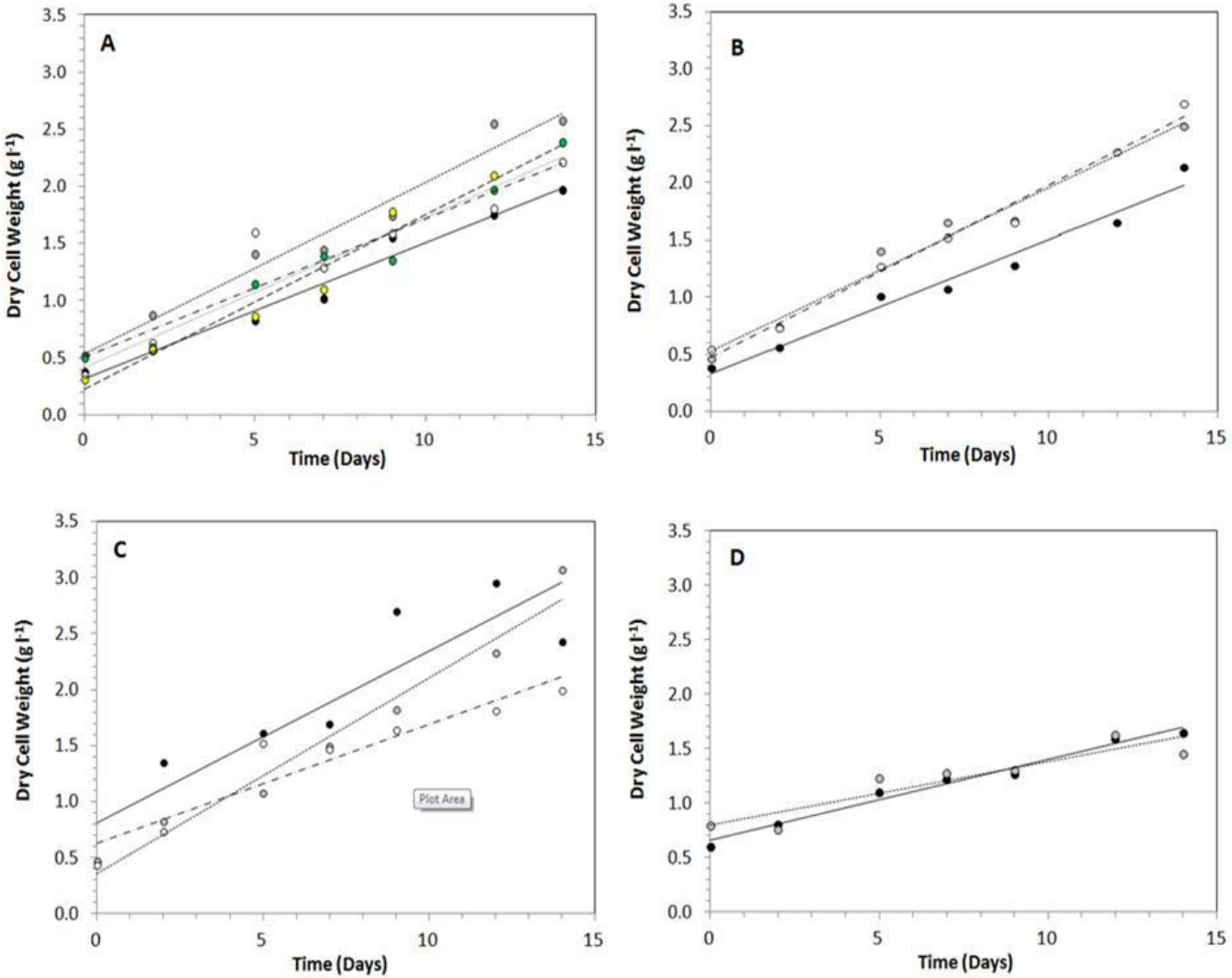

Figure 11 - Growth of *B. braunii* under four different lighting regimes.

B. braunii was grown for 14 days using warm white fluorescent bulbs at 300 µmol m^{-2} s^{-1} and a warm white LED shroud at 300, 450 and 600 µmol m^{-2} s^{-1}. Each chart shows successive runs carried out for each lighting system: Panel A - 300 FLU. Panel B - 300 LED. Panel C - 450 LED. Panel D - 600 LED. Increases in growth rate can be seen at 300 FLU, 300 LED, 450 LED repeats 1 and 2 whereas 450 LED repeat 3 and both runs at 600 LED show a decline.

The specific growth rate (SGR) of each culture was calculated using the equation:

$$\mathrm{SGR} = \frac{DCW_{t_2} - DCW_{t_1}}{t_2 - t_1}$$

Where, $DCWt_1$ is the initial dry biomass at time point 1 (t_1), and $DCWt_2$ is the dry biomass as time point 2 (t_2). The units of the growth rate are in grams per litre per day (g l^{-1} d^{-1}). There is no obvious increase in mean growth rate between runs of the same intensity and illumination type (Fluorescent lights or LED's) (Table 5). The SGR of *B. braunii* under 300 FLU and 300 LED have a mean of 0.1511 g l^{-1} d^{-1} (± 0.0149) and 0.1561 g l^{-1} d^{-1} (± 0.0053), respectively. The means were compared using a student's t-test, and found to be non-significantly different (P = 0.52) at the 95 % confidence level (Table 5). This result correlates to the similarity in spectral data obtained from both fluorescent and LED lighting systems in relation to the amount of Photosynthetically Active Radiation (PAR) or usable light in the blue and red regions (Figure 12).

Increasing the irradiance from 300 µmol m^{-2} s^{-1} (300 LED) to 450 µmol m^{-2} s^{-1} (450 LED) resulted in a 6 % increase in growth rate from an average of 0.1561 g l^{-1} d^{-1} (± 0.0053) to an average of 0.1661 g l^{-1} d^{-1} (± 0.0610). This difference was considered significant at the 95% confidence level, as determined by the student's t-test (P = 0.0048). Increasing the irradiance further to 600 µmol m^{-2} s^{-1} (600 LED) had a detrimental effect on the culture and caused a substantial decrease in mean SGR to 0.0735 g l^{-1} d^{-1} (± 0.0007).

When successive runs were analysed individually, an interesting and unexpected result emerged, and probably arose from the manner in which the experiments were performed. Successive cultures had similar growth rates when illuminated with 300 FLU and 300 LED. A 25 % increase in individual SGR was observed for the first two runs in 450 LED (0.2021 g l^{-1} d^{-1} and 0.2005 g l^{-1} d^{-1}) compared to the SGR in 300 LED, but then a collapse in SGR occurred from 0.2005 g l^{-1} d^{-1} (450 LED run 2) to 0.0957 g l^{-1} d^{-1} (450 LED run 3) (Figure

13). This represents over a 50 % reduction in SGR compared to that observed for the two earlier cultures at 450 LED (Figure 13).

Microscopic observations, however, showed that the *B. braunii* cells in 450 LED run 3 were not necrotic or ruptured. Moreover, no increase in bacterial contamination relative to previous cultures was observed. Therefore a possible explanation for the observed crash in SGR between 450 LED run 2 and 3 is the effect of photoinhibition and the progressive accumulation of irreparable photodamage and even though cells appear healthy, they are not viable. This explanation may also account for the further 30 % reduction in SGR observed between 450 LED run 3 (0.0957 g l^{-1} d^{-1}) and 600 LED run 1 (0.0735 g l^{-1} d^{-1}). Similarly, there were no major microscopic differences between 450 LED run 3 and 600 LED run 1 (Figure 20, panel B, C and D). Due to equipment failure, microscopic analysis was performed for 450 LED Run 3, but no images are available.

Irradiance (µmol m^{-2} s^{-1})	300 FLU	300 LED	450 LED	600 LED
SPR ± SD (g l^{-1} d^{-1})	0.1511 ± 0.0149	0.1561 ± 0.0053	0.1661 ± 0.0610	0.0735 ± 0.0007
t-test Comparison	P = 0.2620 (NS)			
		P= 0.0048 (S)		
			N/A*	

Table 5 - Average specific growth rates (SGR) and significance values (P values) for growth of *B. braunii* in different illumination conditions.

The average SGR for each illumination condition were analysed using an unpaired t-test assuming unequal variances. Comparisons were made between fluorescent and LED lighting at 300 µmol m^{-2} s^{-1}; at an increase in irradiance from 300 to 450 µmol m^{-2} s^{-1} (LED) and an increase from 450 to 600 µmol m^{-2} s^{-1} (LED). P values are given in the light green boxes. Differences between data sets are either considered S – Significant or NS – Non Significant at the 95 % confidence level. * No statistical data analysis was possible between 450 LED and 600 LED due to the number of replicates (*i.e*. 2) performed in 600 LED.

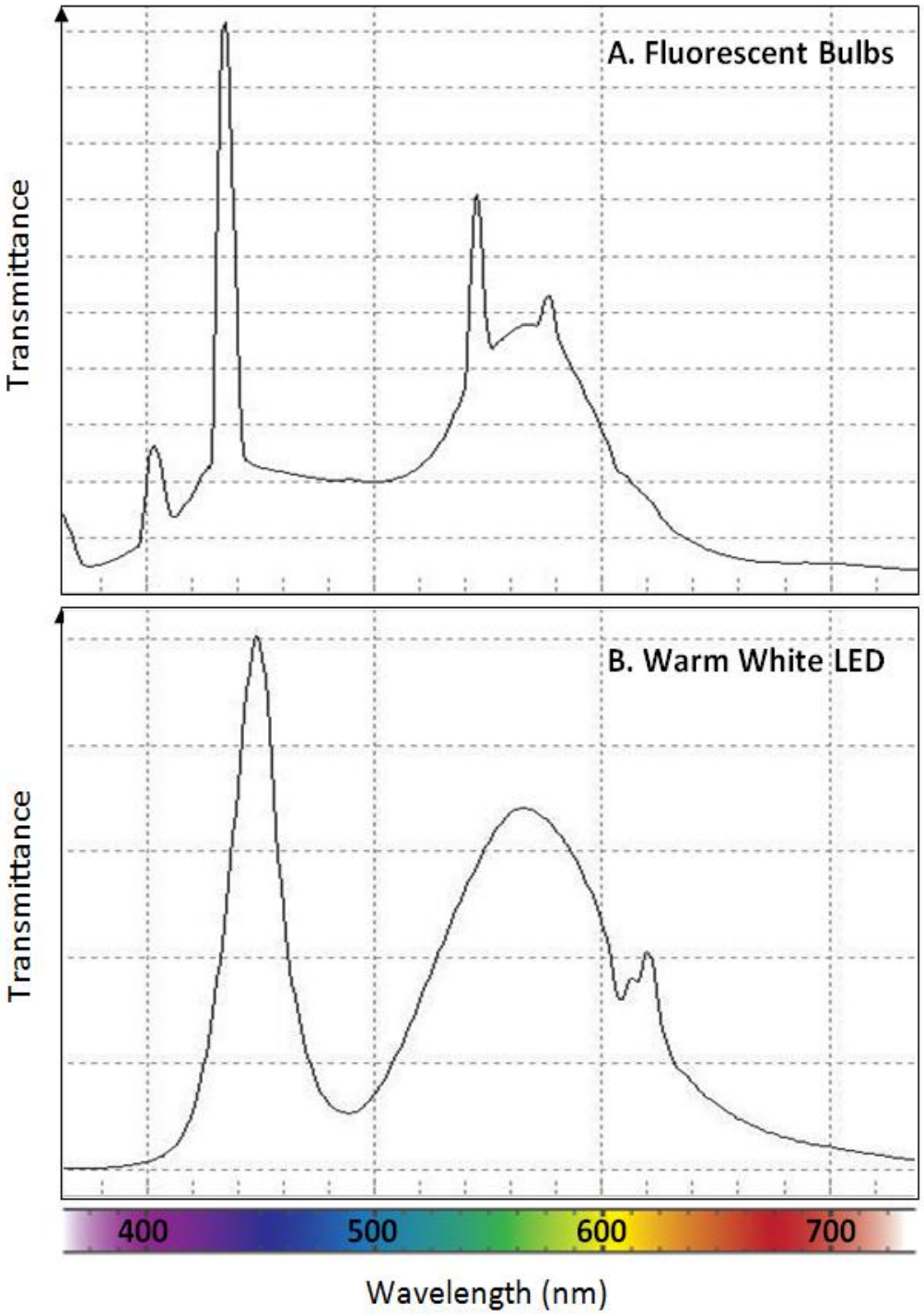

Figure 12 – Spectra of emitted light from Fluorescent (FLU) and LED lighting systems.

Absorption spectrum of Fluorescent (FLU) and LED lighting systems. Both systems give out light from the blue (peaking at around 450 nm) and red (peak at 565 nm) parts of the spectrum. There is a large spectral region between 490 nm and 570 nm where very little light is emitted (green region). NOTE: There is no scale for transmittance, despite differences in light intensity, the spectra remained the same.

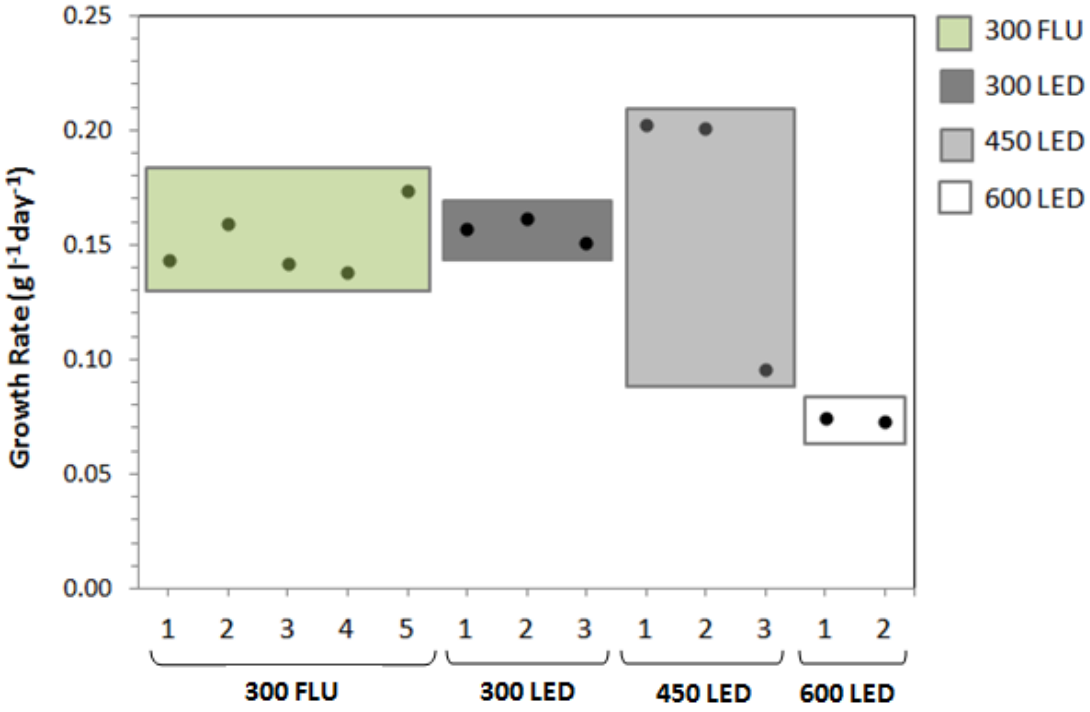

Figure 13 - Comparison of growth rate of *B. braunii* under four different lighting regimes 300 FLU, 300 LED, 450 LED and 600 LED.

B. braunii shows linear growth. Growth rates were calculated as the gradient of the line of best fit from the growth curves (DCW). Early and late data points were excluded to eliminate the effect of the lag and stationary phases. All light intensities are expressed in µmol m^{-2} s^{-1}.

3.2 Growth and Terpene production

Botryococcus braunii produces high levels of liquid terpenoid hydrocarbons called botryococcenes. Terpenes were extracted directly from fresh cells by liquid-solvent extraction using ethyl acetate. This solvent is able to breakdown the extracellular matrix and disrupts cell membranes and therefore provides a measure of total oil content. Samples were taken regularly throughout the growth period to determine how illumination type and irradiance intensity effects terpene production. Terpene extractions were performed in triplicate. The large error bars are associated with the variations in measured terpene value between runs at the same light intensity. This was due to the small sample volume that only allowed a single measurement to be performed at each time point.

As observed in other investigations (Kojima & Zhand, 1999), *B. braunii* shows increasing terpene production during the culture period (Figure 14, panel A). However, when the terpene content was normalised relative to the dry cell mass, terpene production is relatively constant, indicating that production is proportional to cell growth or, more specifically, that terpene production kinetics is growth-associated (Figure 14, Panel B).

The specific terpenes production rate was determined as the slope of the regression line between terpene concentration and time. A 50 % increase in terpene production rate was observed between 300 LED and 450 LED from 47.2410 mg l^{-1} day^{-1} ($\pm$ 9.6590) to 76.2033 mg l^{-1} day^{-1} ($\pm$ 42.8031) respectively.

Figure 15 displays the specific terpene production rate as a function of the specific growth rate under the various illumination conditions. With the exception of 450 LED Run 1 which has an extremely high rate of terpene production, there is a positive linear correlation between all data points. This analysis suggests that terpene production is very strongly growth associated and appears to be unaffected by changes in illumination condition *i.e*. the terpene production per cell remains the same for 300 FLU, 300 LED, 450 LED

and 600 LED. An r^2 value of 0.8144 indicates a good regression fit, but reflects the variation in terpene content observed between adjacent time points. The formula of the line is 330.37 µ. This is lower than a value of 406 µ reported by Kojima and Zhang (1999), but could be due to differences in extraction method.

B. braunii grown under 450 µmol m^{-2} s^{-1} for the first time (450 LED Run 1) displayed a rapid increases in measured terpene content at day 9 and day 12. This was over double the quantity compared to 450 LED run 2 and three times that for 450 LED run 3 at the same time points. While earlier time points were also higher the difference was not as significant. It was these values that lead to the exceptionally high specific terpene production rate for 450 LED run 1.

Due to the observed variation in terpene content the result for 450 LED could be anomalous. However, it has been reported that terpenes, especially β-carotenoid have a photoprotective function by preventing chlorophyll destruction by inactivating reactive oxygen species (Ge *et al*, 2011). If this is the case overproduction of terpenoid at 450 LED run 1 could have prevented damage to the photosynthetic machinery at the higher intensity and allowed an increase in growth rate. Run 2 at 450 µmol m^{-2} s^{-1} did not show overproduction of terpenes, but the growth rate remained the same. Here the rate of photodamage and protection / repair was tolerated and the cells sustained normal function. By run 3 the accumulation of photodamage may have been sufficient to cause a drop in growth rate.

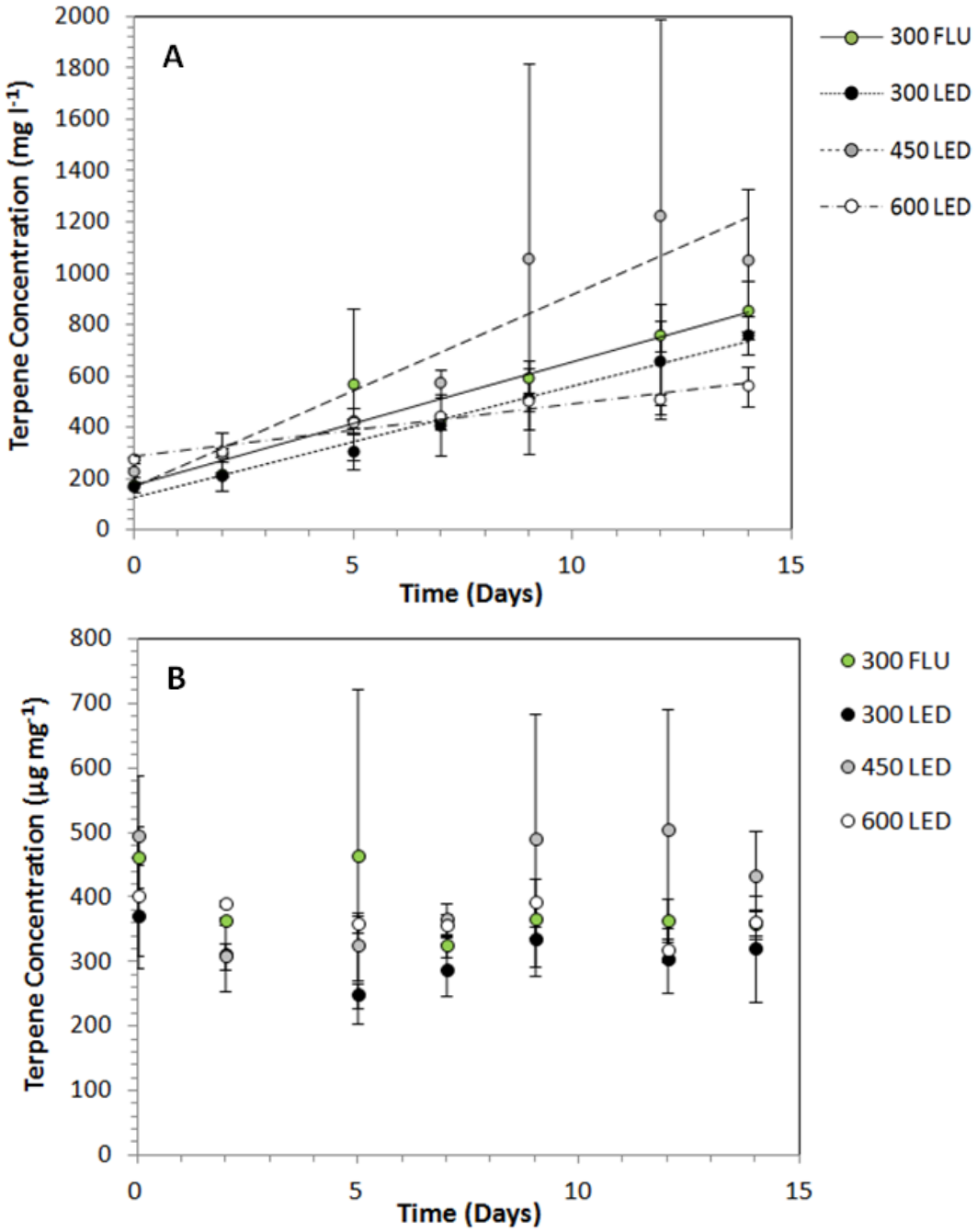

Figure 14 – Terpene content of *B. braunii* over 14 day growth period with illumination provided by 300 FLU, 300 LED, 450 LED and 600 LED.

Panel A: Terpene concentration per unit volume of culture. Panel B: Terpene concentration expressed as μg of terpene per mg of dry cell weight of the microalga. Each data points represent the average of 4, 3, 3 and 2 replicates for 300 FLU, 300 LED, 450 LED and 600 LED respectively with standard error bars shown. No data obtained for 300 LED Run 1. When error bars are not seen, they are masked by the symbol. All light intensities are expressed in μmol m^{-2} s^{-1}.

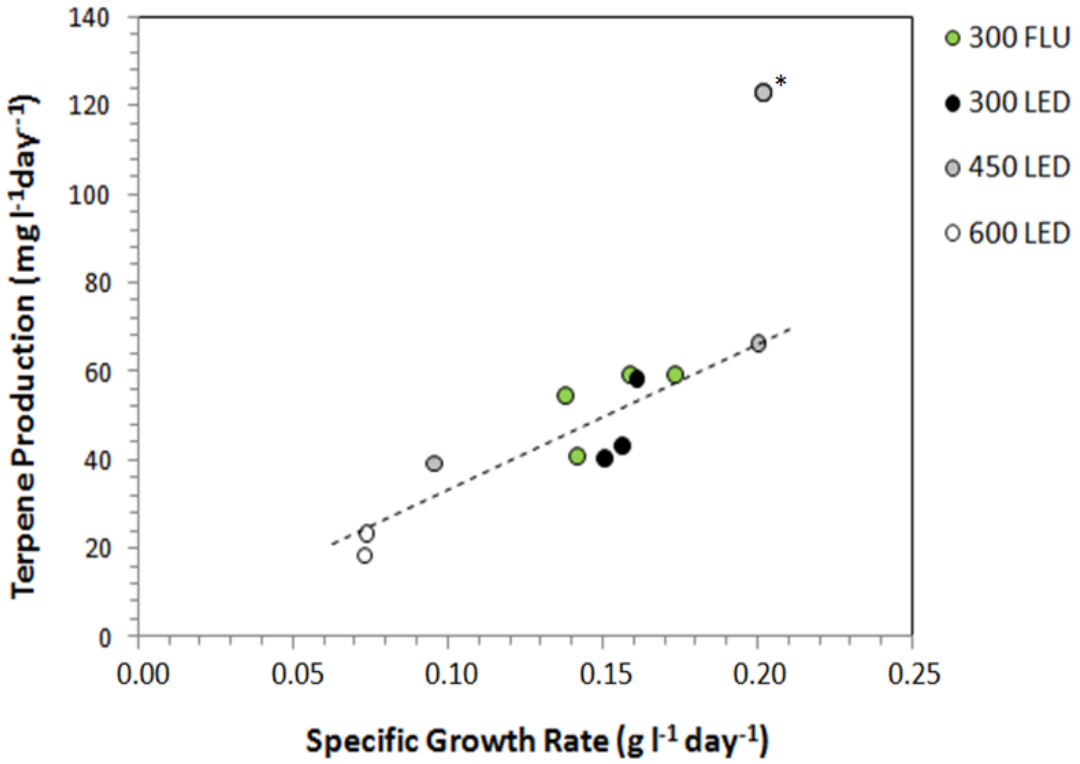

Figure 15 – Specific hydrocarbon production rates plotted as a function of the specific growth rate.

Correlation between specific growth rate and hydrocarbon production rate of *B. braunii* cultured under 300 FLU, 300 LED, 450 LED and 600 LED. Chart shows data for individual runs. Terpene production rate was determined as the slope of the regression line in the linear phase. Early and late data points were excluded to eliminate the effect of the lag and stationary phases. * represents the value for 450 LED Run 1.

3.2.1 Total Extractable Lipid at Day 14

Botryococcus braunii does not simply produce secreted hydrocarbons, but also synthesises different lipids that are not secreted but may be converted to useable biofuels, such as triacylglycerides (TAGs). TAGs do not constitute a dominant class of lipids but occur widely in organisms in which they constitute storage lipids (Metzger *et al*, 1989). The accumulation of neutral lipids by microalgae differs from those regarding the production of terpene.

Extractions were performed using a Dionex ASE 300 Accelerated Solvent Extraction (ASE) with extracts analysed by GC. ASE extractions give an definitive measure of oil content, however, they are labour intensive and time consuming. They also require a larger sample volume. To determine the total lipid content of *B. braunii* at the end of the culture, at least 0.1 g of fresh cell paste would be required, equating to approximately 50 - 200 ml of fresh culture depending on the cell density. The large sample volume would quickly diminish reactor volume below the minimum working level, making it impossible to take in-process measurements and track lipid content over the growth period. Consequently, neutral lipid was only measured on harvested material. With the exception of 600 LED run 1, all standard deviations for the total extractable yield are less than 2 which shows the reproducibility of the method and accuracy of the data (Figure 16, Panel B).

Cells were dewatered by filtration, and therefore secreted hydrocarbons may be lost. However, heptane extraction of the filtrate followed by GC analysis showed lipid loss to the flow-through medium was minimal (< 1%). Alternative dewatering methods such as centrifugation were not feasible due to the high oil content of *B. braunii* which results in the cells remaining in suspension. Freeze drying has often been the laboratory method of choice for processing wet biomass as it is assumed it gives total disruption of cells thereby allowing easier extraction of both intracellular and extracellular lipids. However, a sample volume of up to 50 ml would be required to recover enough material for extraction which would take several days to process, making this approach

impractical. Also, as freeze drying disrupts cells it will only allow for determination of total oil content, again making it unsuitable for this set of experiments.

Once cells had been recovered by filtration, the cell paste was subject to a two stage extraction; heptane for recovery of oil secreted into the extracellular matrix, followed by chloroform:methanol extraction (1:2) for purification of the remaining intracellular lipid. The two stage extraction allowed changes in distribution of intra- and extra-cellular lipid to be identified in addition to the comparison of lipid composition over successive runs at the same intensity and where intensity was increased. All material was treated immediately on the day of harvest to remove the possibility that an increase in yield was caused by cell degradation through natural processes.

The total lipid yield is interchangeably used with neutral lipids yield and is defined as triacylglycerides (TAG's), diacylglycerides (DAG's), monoacylglycerides (MAG'), free fatty acids (FFA's) and sterols. Small amounts of esters and alcohols sometimes observed.

Figure 16, panel A shows the total extractable yield of neutral lipid expressed as a percentage of the DCW for *B. braunii* grown under various illumination conditions. With the exception of cells grown under 300 FLU, the yield of total extractable material increased with irradiance to a maximum of 77 % of the DCW at 450 LED run 2. This was over double that for the lowest yield obtained for 300 LED run 1 at just 36 %. The largest increase in extractable material was 58 % observed between run 1 and 2 with illumination provided by LED at 450 µm m^{-2} s^{-1}. The increase in neutral lipid yield contradicts previous results for terpene production which was growth associated *i.e.* terpene production was constant relative to growth regardless of the illumination condition and is probably due to differences in synthesis and storage mechanisms.

Although the yield dropped to 56 % when the irradiance was increased to 600 LED (600 LED run 1), levels returned to 77 % on run 2. The increase in

extracellular oil yield could be attributed to the lysis of cells due to the effects of photoinhibition (Kojima & Zhang, 1999) allowing the hydrocarbons to be freely to be recovered as extracellular oil during the heptane extraction. Cell lysis at 600 µm m^{-2} s^{-1} was not confirmed by microscopic analysis (Figure 20 Panel B, C and D).

Illumination provided by 300 FLU does not show this trend. Total extractable yield starts at 70 % of the DCW which is nearly as high as that seen at 450 LED run 1, and decreases throughout the successive runs at the same intensity in increments of 13 % to a value of 50 % at run 3. All yields for 300 LED were lower than those observed for 300 FLU. This contradicts results so far with respect to growth rate and specific terpene production rate where 300 FLU and 300 LED have been comparable. The discrepancy could be related to the conditions the inoculum was grown under prior to starting this set of experiments rather than the effect of the illumination type i.e. it was acclimated to previous culture conditions.

Irradiance has no observed effect on the distribution of intra and extra-cellular lipid for all illumination conditions investigated. It remains relatively constant with 70 – 80 % of the lipid being found externally. This is no surprise due to the presence of an extracellular matrix.

An increase in irradiance also seem to have no effect on the composition of extractable material with approximately 40 % of components identifiable as neutral lipid by GC for 300 LED, 450 LED and 600 LED (Figure 16, panel B). This is supported by Kojima & Zhang (1999) who found that the hydrocarbon content of cells grown under low and high irradiance was maintained at around 50 % of DCW. The exception to this is 300 FLU with identifiable components making up an impressive 60 - 70 % of the total extractable yield for runs 1 and 2.

This is supported by Figure 17 which shows the relative amounts of neutral lipid in each of the extracts. Extracellular oil is composed almost entirely of terpenes

for all conditions investigated (Figure 17, panel A). It is worth noting that as a limitation of GC used in the compositional analysis of extracts, terpene elutes in same area of chromatogram as MAG therefore it is impossible to differentiate between the two. However, it assumed that there is very little MAG is present. Small quantities of MAG, DAG, TAG, Sterols and FFA are present but account for less than 10 % of identifiable components. The high levels of terpene is no surprise as it is the one of the main component of the extracellular matrix. Intracellular lipid extracts were compositionally identical (Figure 17, panel B).

The majority of the oil is externally localised which is consistent with findings by Eroglu & Melis (2004) and is either stored within the outer walls or located within the extracellular matrix. Furthermore results are consistent with findings from Wolf *et al*, who estimate that only 7 % of the botryococcene fraction was intracellular and that the remainder was located within the extracellular matrix; Largeau *et al* (1980) state that greater that 95 % of *B. braunii* hydrocarbons are located in the external pool with other classes of lipid are present in noticeable amounts.

300 FLU run 3 gave inconsistent results where the yield of total extractable material remained at 53 % of the DCW, but only 8 % was identifiable by GC. A high yield suggests a successful ASE extraction. Compositionally there was a marked increase in FFA for lipid located both internally and externally of the cell with complete absence of MAG, DAG, TAG and sterols (Figure 17) indicating degradation of the lipid may have occurred. This effect is usually observed as a result of storage or pre-treatment of alga samples, not on fresh harvested material like in this case. Comparable results obtained by GC analysis of lipid extracts from two separate extractions performed on the same material validate the results.

The decrease in total extractable yield, but more so with the drop in identifiable components over runs at 300 FLU could also be due to colony aging rather than the effect of lighting type itself. This has been observed in previous work. In this case the change coincides with a change in lighting type from FLU to LED.

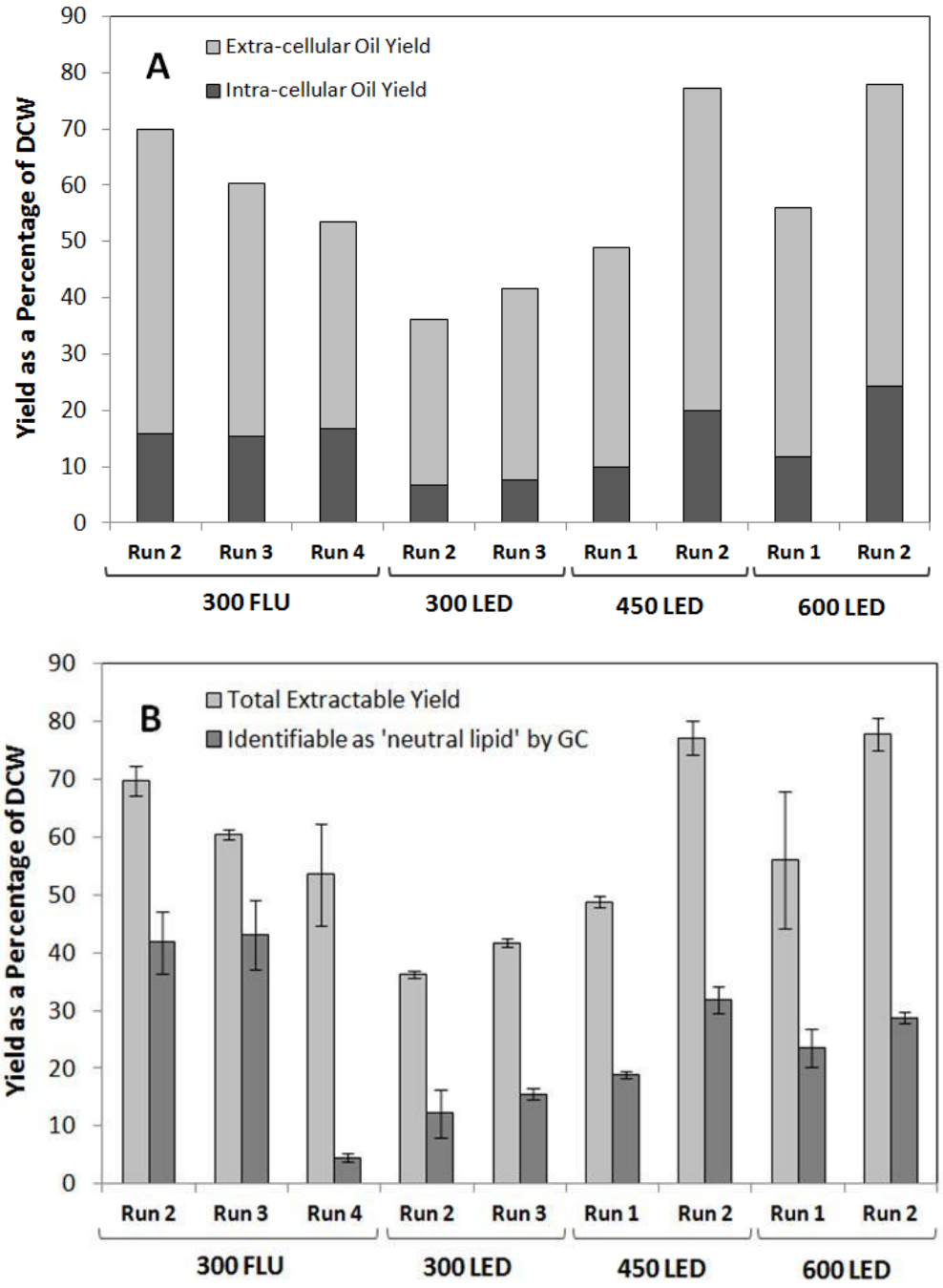

Figure 16 - Lipid yield of *B. braunii*.

Panel A shows the extra- and intracellular lipid as a proportion of the total extractable material. Panel B shows the proportion of the extractable material that was identifiable as neutral lipid by GC. An sequential ASE extraction was performed on harvested *B. braunii* cells with to differentially recover extracellular and intracellular lipids. Neutral lipid is defined as triacylglycerides (TAG's), diacylglycerides (DAG's), monoacylglycerides (MAG'), free fatty acids (FFA's) and sterols. Terpene elutes in same area of chromatogram as MAG so is impossible to differentiate, however, it assumed that there is very little MAG is present. Experiments were run in duplicate, average values reported and error bars are shown (Panel B only). NOTE: No ASE data was obtained for 300 FLU Run 1 and Run 5, 300 LED Run 1 or 450 LED Run 3.

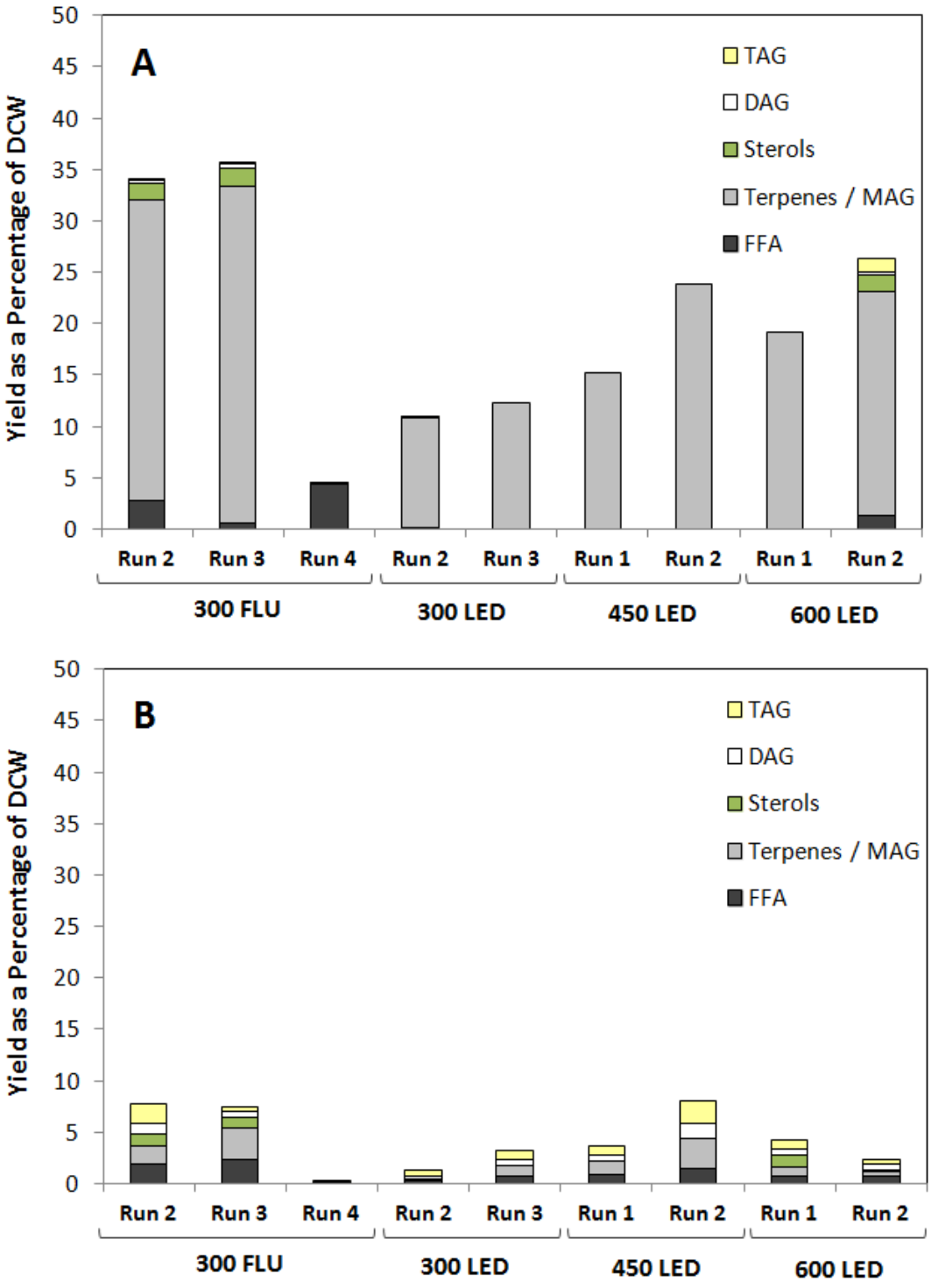

Figure 17 – Neutral lipid and terpene composition of extracellular (A) and intracellular (B) material determined by GC.

Neutral lipid is defined as triacylglycerides (TAG), diacylglycerides (DAG), monoacylglycerides / terpene (MAG), free fatty acid (FFA) and sterols. Experiments were run in duplicate, average values report but error bars are not shown. NOTE: No ASE data was obtained for 300 FLU Run 1 and Run 5, 300 LED Run 1 or 450 LED Run 3.

3.3 Ion and Nutrient Analysis

The concentration of inorganic cation and anions were monitored over the 14 day growth period for *B. braunii* cultured under each illumination condition. The only significant change was observed in the nitrate and phosphate ions as shown in Figure 18. Levels of sodium, potassium, magnesium, chloride and sulphate ions remained constant over the 14 day period, as such they are not included in the figure.

Photobioreactors had an initial nitrate concentration of 240 mg l^{-1}. *B. braunii* cultured under 300 FLU, 300 LED and 450 LED showed a steady decline in nitrate levels over the entire growth period until the nitrate was completely consumed. Much of the nitrate was removed from the media between day 0 and day 12 with uptake rates of 20.36, 22.014 and 18.026 mg l^{-1} day^{-1} for 300 FLU, 300 LED and 450 LED respectively. Rates were determined from the gradient of the trend lines (data not shown). Differences in nitrate usage between 300 FLU, 300 LED or 450 LED were non-significant ($P > 0.05$), therefore illumination type or irradiance does not influence nitrate uptake in these conditions. The exception is 600 LED where there was only a 25 % decrease in media nitrate levels from the initial concentration. Nitrate uptake was calculated at just 12.117 mg l^{-1} day^{-1} which is highly significant ($P < 0.01$) from those obtained from 300 FLU, 300 LED and 450 LED.

Phosphate ions started at a concentration of around 55 - 60 mg l^{-1} and were reduced by around 50 % during the course of each run for 300 FLU, 300 LED and 450 LED. Uptake rates were calculated at 1.3826, 1.1779 and 1.7468 mg l^{-1} day^{-1}. The phosphate uptake rate for 300 LED was lower than the others but only considered significantly different from 300 FLU. There is no reasonable explanation for this difference. A two third reduction in phosphate ions uptake rate was observed with 600 LED to just 0.7244 mg l^{-1} day^{-1}. The difference is significant at the 95 % confidence level from those obtained from 300 FLU ($P = 0.045$) and 450 LED ($P = 0.050$).

The experiment was only run for 14 days so it was unlikely that a deficiency of either nitrate or phosphate would be limiting *B. braunii* growth in the later stages of cultivation. Overall, there was no noticeable difference in the uptake of either nitrate or phosphate ions by *B. braunii* under 300 FLU, 300 LED and 450 LED. Therefore, rate does not appear to be influenced by illumination type or an increase in irradiance. The exception is 600 LED where the rates of nitrate and phosphate assimilation were reduced, possibly due to the effects of photoinhibition on growth.

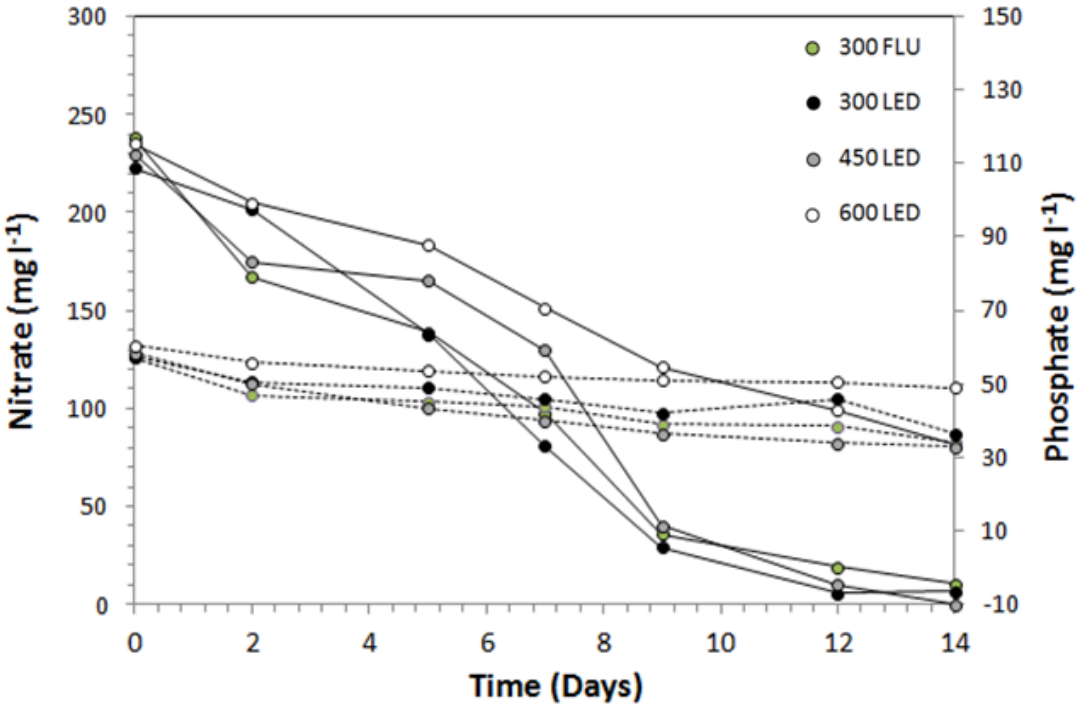

Figure 18 – Concentration of Nitrate (solid line) and phosphate (dashed line) within the photobioreactor over the 14 day growth period of *B*otryococcus *braunii*.

Cation and anion concentrations were tracked over the 14 day growth period of *B. braunii* under all illumination conditions. Each data points represent the average of 3, 3, 2 and 2 replicates for 300 FLU, 300 LED, 450 LED and 600 LED respectively. All light intensities are expressed in µmol m^{-2} s^{-1}.

3.4 Microscopic Analysis of *B. braunii*

3.4.1 Morphology

The morphology of *B. braunii* colonies as well as individual cells were compared over the course of each 14 day run and between illumination condition using differential interference contrast (DIC) microscopy. BODIPY 505/515 staining was used to assess the intracellular and secreted oil content of cells. The general health of the culture was assessed by the presence of damaged or disrupted cells, contamination and debris, cluster sizing (section 3.4.2) and levels of oil secretion. Microscopic analysis also allowed the culture to be examined at a cellular level in terms of membrane integrity and condition of intracellular organelles.

Typically *B. braunii* were pyriform-shaped cells, forming tightly packed colonies with three-dimensional amorphous structure, held together by an extracellular matrix (Figure 19, Panel A and B). Lipophilic matter was confirmed by BIODIPY 505/515 staining which revealed the presence of intracellular oil vacuoles and high quantities of hydrocarbons within the extracellular matrix (Figure 19, Panel C). The internal lipid vacuoles are presumed to be site of botryococcene sequestration (Eroglu & Melis, 2010) and are visually indistinguishable from TAG-containing lipid bodies in other algae (Weiss, 2012). Clusters of cells may be linked by refracting threads, thereby allowing the formation of larger colonies (Figure 19, Panel A). Many of the microscopic images showed droplets of oil budding from the periphery of the colony. This results from the compression of the three dimensional structure during application of the cover slip, causing droplets of extracellular matrix to be squeezed from of the colony (Figure 19, Panel D) (Eroglu & Melis, 2010).

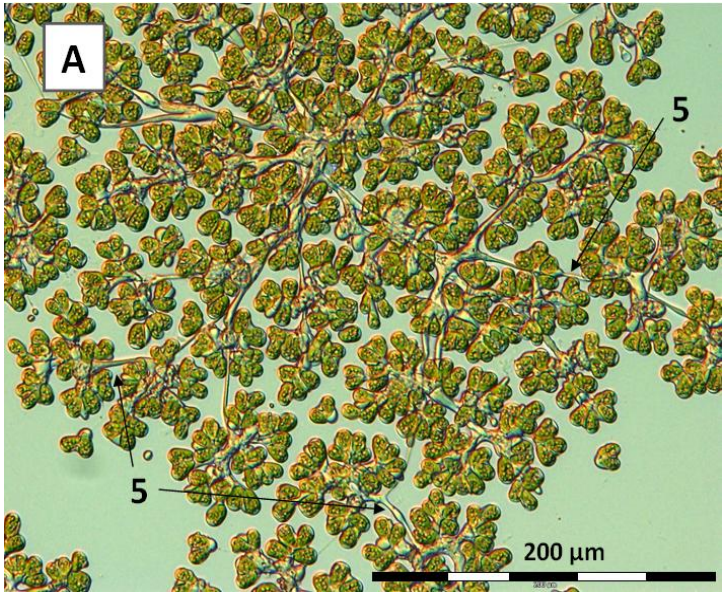

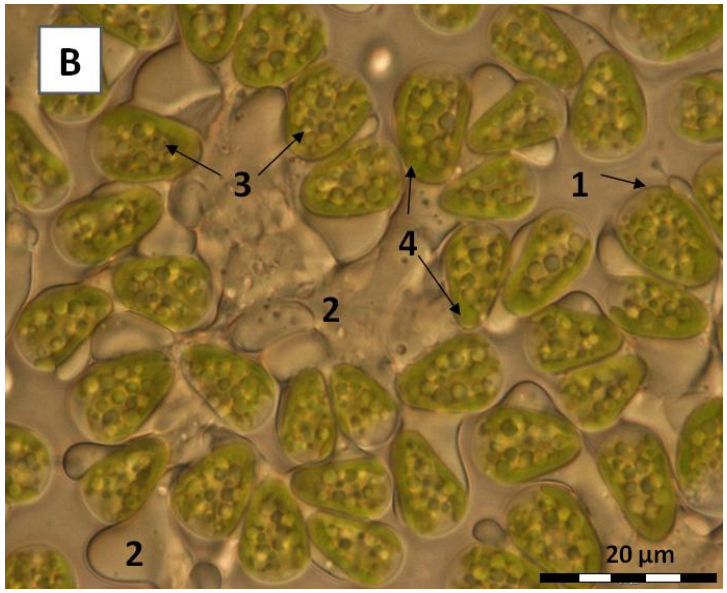

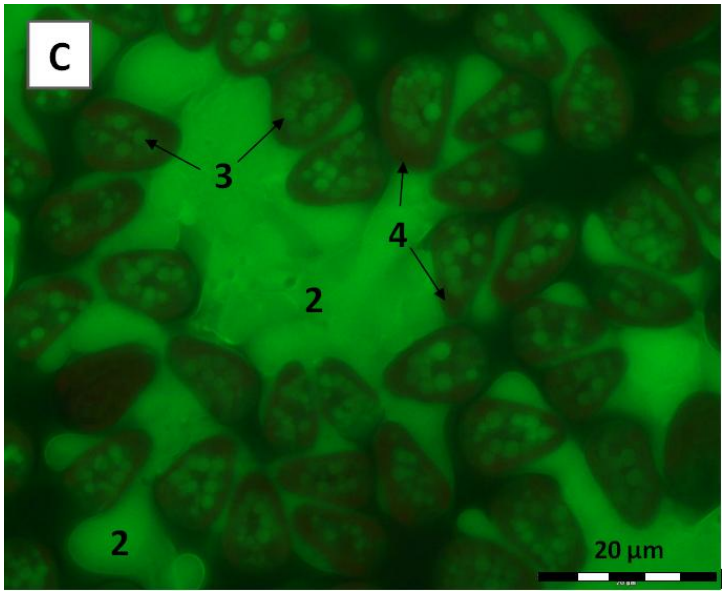

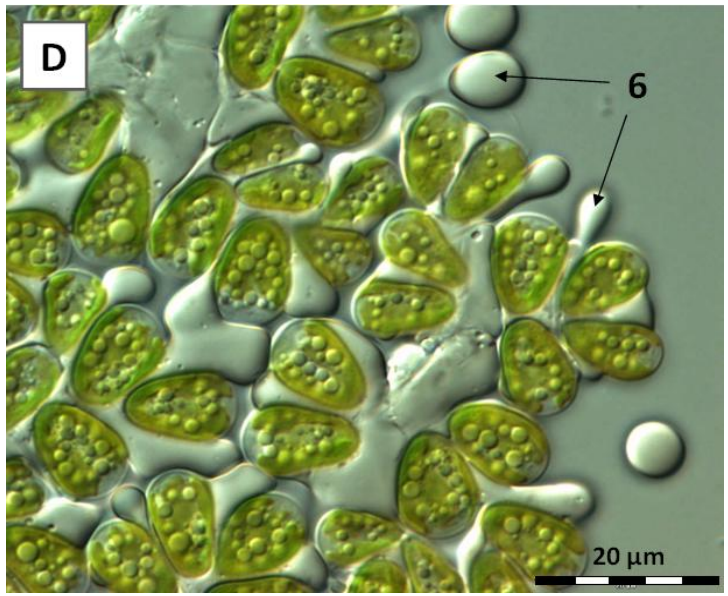

Figure 19 - Microscopic images of a *B. braunii* colony.

Differential Interference Contrast (DIC) microscopy images of a *B. braunii* colony at various magnifications (A x 20 and BCD x 100). The numbers depict the following: (1) individual cell, (2) extracellular matrix, (3) cytoplasmic inclusions (oil vacuoles) (4) chloroplast, (5) refracting threads linking clusters of cells, (6) budding oil droplets.

Panel A - 300 FLU Run 1, Day 5 (x 20) refracting threads linking smaller cluster of cells to form larger colonies;

Panel B - 300 FLU Run 2, Day 14 (x 100), *B. braunii* cells embedded in the extracellular matrix;

Panel C - 300 FLU Run 2, Day 14 (x100), BIODPY staining indicating a high oil content of the extracellular matrix and the location of intracellular oil vacuoles (green fluorescence);

Panel D - 300 FLU Run 2, Day 14 (x 100), oil droplets extruding from the periphery of the colony.

No difference in morphology was observed between *B. braunii* grown under fluorescent bulbs (300 FLU) or warm white LEDs at 300 µm m^{-2} s^{-2} (300 LED). Cells looked healthy, were of uniform size and maintained their pyriform shape in all runs. Intracellular organelles were well defined; individual cells contained 15 - 20 small lipid vacuoles (< 2 µm) and had pronounced chloroplasts which occupied 80 - 90 % of the visible cell area (Figure 19, Panel A and Panel C). High numbers of actively dividing cells were observed on day 14 for all runs at 300 µmol m^{-2} s^{-1} which is consistent with the increases in biomass observed throughout the whole 14 day growth period.

Thick, relatively compact colonies dominated with a median diameter of 17 µm as determined by colony size analysis (section 3.4.2). Regions of single cells and smaller colonies were also present. Day 12 - 14 saw an increase in cluster variation where lacy, open colonies with significant amounts of extra cellular lipid replaced compact clusters. No disrupted cells or debris were identified, there was however low levels of bacterial cells floating free in the media. Contamination levels increases slightly by day 14, but quantities were significantly reduced by 'washing' before cells were recycled and used to inoculate subsequent runs. Contamination was most evident during 300 LED run 1, day 14 where moderate levels of bacteria were present. The subsequent run (300 LED run 2, day 0) showed a significant reduction in contaminant load when examined immediately after inoculation thus support the effectiveness of the washing procedure.

When irradiance was increased to 450 LED µmol m^{-2} s^{-1} (450 LED Run 1) *B. braunii* was characterised by thick, compact clusters with moderate amounts of extracellular lipid. Exceptionally high levels of extracellular lipid were noted at day 12 and 14. Individual cells were of uniform size and shape, had well defined chloroplasts and contained 15 - 20 oil vacuoles. The culture was generally healthy, there were relatively few areas of dead cells with low levels of bacterial contamination of the media at day 3, increasing to moderate levels at day 7. At day 14 bacteria were associated with the media and extracellular matrix. The presence of dividing cells together with a high specific growth rate (SGR) of 0.2021 g l^{-1} d^{-1} (Figure 13) showed that contamination and an increase in irradiance did not appear to have a detrimental effect on the growth of the *B. braunii* in this culture.

Microscopy of cells from subsequent PBR runs at 450 µmol m^{-2} s^{-1} (450 LED Run 2 and Run 3) showed mainly thick, compact colonies and levels of bacterial contamination that were comparable to 450 LED Run 1. For 450 LED Run 2 the overall good health of the culture was confirmed by presence of dividing cells throughout the whole run and a high SGR of 0.2005 g l^{-1} d^{-1} (Figure 13). Individual *B. braunii* cells had intact cell membranes and chloroplasts appeared normal, however there was increased variation in the size of intracellular oil vacuoles with some in excess of 4 - 5 mm in diameter (Figure 20, Panel A). Conversely, 450 LED Run 3 saw a 50 % reduction in SGR. When cells were examined under the microscope there was no obvious reason for such a significant drop in SGR; there was no necrotic or ruptured cells, no increase in bacterial contamination relative to the previous run (450 LED Run 1) and individual cells appeared reasonably healthy. Due to equipment failure microscopic analysis was performed for 450 LED Run 3, but due to a technical error no images are available.

Exposure to 600 µmol m^{-2} s^{-1} saw increased variation in *B. braunii* colony size which was confirmed by colony size analysis (Figure 22). Colonies were mainly large, thick and compact with significant amounts of extracellular material. Moderate levels of bacterial contamination were visible in both 600 LED Run 1 and 600 LED Run 2; 600 LED Run 1, day 9 saw an increase in bacterial contamination associated with the extracellular matrix and surrounding the colony, but this reduced by day 12 and 14. There were only few regions of disrupted cells present. Unlike Wolf *et al* (1985), no change in colony colour was observed in response to high light intensities where the increase in carotenoid/chlorophyll ratio resulted in orange colonies.

Individual *B. braunii* cells grown at an irradiance of 600 µm m^{-2} s^{-1} appeared reasonably healthy and most had well defined chloroplasts. Cells were however irregular in sizes and shape and contained enlarged oil vacuoles similar to 450 LED Run 2 (day 14). A small number of cells had completely lost definition of their internal organelles while their outer membrane remained intact (Figure 20 Panel B). Where cells were embedded in the extracellular matrix, they had lost their pyriform shape (Figure 20 Panel B). Finally, it looked as if the *B. braunii* cells had undergone abnormal cells division where two cells were contained within an outer membrane, with uneven distribution of cytoplasmic organelles (Figure 20 Panel B and Panel C).

Even though cells grown under 600 µm m^{-2} s^{-1} appeared healthy, they were not viable which was confirmed a very low SGR of 0.0735 g l^{-1} d^{-1} (Figure 13). A possible explanation for the observed is the effect of photoinhibition and the progressive accumulation of irreparable photodamage.

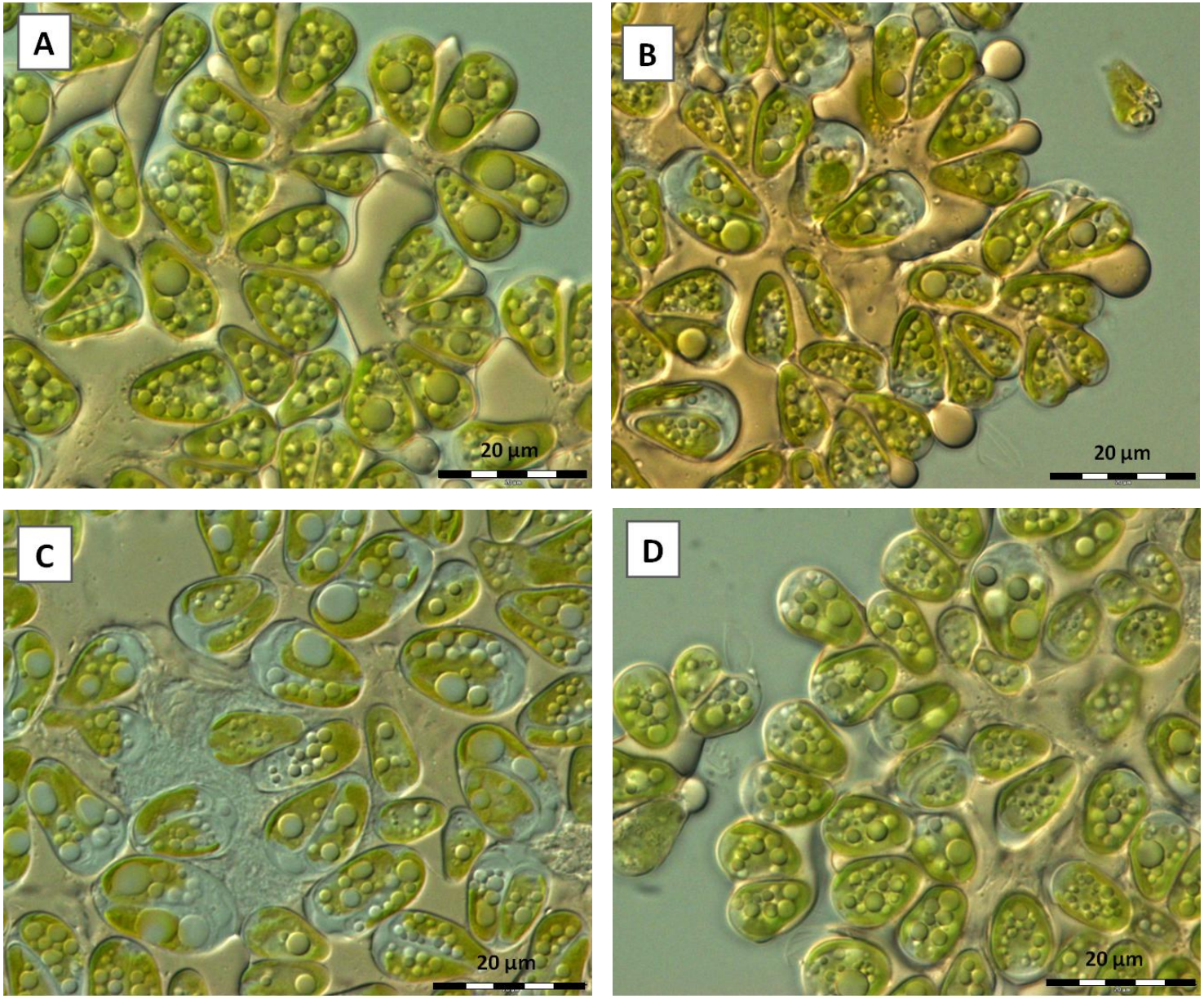

Figure 20 - Microscopic images of a partial B. braunii colony.

Differential Interference Contrast (DIC) microscopy images of a *B. braunii* colony at various magnifications (x 20 and x 100).

Panel A - 450 LED Run 2, Day 9 (x 100). *B. braunii* cells embedded in the extracellular matrix. Substantial amount of extracellular oil within the colony. Actively dividing cells and large oil vacuoles present.

Panel B - 600 LED Run 1, Day 0 (x 100).

Panel C - 600 LED Run 1, Day 14 (x 100) loss of chloroplasts;

Panel D - 600 LED Run 2, Day 14 (x 100)

3.4.2 Colony Size

Analysis of colony size was performed for *B. braunii* cells grown under each lighting condition. No data was obtained for the 300 LED run 3. The imaging process was automated allowing more than 30 screen shots to be analysed for each sample. Although this produced a substantial sample size of between 800 and 10000, not all of the data was useful as it took each and every cluster into account. To eliminate the effect of particulates and contaminants clusters of less than 10 µm were ignored.

The colony size distribution of the raw data was asymmetric and positively skewed with huge variation in 75^{th} percentile (Figure 21). Due to deleterious effect on accuracy and inflated error the data was truncated to include only the top 95 % of values. The top 5% of measurements were considered outliers. This assumption significantly reduced the spread of the data, enabling more accurate conclusions to be drawn from the images; cultures illuminated with 300 FLU saw a 10 fold reduction in maximum colony size from 887.2724 µm to 90.5006 µm; a 70 % drop from 120.4252 µm to 35.3581 µm was seen for 300 LED; finally the maximum colony size for 450 and 600 LED was reduced to one third of the original value.

It is possible that outliers came from inherent variability in colony size rather than errors in measurement including those from sampling error and standardisation failure. A sample could have been inadvertently drawn from a different population than the rest of the sample depending on how randomised the method was for taking a screenshot. Other factors include the time the culture was left standing between sampling and analysis, whether the culture was agitated prior to taking a sample for microscopy. Both of these conditions allow time for *B. braunii* cells to change their distribution within the sample; healthy, oil rich cells will float to the surface; healthy intact colonies will remain in suspension and ‘sick’ colonies will sink.

The median represents the location of the main body of data better the mean in asymmetric distributions or where outliers are present. Colony size distribution is of *B. braunii* is therefore displayed as a box plot diagram (Figure 22).

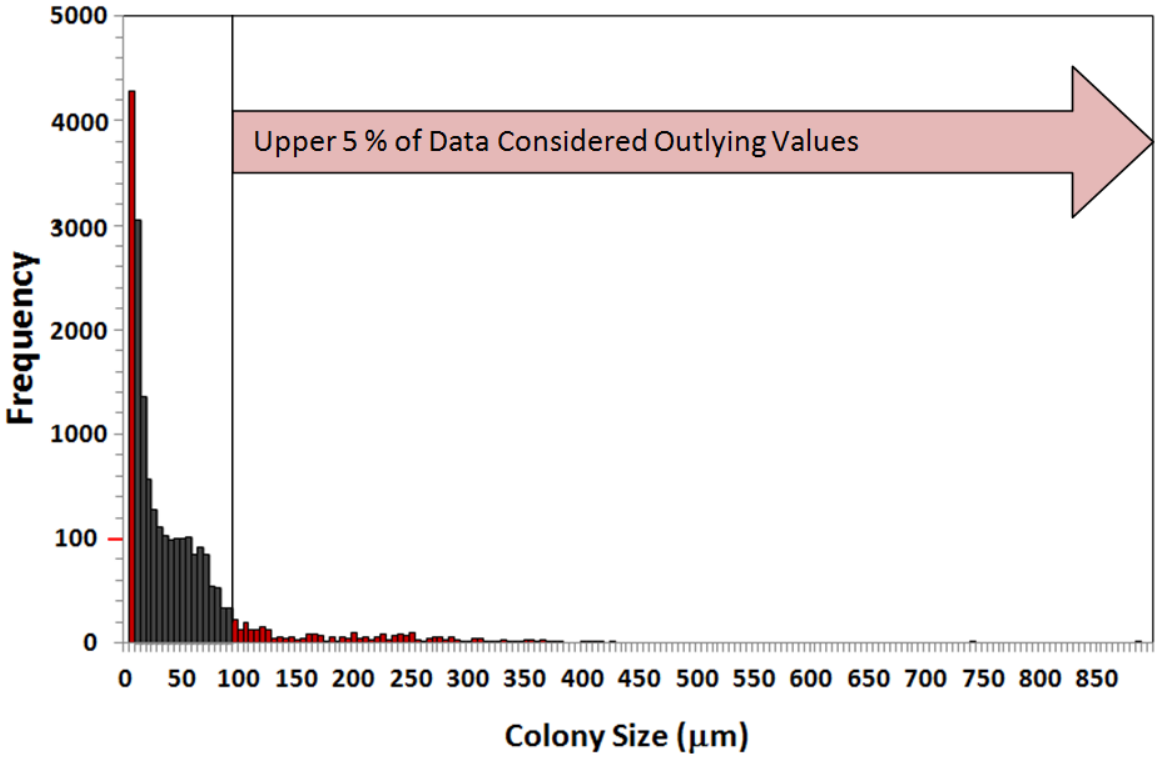

Figure 21 - Frequency diagram showing the colony size distribution of *B. braunii* grown at 300 µmol m^{-2} s^{-1} with illumination provided by fluorescent lighting (300 FLU Run 1).

Cluster size analysis for 300 FLU Run 1 produced a sample size of 11'361 values. Clusters of less than 10 µm were ignored to eliminate the effect of particulates and the effect of outliers was reduced by truncating the data at 95 % of values (accounting for 4380 and 324 data points respectively). Clusters were grouped into intervals of 5 µm. The grey bars identify values which were used in the analysis of colony size. Excluded data is shown by the red bars.

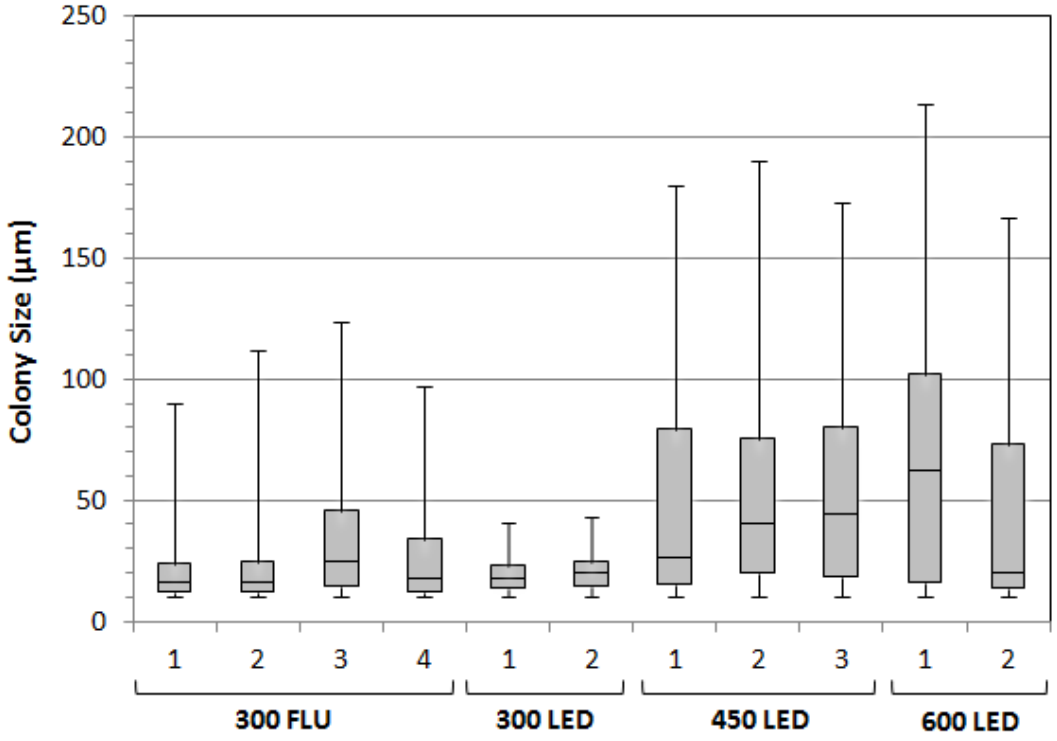

Figure 22 – Box plot to demonstrate the colony size distribution of *B. braunii* grown under each illumination condition.

Box plot diagram illustrating the colony size distribution of *B. braunii* cultured in 300 FLU, 300 LED, 450 LED and 600 LED. Data is shown for individual PBR runs. Boundaries of the box are 25th and 75th percentiles and whiskers (error bars) are clusters greater than 10 µm (lower) and 95th percentiles (upper).

The median colony size for 300 FLU and 300 FLU were approximately 17 µm when the data for each run at each lighting condition was taken into account. The maximum colony size for 300 LED measured one third of the value for 300 FLU (35.3581 and 90.5056 µm respectively). In addition, *B. braunii* cultured under 300 FLU shows greater variability in colony size than those under 300 LED. The semi-interquartile range for 300 LED is 25 % less than that seen with fluorescent lighting at 4.6524 and 6.2991 µm. This means that 50 % of the data value falls within a 10 µm range for 300 LED, 15 µm for 300 FLU. Moreover, within the 75 % percentile, LED illumination resulted in more consistent results than fluorescent light, *i.e.* a reduced spread in colony size. Consequently, illumination provided by LEDs appears to be a more stable light source that fluorescent bulbs.

A comparison between all illumination conditions revealed that the median colony size increased with irradiance. *B. braunii* grown under 450 LED had a median of 33 µm, almost double that for 300 µmol m^{-2} s^{-1}. Unlike 300 µmol m^{-2} s^{-1} consecutive runs demonstrated a change in the median; there was a 33 % increase in colony size from 24.2131 µm in 450 LED run 1 to 40.4508 µm in run 3. Furthermore, the first run at 600 µmol m^{-2} s^{-1} showed a further 50 % increase in the median to almost 60 µm. Data from 600 LED run 2 was excluded as it did not show the same trend; a 3 fold reduction in the median was observed due to the effects of photoinhibition.

When looking at the distribution of data it is more accurate to say a higher irradiance gives rise to a greater range of colony size with a shift in the median value (Figure 22). The majority of variation occurs within the 75 % percentile for all illumination conditions. This is variation in the top 25 % of data only. The lower quartile shows the lowest degree of variation due to elimination of particles less than 10 µm in length.

Despite the shift in median value, consecutive runs at 450 LED display similar spreads. Each had a semi-interquartile range of around 24 µm with colonies ranging from 17 to 65 µm in length.

3.5 Chlorophyll measured by Spectroscopy

The Chlorophyll a (Chl a) and Chlorophyll b (Chl b) content of *B. braunii* was quantified by UV-VIS spectroscopy. Measurements were taken throughout the 14 day growth period for each illumination condition. Chl a and Chl b absorb in overlapping spectral regions with absorption maxima (λ_{max}) of 665 and 650 nm (Figure 23). Cells were recovered by vacuum filtration onto a glass fibre filter and the intracellular chlorophyll extracted by sonication with methanol. Samples were cleaned-up by centrifugation and the absorbance read at the absorption maxima as above. The concentration of Chl a and Chl b was calculated using specific absorption coefficients as provided by Becker (1994).

The Chl a, Chl b and total chlorophyll content was normalised to DCW and expressed as µg of chlorophyll per mg of dry algal biomass (Figure 24 and Figure 25). Measurements were made on five, three, three and two replicates for 300 FLU, 300 LED, 450 LED and 600 LED respectively (from different cultures) and the results expressed as means and standard errors. A two way ANOVA was performed to determine the significance of changes in total chlorophyll, Chl a and Chl b concentrations of *B. braunii* grown under the different illumination conditions. The effect of time on the concentration of each chlorophyll was also analysed by means of a student t-test. All conclusions are based on a level of significance of at least 5% ($P < 0.05$).

Figure 24 shows the relationship between the total chlorophyll content of *B. braunii* and time for the four illumination conditions investigated. In a two way analysis of variance, irradiance had a significant effect on the total chlorophyll content of *B. braunii* ($P < 0.0001$ for illumination condition effect, $P = 0.0005$ for the effect of time). There is a statistically significant interaction between these two independent factors.

Changes in the content of the individual chlorophylls (Chl a and Chl b) were also measured for each illumination condition over the growth period (Figure 25). ANOVA analysis showed both irradiance and/or lighting type and

cultivation period to have a significant or extremely significant effect on the Chl a and Chl b content of *B. braunii* (chlorophyll a, $P < 0.0001$ for illumination condition effect, $P = 0.0134$ for the time effect; chlorophyll b, $P < 0.001$ for illumination condition effect and $P = 0.005$ for time). This significance mirrors that of the total chlorophyll content, however, there is no interaction between the two factors. The differences in Chl a, Chl b and total chlorophyll content of *B. braunii* grown in each illumination condition and their associated significance levels are shown in Table 6.

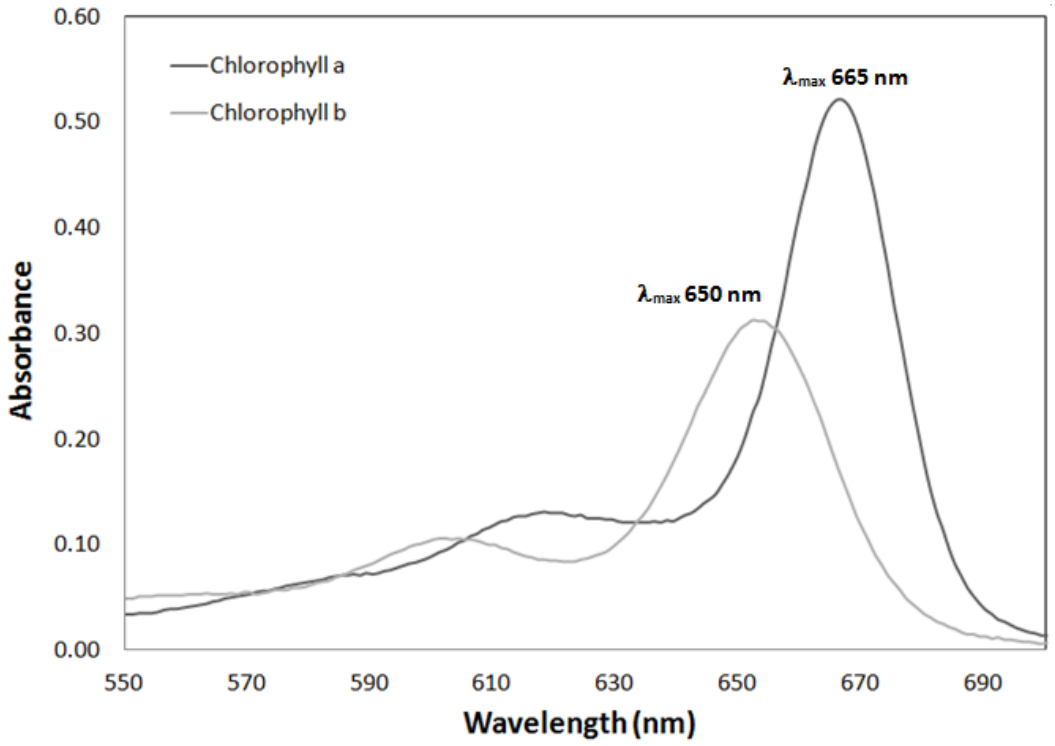

Figure 23 - Absorbance spectra of Chlorophyll a and Chlorophyll b in methanol.

Absorbance spectra of chlorophyll a and b for spinach in HPLC grade methanol(Sigma P/N C5753 and C5878). Both compounds were measured at a concentration of 8 mg l^{-1}. Results are shown between 550 and 700 nm only. The absorption maxima (λ_{max}) for each pigment is was is shown.

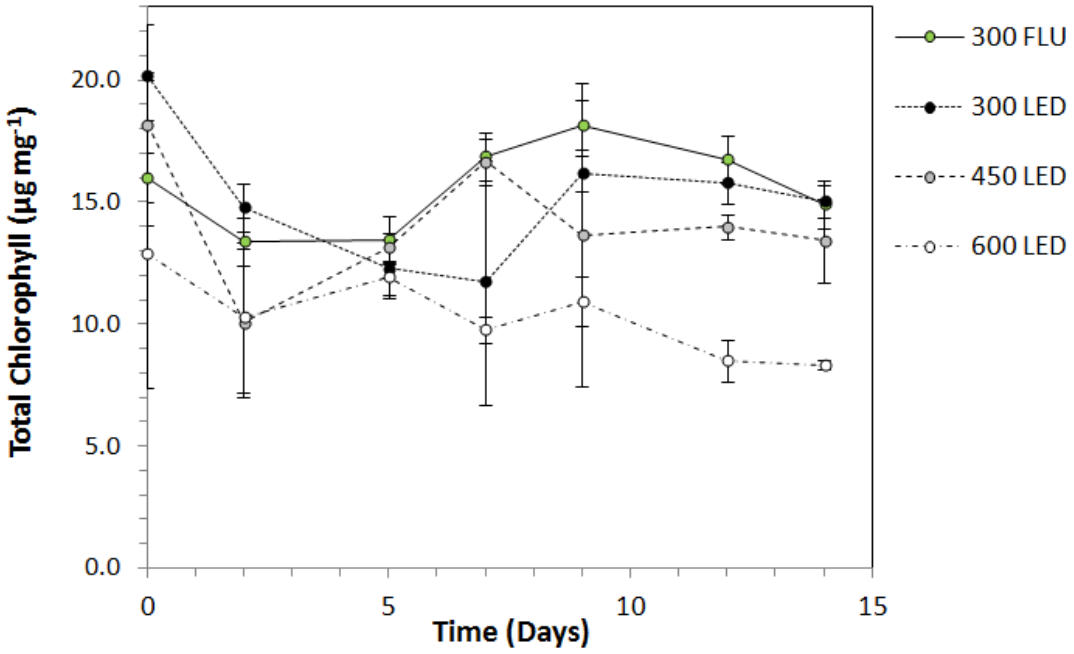

Figure 24 - Changes in the total chlorophyll content of *B. braunii* as determined by UV-VIS spectroscopy, over a run time of 14 days.

B. braunii was grown for 14 days using LED lighting systems at 300, 450 and 600 µmol m^{-2} s^{-1} and fluorescent systems at 300 for comparison of light quality. Pigments were measured by UV-VIS Spectrophotometric. Results are expressed as µg of pigment per mg of dry cell weight (DCW). Each data points represent the average of 5, 3, 3 and 2 replicates for 300 FLU, 300 LED, 450 LED and 600 LED respectively with standard error bars shown. When error bars are not seen, they are masked by the symbol. Trend lines show the relationship for each series.

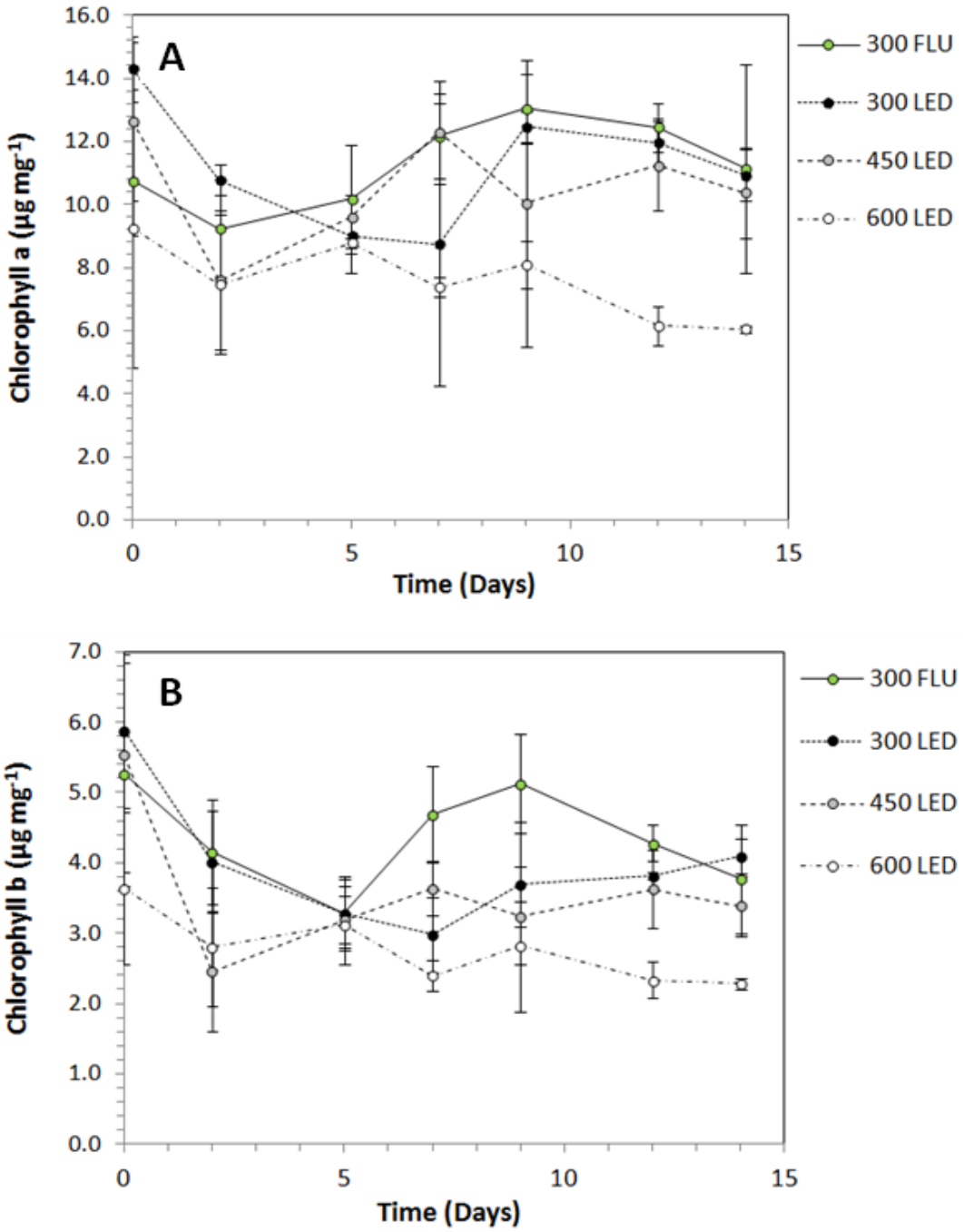

Figure 25 - Changes in chlorophyll a and b content of *B. braunii* over a run time of 14 days shown in charts A and B respectively.

B. braunii was grown for 14 days using LED lighting systems at 300, 450 and 600 µmol m^{-2} s^{-1} and fluorescent systems at 300 for comparison of light quality. Pigments were measured by UV-VIS Spectrophotometric. Results are expressed as µg of pigment per mg of dry cell weight (DCW). Each data points represent the average of 5, 3, 3 and 2 replicates for 300 FLU, 300 LED, 450 LED and 600 LED respectively with standard error bars shown. When error bars are not seen, they are masked by the symbol. Trend lines show the relationship for each series.

Typically, *B. braunii* cultured under 300 LED had the highest Chl a, Chl b and total chlorophyll content of all illumination conditions investigated. There were however no significant quantitative change in pigment composition between 300 FLU and 300 LED at any of the time points ($P > 0.05$) (Table 6). This probably result from the similarity in spectral data from both fluorescent and LED lighting systems (Figure 12). Differences in all chlorophyll measurements for 300 LED and 450 LED were also considered non-significant at the 95 % confidence level.

Significant changes in chlorophyll content were only observed between extremes of irradiance, with cultures grown at 300 FLU and 600 LED showing the largest difference. Looking only at total chlorophyll content, differences between 300 FLU and 600 LED were highly significant at days 7, 9 and 12 ($P < 0.01$) and significant at day 14 ($P < 0.05$). The changes in total chlorophyll was lesser between 300 FLU and 600 LED where days 0, 12 and 14 were considered different at the 95 % confidence level ($P < 0.05$). An increase in irradiance from 450 LED to 600 LED only showed a significant difference in measured total chlorophyll value at day 7 ($P < 0.05$). The same effect can be observed for chlorophyll a and chlorophyll b (Table 6). Generally, as the difference between irradiance decreased, the change in measured chlorophyll (Chl a, Chl b and total chlorophyll) became less noticeable.

A high Chl a, Chl b and total chlorophyll content were observed at day 0 for *B. braunii* grown in 300 FLU, 300 LED and 450 LED, when the sample was taken immediately after inoculation (Figure 24 and Figure 25). It is assumed these changes are caused during inoculum preparation and the recycling of cell between runs. During harvest, cells are removed from a stable illuminated environment, subject to centrifugation and washing and then stored in a flask until inoculation. In this process, cells are concentrated from 7000 ml to 200 ml to produce the seed for the next experiment (OD > 20 (Ab_{680})) and become light limited due to reduced light availability and self shading. Although the time cells were taken out of the reactor was minimised at 3 and 4 hours, the competition for light could causes a short-term increase in chlorophyll concentration.

With the exception of 600 LED, there was a 40 % drop in initial Chl a and Chl b concentrations when light was abundant and the cell density low (Figure 25 A and B). This may be attributed to the acclimation of the cells to the new lighting regime, in relation to adjustment of antenna size and a reduction in the number of chlorophyll molecules. This effect was observed at day 5 for cultures illuminated by 300 LED. The means were compared using a student's t-test and found to be highly significant for chlorophyll a ($P = 0.002$) and significant at the 95 % confidence level for chlorophyll b ($P = 0.03$). At 450 LED the decrease occurred at day 2; the decline in Chl a was considered non-significant ($P > 0.05$), however, the drop in Chl b concentration was highly significant ($P = 0.002$). Although 300 FLU showed the typical 40 % reduction in Chl b value at day 5, there was only a 15 % decrease in Chl a at day 2. The means were found to be non-significantly different at the 95 % confidence level (Chl a: $P = 0.30$; Chl b: $P = 0.09$).

Despite initial decrease in Chl a, no other time points for 300 FLU, 300 LED or 450 LED showed a significant change in pigment levels ($P > 0.05$). Similarly, no time points showed a significant change in chlorophyll b at the intensity of 450 µmol m^{-2} s^{-1} (LED) ($P > 0.05$). Contrary to this the average chlorophyll b content of *B. braunii* grown at 300 FLU saw an increase back to initial levels by day 9. The increase in chlorophyll b content was considered highly significant at the 99 % confidence level ($P = 0.003$). A maximum of 5.126 ± SD 1.112 µg mg of DCW was reached before levels declined at days 12 and 14 ($P < 0.05$). The Chl b content of *B. braunii* grown under 300 LED steadily increased over the entire growth period to a maximum value of 4.096 ± SD 0.241 µg mg of DCW on day 14. A significant increase in chlorophyll b concentration was observed between day 7 and day 9 ($P = 0.049$). The lower cellular concentrations chlorophyll a, an accessory pigment, may be the reason why changes are not as evident as with chlorophyll b, the major light harvesting pigment.

Although there were fluctuations in the Chl a and Chl b content of *B. braunii* cells grown at 600 LED, the overall trend was a decline in levels over the 14 day

growth period. A t-test was used to compare values between time points and they were all found to be non-significant ($P > 0.05$). Taking the same time point into consideration, the Chl a and Chl b measurements were 40 % lower than the maximum values achieved under both 300 µmol m^{-2} s^{-1} and 450 LED. The reduction at 600 LED is most likely to be due to the effects of photoinhibition.

Eroglu & Melis (2010) found spectrophotometric quantification of extracellular hydrocarbons yielded comparable results, however in this study there is huge variability between repeat measurement. This is probably attributed to do differences in the extraction procedure. Whereas Eroglu & Melis vortexed the culture with glass beads in the presence of heptane, in this study the culture was sonicated in the presence of heptane. The glass beads are reported to result in extensive loosening of the normally tightly packed cells and a substantial release of botryococcenes from the extracellular matrix without compromising cell integrity.

TOTAL CHLOROPHYLL			
Irradiance ($\mu mol\ m^{-2}\ s^{-1}$)	**300 LED**	**450 LED**	**600 LED**
300 FLU	**NS**	**NS**	**S (P < 0.05) = 14 HS (P < 0.01) = 7, 9, 12**
300 LED		**NS**	**S (P < 0.05) = 0, 12, 14**
450 LED			**S (P < 0.05) = 7**
CHLOROPHYLL A			
Irradiance ($\mu mol\ m^{-2}\ s^{-1}$)	**300 LED**	**450 LED**	**600 LED**
300 FLU	**NS**	**NS**	**S (P < 0.05) = 7, 9, 14 HS (P < 0.01) = 12**
300 LED		**NS**	**S (P < 0.05) = 0, 12**
450 LED			**S (P < 0.05) = 12**
CHLOROPHYLL B			
Irradiance ($\mu mol\ m^{-2}\ s^{-1}$)	**300 LED**	**450 LED**	**600 LED**
300 FLU	**NS**	**S (P < 0.05) = 2, 9**	**S (P < 0.05) = 12 HS (P < 0.01) = 7, 9**
300 LED		**NS**	**S (P < 0.05) = 0**
450 LED			**NS**

Table 6 – A two way ANOVA demonstrating the significance (P value) of changes in total chlorophyll, Chl a and Chl b content of *B. braunii* grown at four illumination conditions and at all time points investigated.

A two way ANOVA was performed to determine the significance of changes in total chlorophyll, Chl a and Chl b content of *B. braunii* between each illumination condition (300 FLU, 300 LED, 450 LED and 600 LED) at all time points investigated. Differences between data sets are considered NS – Non Significant (P > 0.05); S – Significant (P < 0.05) or HS – Highly significant (P < 0.01) at the days listed.

Like many other photosynthetic organisms *B. braunii* can modify the components of photosynthetic membranes in accordance with environmental conditions. Table 7 shows the chlorophyll a to chlorophyll b ratio (Chl a:b) for each time point over the 14 day growth period and for each illumination condition investigated. In all cases chlorophyll a is the major pigment and chlorophyll b as an accessory pigment. This finding is consistent with the literature (Lee, 2008; Lichtenthaler, 1987).

Typically, there was an increase in the weight ratio of Chl a to Chl b after exposure to increasing irradiance. The lowest Chl a:b ratio was obtained from cells grown at 300 FLU with a range of 2.16 to 3.15 and average of 2.658 over the whole growth period. Illumination provided by 300 LED was nearly 8 % higher at 2.52 to 2.38 with an average of 2.863. The highest ratio was observed in cells cultured under 450 LED with ratios in the range of 2.35 to 3.36 and average of 3.017. This was a 5 % increase on those observed with 300 LED. Despite showing signs of photoinhibition 600 LED demonstrated a ratio of similar range at 2.47 to 3.10 with a run average of 2.749.

In a two way analysis of variance there were no significant change in Chl a:b ratio between all illumination conditions at any of the time points investigated ($P > 0.05$) (Table 8). Furthermore, differences in the Chl a:b ratio were compared between sampling points for individual runs using a student's t-test, and found to be non-significant at the 95 % confidence level ($P > 0.05$). Regardless of differences in the Chlorophyll to DCW ratio all illumination conditions had similar Chl a:b ratio which suggests similar organisation of their photochemical apparatus.

Day	Chlorophyll a:b Ratio			
	300 FLU	300 LED	450 LED	600 LED
0	2.160 ± 0.632	2.515 ± 0.656	2.354 ± 0.370	2.467 ± 0.481
2	2.251 ± 0.363	2.738 ± 0.449	3.150 ± 0.271	2.669 ± 0.019
5	3.150 ± 0.655	2.794 ± 0.618	3.041 ± 0.528	2.864 ± 0.454
7	2.613 ± 0.252	2.805 ± 1.123	3.364 ± 0.130	3.089 ± 0.165
9	2.589 ± 0.482	3.377 ± 0.091	3.049 ± 0.171	2.864 ± 0.004
12	2.917 ± 0.256	3.134 ± 0.156	3.101 ± 0.091	2.642 ± 0.023
14	2.926 ± 0.441	2.678 ± 0.340	3.058 ± 0.123	2.649 ± 0.043

Table 7 - Weight ratio of chlorophyll a to chlorophyll b (a:b ratio) of *B. braunii* grown under various illumination conditions.

B. braunii was grown for 14 days using LED lighting systems at 300, 450 and 600 µmol m^{-2} s^{-1} and fluorescent systems at 300 for comparison of light quality. Each data points represent the average of 5, 3, 3 and 2 replicates for 300 FLU, 300 LED, 450 LED and 600 LED respectively. Pigments were measured using UV-VIS Spectrophotometric. All weight ratios given in the table are for Chl b, Chl a is always 1.

Irradiance (µmol m^{-2} s^{-1})	300 LED	450 LED	600 LED
300 FLU	**NS**	**NS**	**NS**
300 LED		**NS**	**NS**
450 LED			**NS**

Table 8 - A two way ANOVA determining the significance of changes in the Chlorophyll a:b ratio of *B. braunii* grown under different illumination.

A two way ANOVA was performed to determine the significance of changes in total chlorophyll, Chl a and Chl b content of *B. braunii* between each illumination condition (300 FLU, 300 LED, 450 LED and 600 LED) at all time points investigated. Differences between data sets are considered NS – Non Significant ($P > 0.05$); S – Significant ($P < 0.05$) or HS – Highly significant ($P < 0.01$) at the days listed.

3.5.1 Photosynthetic Pigments by HPLC

B. braunii is reported to contain chlorophyll a, chlorophyll b, β-carotene, antheraxanthin, zeaxanthin, violaxanthin, lutein and neoxanthin (Zigman *et al*, 2012). The change in pigment composition of *B. braunii* was followed over a period of 14 days, for three illumination conditions; 300 LED, 450 LED and 600 LED. Figure 26 shows a typical chromatogram of pigments extracted from *B. braunii* obtained from 450 LED run 2 (Day 7). Four main liposoluble pigments were identified: Chlorophyll a, chlorophyll b, zeaxanthin and β-carotene. However none of the other xanthophyll pigments were found in the extracts. The β-carotene and zeaxanthin content of *B. braunii* was normalised to DCW and expressed as µg of pigment per mg of dry algal biomass (Figure 28). The results were also expressed as pigment to chlorophyll a ratio with means and standard deviations (Figure 27 and Figure 29). No HPLC data was obtained from 300 FLU due to insufficient sample available for pigment extraction.

Many of the results obtained were at or below the detection limit for HPLC due to small sample size and low pigment concentrations within the extract. These samples were therefore omitted from the subsequent analyses. Where possible, a two way ANOVA was performed to determine the significance of changes in zeaxanthin and β-carotene concentrations as well as the pigment ratios (relative to Chl a) of *B. braunii* grown under the different illumination conditions. The effect of time on the concentration of each type of chlorophyll was also analysed by means of a student t-test. All conclusions are based on a level of significance of at least 5% ($P < 0.05$).

In agreement with spectroscopy data, pigments measured by HPLC identified chlorophyll a as the major photosynthetic pigment and chlorophyll b as an accessory pigment. Figure 27 shows changes in the chlorophyll a:b ratio of *B. braunii* cultured at 300 LED, 450 LED and 600 LED over the 14 day growth period. Taking all data points for each level of irradiance into consideration, the average weight ratio of Chl a-to-Chl b for 300 LED was 1.0904 ± 0.0969. The highest Chl a:b ratio was observed in cells cultured at 450 LED with an average

of 1.3147 ± 0.1819. This represented a 20 % increase in weight ratio of Chl a-to-Chl b than was observed at 300 LED. The lowest Chl a:b ratio was obtained from cells grown at 600 LED with an average of 1.0451 ± 0.1838 over the whole growth period. This was a 25 % decrease in ratio compared to 450 LED.

In a two way analysis of variance, exposure of cells to increasing irradiance (300 µm m^{-2} s^{-1} to 450 µm m^{-2} s^{-1}) resulted in a significant increase in the Chl a:b ratio ($P > 0.05$) (Table 8). However, as irradiance was increased from 450 to 600 µm m^{-2} s^{-1} there was a decrease in the Chl a:b ratio ($P > 0.05$) which may be attributable to the effects of photoinhibition (Table 8). With the exception of day 0 and day 2, there was no significant difference in the Chl a:b ratio of *B. braunii* grown at 300 LED or 600 LED ($P > 0.05$).

The differences in Chl a:b ratio were compared within each light intensity using the student's t-test. *B. braunii* grown at 300 LED showed a decline in Chl a:b ratio throughout the growth period; these were however non-significant ($P > 0.05$). A high initial Chl a:b ratio was observed for both 450 LED and 600 LED, but this dropped by 25 % at day 2 for cultures grown at 450 LED ($P < 0.05$) and 45 % for cultures grown at 600 LED ($P < 0.01$). Although the Chl a:b ratio was unaffected when pigments were quantified by spectroscopy, there was an increase in starting concentration of pigment for all runs which was thought to be as a result of the washing procedure and subsequent enrichment with young colonies at the start of each run. Irrespective of the initial drop in Chl a:b ratio, it increased again as the culture matured. This increase could be due to acclimation of the cells to high light conditions where the amount of accessory pigments relative to Chl a within the light harvesting antenna are reduced in order to limit the excessive absorption of photons. The increase was found to be non-significant at any time point investigated ($P > 0.05$).

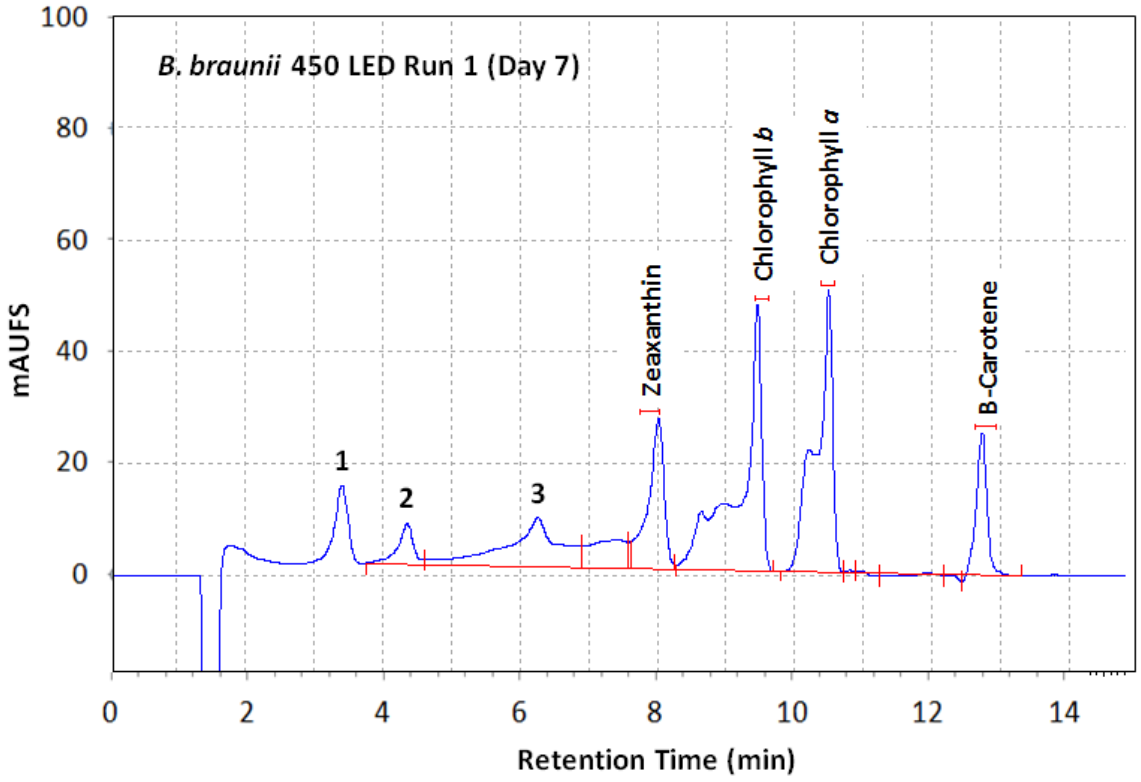

Figure 26 – HPLC Chromatogram of a pigment extract of *B. braunii*.

HPLC Chromatogram of a pigment extract of *B. braunii* cultured at 450 µm m^{-2} s^{-2} (Run 1 Day 7). The following pigments were identified: Peak 1 Unknown; Peak 2 Unknown; Peak 3 Unknown; Zeaxanthin; Chlorophyll b; Chlorophyll a; β-Carotene.

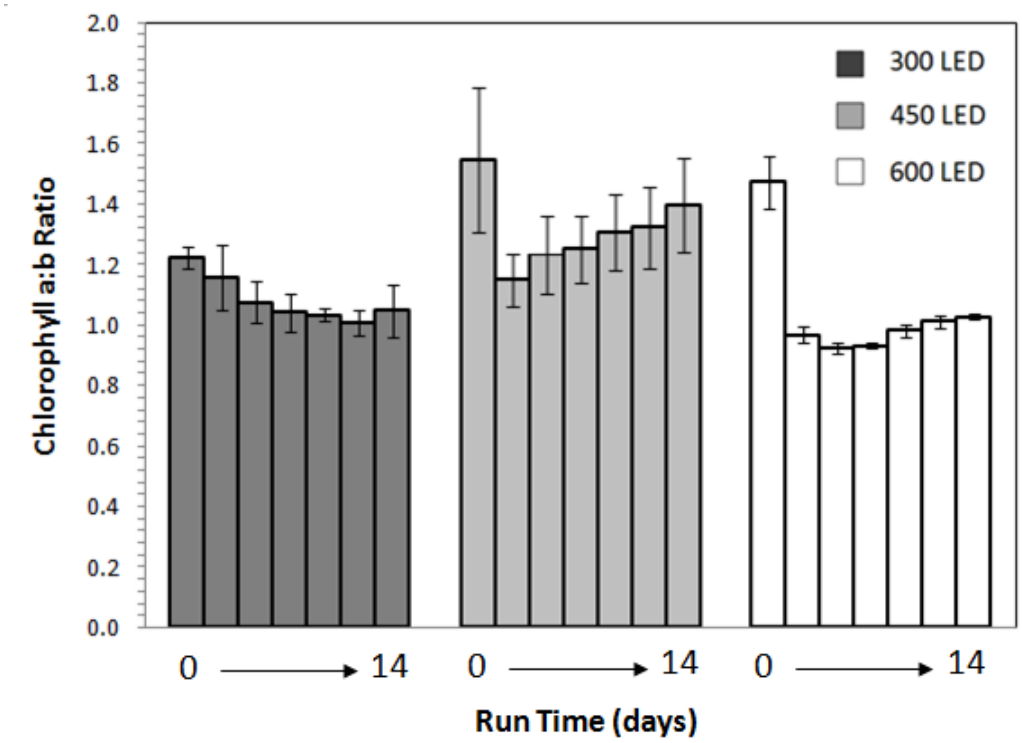

Figure 27 - Weight Ratio of Chlorophyll a to Chlorophyll b for *B. braunii* cultured under various illumination conditions.

B. braunii was grown for 14 days using LED lighting systems at 300, 450 and 600 µmol m^{-2} s^{-1}. The weight ratio of Chlorophyll a relative to chlorophyll a was determined for each illumination condition at all time points investigated. Each data points represent the average of 6, 6 and 4 replicates for 300 FLU, 300 LED, 450 LED and 600 LED respectively. Pigments were measured using HPLC. Weight ratios given in the table are for Chl b, Chl a is always 1.

CHLOROPHYLL A: CHLOROPHYLL B RATIO		
Irradiance (µmol m^{-2} s^{-1})	**450 LED**	**600 LED**
300 LED	HS (P < 0.01) = 0, 7, 9, 12, 14	S (P < 0.05) = 2 HS (P < 0.01) = 0
450 LED		HS (P < 0.01) = 5, 7, 9, 12, 14

Table 9 - A two way ANOVA determining the significance of changes in Chl a:b ratios of *B. braunii* under various illumination conditions.

A two way ANOVA was performed to determine the significance of changes in the weight ratio of Chlorophyll b relative to chlorophyll a for each illumination condition (300 FLU, 300 LED, 450 LED and 600 LED) at all time points investigated (day 0, 2, 5, 5, 9, 12 and 14). Differences between data sets are considered NS – Non Significant (P > 0.05); S – Significant (P < 0.05) or HS – Highly significant (P < 0.01) at the days listed.

Changes in the β-carotene and zeaxanthin content of *B. braunii* are shown in Figure 28. Initial β-carotene concentrations at 300 LED and 450 LED were comparable (Figure 28). β -carotene was not identified in pigment extracts obtained during PBR runs 1 and 2 at 300 μm m^{-2} s^{-1}, however during run 3 cells β-carotene content remained relatively constant throughout the growth period (approximately 0.18 μg mg^{-1}). There was a marked increase in β-carotene levels in *B. braunii* cultured at 450 μmol m^{-2} s^{-1}, with a 2.6-fold increase observed from day 0 and peaking at day 9 (1.510 ± 0.0670 μg mg^{-1} to 4.031 ± 0.1307 μg mg^{-1}). This peak was the highest average concentration of β-carotene compared to all lighting conditions investigated. Levels decreased between day 9 and 14 possibly due to the effect of to self-shading in the photobioreactor and a reduced rate of photodamage.

Initial β-carotene levels for *B. braunii* cultured at 600 μmol m^{-2} s^{-1} were 60 % lower than for 300 LED and 450 LED (0.908 μg mg^{-1}). A 2.5-fold increase was observed in β-carotene levels up to day 5 but this dropped back down to the initial concentration by day 14. The pigment β-carotene was the only measured value at intensities of 600 μmol m^{-2} s^{-1} that showed a change over the growth period.

Like β-carotene, zeaxanthin was not detected in pigment extracts from *B. braunii* cultured during run 1 or run 2 at 300 μmol m^{-2} s^{-1}. For 300 LED run 3, the cellular zeaxanthin content fluctuated at around 0.02 μg mg^{-1} over the whole growth period (Figure 28). A 3-fold increase in zeaxanthin levels was observed for *B. braunii* cultured at 450 μmol m^{-2} s^{-1} between day 0 and day 9 (0.0559 ± 0.0227 μg mg^{-1} to 0.1439 ± 0.0534 μg mg^{-1}). This was the highest average zeaxanthin concentration obtained for all illumination conditions investigated and coincides with the accumulation β-carotene. After day 9, zeaxanthin levels stayed high at around 0.143 μg mg^{-1} until the end of the run.

Initial exposure to 600 μmol m^{-2} s^{-1} resulted in a 2.7-fold decrease in average zeaxanthin content from 0.1370 μg mg^{-1} to 0.0442 μg mg^{-1}. Typically,

zeaxanthin levels for cells cultured at 600 LED remained fairly constant over the whole run at a concentration of 0.0442 ± 0.0044 μg mg^{-1}; the lowest observed in all illumination conditions. This result is surprising as the accumulation of zeaxanthin is associated with photoprotection and the dissipation of excess energy when cells are exposed to irradiance stress.

Taking individual runs into consideration, both the β-carotene and zeaxanthin content of *B. braunii* increased with irradiance over successive runs from 300 LED Run 1 through to 450 LED Run 2. The up-regulation of both xanthophylls under high irradiance suggests their role in a photoprotective function and is indicative of an acclimative response of *B. braunii* to increasing light intensities. A irradiance was increased to 600 μmol m^{-2} s^{-1} there was a 20 % reduction in β-carotene from 450 LED Run 2 and Run 3 which correlates with the inability of cells to maintain normal function after the first signs of photodamage were evident. This decrease in β-carotene for 450 LED Run 3 accounts for the high variation in measured values obtained for this intensity. Contrary to the observations for β-carotene, there was no observed decreased in cellular zeaxanthin concentration for *B. braunii* grown at 450 LED Run 3.

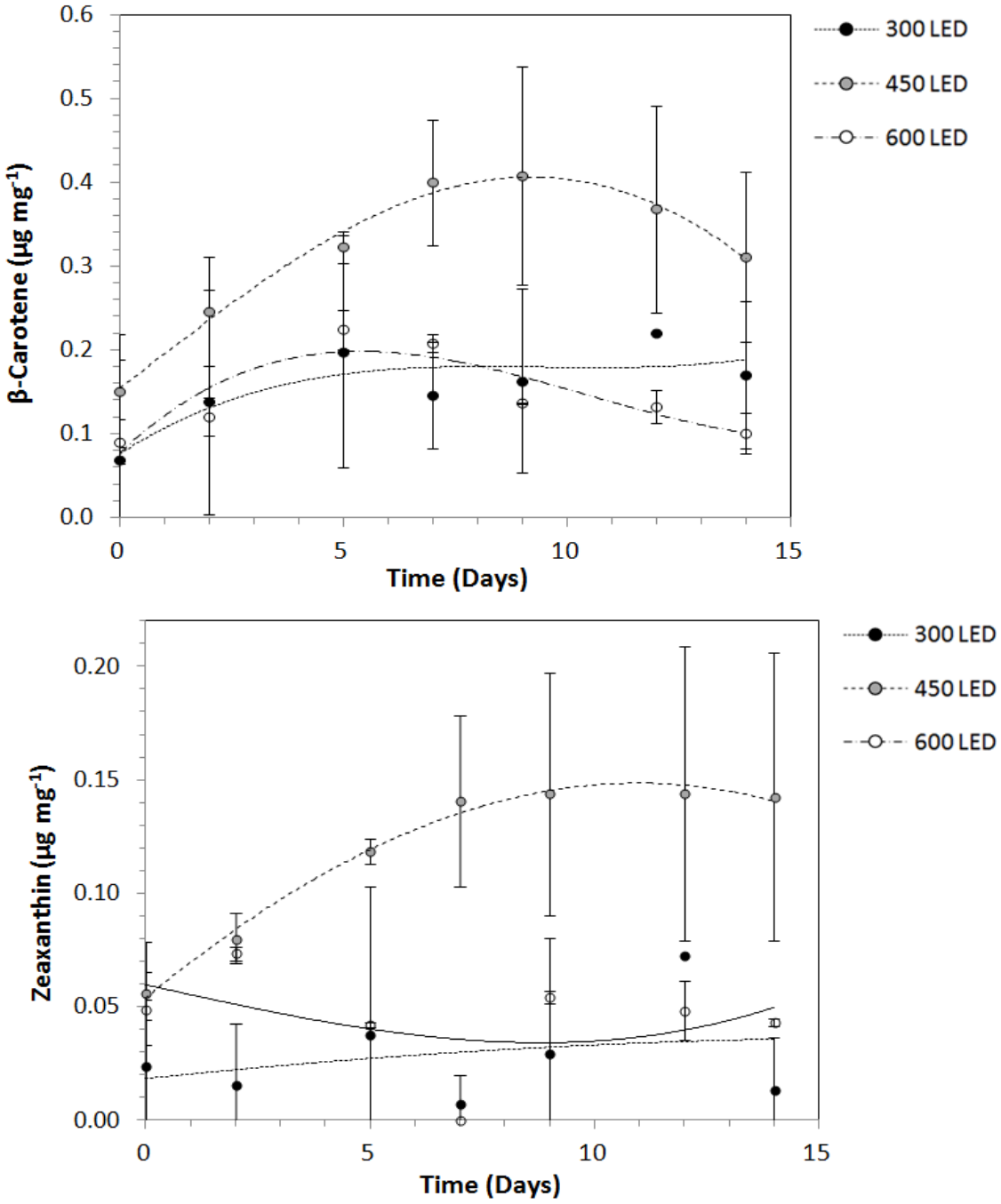

Figure 28 - Changes in the zeaxanthin and β-carotene content of *B. braunii* over a run time of 14 days under three LED lighting systems.

B. braunii was grown for 14 days using LED lighting systems at 300, 450 and 600 µmol m^{-2} s^{-1} for comparison of light quality. Extracts were analysed by HPLC, the concentration of zeaxanthin and β-carotene were normalised to DCW and expressed as µg of chlorophyll per mg of dry algal biomass. Each data points represent the average of 3 true replicates from different PBRs for 300 LED and 450 LED with 2 replicates at 600 LED; duplicate biological replicates for each run were also performed. Standard error bars are shown. When error bars are not seen, they are masked by the symbol.

Estimation of the ratio of chlorophyll a:carotenoid is useful to understand the reaction of photosynthetic organisms to changing environmental light condition (Jodłowska and Latała, 2011) (Figure 27 and **Figure 29**). *B. braunii* cultured at 300 LED showed an increase in Chl a:β-carotene ratio throughout the growth period reaching a maximum of 0.4395 ± 0.1420 μm mg^{-1} at day 14; differences were however non-significant when compared using a student's t-test ($P > 0.05$). At 450 LED there was a 2-fold increase in the Chl a:β-carotene ratio between day 0 and 7 ($P < 0.01$) where β-carotene increased from 14 % to 28 % of Chl a. Similarly, a 2.2 fold increase in Chl a:β-carotene ratio was observed between day 0 and 5 for *B. braunii* cultured at 600 LED (respective increase of 0.1274 ± 0.0035 to 0.2840 ± 0.0116). The β-carotene content of *B. braunii* grown at 450 LED and 600 LED fluctuated between 20 and 30 % of the Chl a content until the end of the run.

In a two way analysis of variance, an increase in irradiance from 300 to 450 μm m^{-2} s^{-2}, and 300 to 600 μm m^{-2} s^{-2} only demonstrated in a significant increase in Chl a:β-carotene ratio at day 14 ($P < 0.01$) (Table 10). Furthermore the weight ratio of β-carotene to Chl a for both 450 LED and 600 LED were comparable at all time point investigated ($P > 0.05$). Exposure of *B. braunii* to increasing irradiance did therefore not result in an increase in Chl a:β-carotene ratio and is not consistent with the observed increase in cellular β-carotene content when *B. braunii* was exposed to high irradiance.

An increase in the Chl a:zeaxanthin ratio was observed throughout the growth period for *B. braunii* cultured at 300 LED and 450 LED. However, due to huge variability within the results, differences were considered non-significant when compared using a student's t-test ($P > 0.05$). For 600 LED the Chl a:zeaxanthin ratio fluctuated to such an extent over the run it was difficult to observe a trend.

Due to missing data points, it was not possible to perform ANOVA analysis on the Chl a:zexanthin ratios. Taking all of the time points for *B. braunii* grown at 300 LED into consideration, the average Chl a:zexanthin ratio was 0.0269 ± 0.0403 ranging from 0.0000 to 0.1026; the lowest ratio of all illumination

conditions investigated. A 3.4-fold increase in the Chl a:zexanthin ratio was observed as irradiance increased from 300 to 450 µm m^{-2} s^{-1} (average 0.0903 ± 0.0266, range 0.0308 to 0.1370). The increase was extremely significant when the whole data set was analysed using a student's t-test ($P < 0.001$). The average Chl a:β-carotene ratio for *B. braunii* cells cultured at 600 LED dropped by 10 % compared to 450 LED with an average of 0.0814 ± 0.0537 (range 0.0588 to 0.1667), but was not considered significant ($P > 0.05$). Thus, an increase in the weight ratio of Chl a to zeaxanthin was observed with increasing irradiance. This result is consistent with the accumulation of zeaxanthin when *B. braunii* was cultured under high irradiance.

The most abundant carotenoid found in all cultures was β-carotene. The zeaxanthin concentration as a percentage of β-carotene was approximately 40 % at 300 LED and 450 LED, but increased to between 40 and 50 % in cells cultured at 600 LED. Even though levels of zeaxanthin had not increased on a cellular basis for *B. braunii* cultured at 600 LED, the ratio of zeaxanthin to β-carotene had increased.

B. braunii cells cultured under 450 and 600 µm m^{-2} s^{-1} showed much less variability in measured value for both carotene and zeaxanthin relative to those grown under 300 LED. This variation may be attributable to the small sample size which was available for pigment extraction, the complexity of the extraction procedure, the susceptibility of the pigments to heat, light and oxygen and the low concentration or absence of these pigments in the algal extracts. As a result pigment concentrations were nearing the detection limit of HPLC.

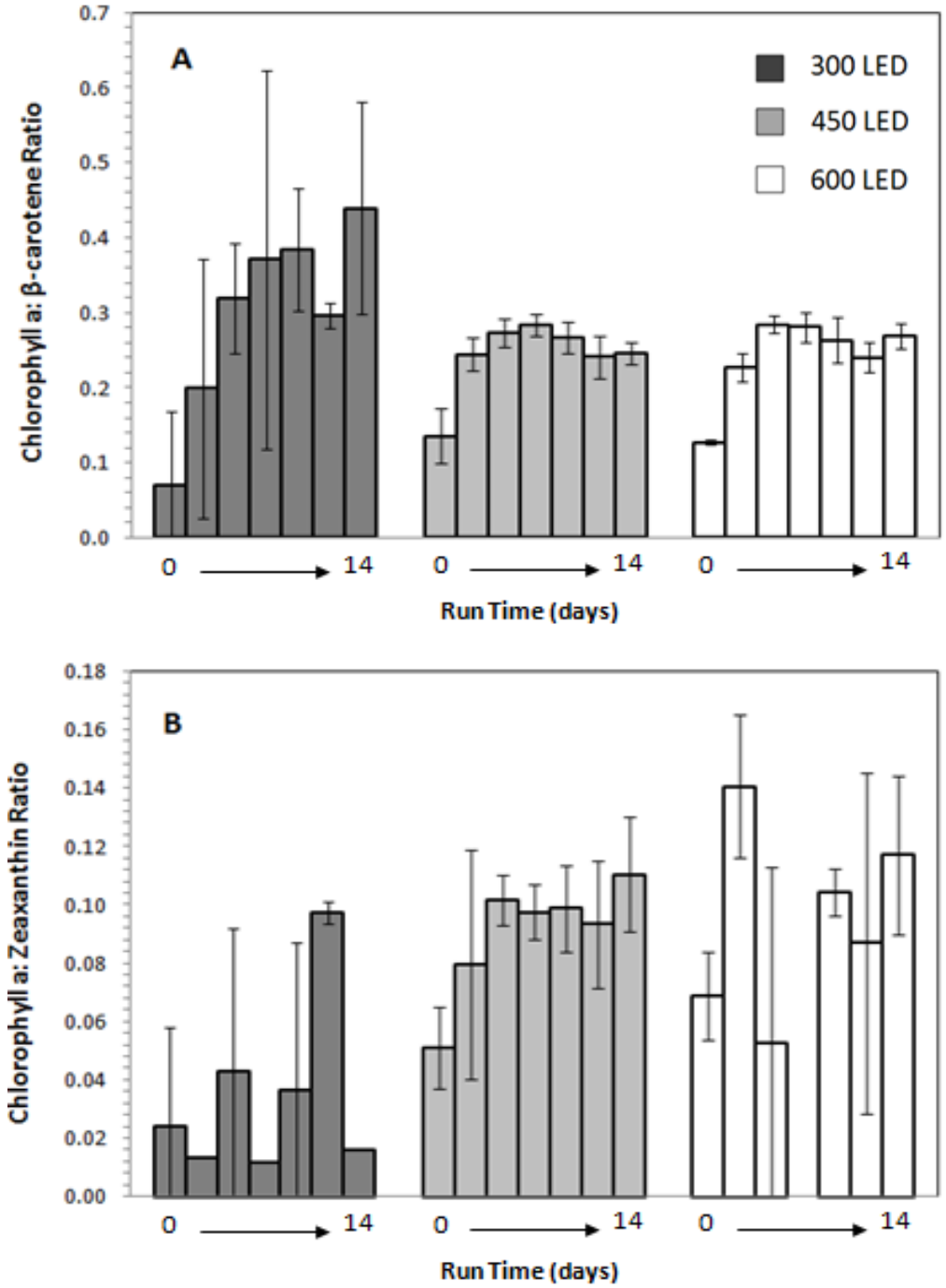

Figure 29 - Weight ratio of β-carotene and zeaxanthin relative to Chlorophyll a for *B. braunii* cultured under various illumination conditions.

B. braunii was grown for 14 days using LED lighting systems at 300, 450 and 600 µmol m^{-2} s^{-1}. The weight ratio of β-carotene and zeaxanthin relative to chlorophyll a was determined for each illumination condition at all time points investigated (day 0, 2, 5, 5, 9, 12 and 14). Each data points represent the average of 6, 6 and 4 replicates for 300 FLU, 300 LED, 450 LED and 600 LED respectively. Pigments were measured using HPLC. Weight ratios given in the table are for Chl b, Chl a is always 1.

CHLOROPHYLL A: β-CAROTENE RATIO		
Irradiance ($\mu mol\ m^{-2}\ s^{-1}$)	**450 LED**	**600 LED**
300 LED	HS (P < 0.01) = 14	S (P < 0.05) = 14
450 LED		NS
CHLOROPHYLL A: ZEAXANTHIN RATIO		
Irradiance ($\mu mol\ m^{-2}\ s^{-1}$)	**450 LED**	**600 LED**
300 LED	N/A	N/A
450 LED		N/A

Table 10 - A two way ANOVA determining the significance of changes in pigment ratios of *B. braunii* grown under various illumination conditions.

A two way ANOVA was performed to determine the significance of changes in the weight ratio of β-carotene and zeaxanthin relative to chlorophyll a for each illumination condition (300 FLU, 300 LED, 450 LED and 600 LED) at all time points. Differences between data sets were considered NS – Non Significant (P > 0.05); S – Significant (P < 0.05) or HS – Highly significant (P < 0.01) at the days listed.

4. Discussion

The results presented in this investigation indicate that the alga *Botryococcus braunii* Guadeloupe are able to adjust their photosynthetic performance to accommodate increasing in irradiance. Furthermore, illumination type had no effect on the growth of *Botryococcus braunii* when cultured at 300 µmol m^{-2} s^{-1}.

4.1 Illumination Type

The growth of *B. braunii* at 300 µmol m^{-2} s^{-1} was comparable irrespective of whether illumination was provided by fluorescent bulbs or LED shrouds. This is true for metabolic aspects including growth rate, terpene production and neutral lipid composition, but also organisation of the photosynthetic apparatus. The equivalence is probably related to the similarity of the spectral data which was obtained from both lighting systems. LED lighting did however prove to be a more reliable light source showing reduced variability in growth rates and colony size analysis than when fluorescent bulbs were used.

For complete comparison, characterisation of *B. braunii* grown at 300 FLU and 300 LED should have been performed in parallel using the same starting culture. This was not possible due to lack of equipment and the inability to produce a consistent, viable master stock. Instead, the inoculum for each batch was derived from the previous one. Repeat runs or replicates cultures were grown under identical conditions, inoculated consistently at the same starting density and sustained for the same period of growth.

4.1.1 Growth Rate

B. braunii displayed linear growth with no lag phase in all lighting regimes and did not reach stationary phase over the 14 day growth period. Of all illumination conditions investigated the highest growth rate was achieved at 450 LED

(0.1661 g l^{-1} d^{-1} ± 0.0610). An increase in irradiance from 300 µmol m^{-2} s^{-1} to 450 µmol m^{-2} s^{-1} resulted in a 6 % increase in growth rate ($P < 0.05$). Increasing irradiance to 600 µmol m^{-2} s^{-1} had a detrimental effect on the growth of *B. braunii* and resulted in a 65 % drop in growth rate.

When analysed individually, there was no apparent increase in growth rate between successive runs for the same lighting condition and therefore no evidence of acclimation. Rather each illumination condition had its own maximum growth rate. These findings are consistent for 300 FLU, 300 LED and 450 LED (run 1 and 2 only). The first signs of photoinhibition were observed during 450 LED Run 3 where a 50 % decrease in growth rate was observed from the previous two runs (0.2013 g l^{-1} d^{-1} to 0.0957 g l^{-1} d^{-1}). If this result is omitted, the average growth rate for 450 LED becomes 0.2013 g l^{-1} d^{-1} ± 0.0011. This is a 25 % increase in growth rate from 300 FLU and 300 LED and represents the maximum achievable SGR for all experimental lighting conditions. After 450 LED Run 3, *B. braunii* cells did not recover and the SPR for cells cultured under 600 µmol m^{-2} s^{-1} reduced by a further 30 % to 0.0735 ± 0.0007 g l^{-1} d^{-1}. A possible explanation for the crash in growth rate is the effect of photoinhibition and the progressive accumulation of irreparable photodamage. This may be associated with the successive nature of the experiments.

Once harvested, *B. braunii* cells were washed to remove bacterial contamination dead cells and particulates. However, the washing process does not differentiate between sick and dying cells from healthy ones. Providing the cells were intact and resided within a colony, they were not removed by centrifugation or sieving. This is significant as microscopic analysis showed photoinhibition to manifest as a change in the size and shape of individual *B. braunii* cells, enlargement of intracellular oil vacuoles and abnormal or incomplete cell division. No areas of damaged or disrupted cells were observed, instead exposure to high irradiance resulted in decreased viability of *B. braunii* cells which was confirmed by microscopic analysis and impaired growth rates. Unhealthy, potentially photodamaged cells were therefore not

removed from the population, but recycled and allowed to accumulate throughout the runs. This increases the risk of failure which would have massive economical impacts on industrial scale biofuel production.

Prior to this investigation, *B. braunii* Guadeloupe was acclimated to growth in 300 µmol m^{-2} s^{-1} for 12 months (300 FLU). Cells were recycled between subsequent runs but a healthy growth rate was maintained throughout; microscopic analysis showed no signs of an aging culture or photoinhibition. Additionally, Zhang and Kojima (1998) recycled *B. braunii* cells between PBR runs but did not observe any detrimental effects on growth rate. However, as the maximum irradiance used was much lower at 217 µmol m^{-2} s^{-1}, the effect of photoinhibition would not be expected. *B. braunii* cells from 600 LED run 2 were re-inoculated under optimum conditions over a 6 week period, but they did not recover. As a result, a third run at 600 LED was unable to be performed.

4.1.2 Hydrocarbon Production

Botryococcenes (terpene) production of *B. braunii* was found to be growth associated during the linear phase irrespective of illumination type and intensity. Therefore, although there was a difference in growth rate between *B. braunii* grown at 300 FLU, 300 LED and 450 LED (Run 1 and Run 2), and limited growth during 450 LED Run 3 and 600 LED, the hydrocarbon as a percentage of dry biomass was conserved. The same trend has been documented previously in studies (Eiichi & Zhand, 1999).

Many of the current issues in large-scale algae biofuel production is the difficulty in releasing the lipids from their intracellular location in the most energy-efficient and cost effective way possible (Scott *et al*, 2010). Results show that up to 80 % of the lipid is secreted, located within the extracellular matrix and internally within lipid globules as is consistent with many studies (Largeau *et al*, 1980; Eroglu & Melis, 2011). Eroglu & Melis (2010) and work carried out at Shell

(Spencer and Spiering, 2011) have shown that *B. braunii* cells retain their viability even after mechanical disruption and heptane extraction for recovery of extracellular hydrocarbons. This is advantageous and lends itself to continuous culture and the idea of milking. A technique was developed for extracting β-carotene from *Dunaliella salina* whereby cells were grown under normal conditions to increase biomass and then stressed by exposure to excess light to produce larger amounts of β-carotene. A bio-compatible organic solvent was then re-circulated through the aqueous phase containing the cells to extract the product (Hejazi and Wijffels, 2004).

Botryococcene production is growth associated for *B. braunii*, therefore providing cells were maintained in the linear phase of growth they will continually synthesise and secrete the valuable product. As the biomass could be continuously reused, cells would not need to be grown again thereby alleviating issues associated with slow growth rate and down time related with biomass accumulation. Recycling of the cells, including any remaining intercellular oil to the reactors allows a recovery process with relatively low efficiency to be economically viable. A key advantage is that the secreted oil can be extracted without contamination by other cellular components such as DNA or chlorophyll (Scott *et al*, 2010). There is also the possibility of converting these long chain botryococcenes into shorted length fuel-type hydrocarbons by catalytic cracking (Eroglu and Melis, 2010). Additionally, milking does not require the harvesting, concentrating and the lysis of cells for extraction of the desired product. All of these advantages are related to simplification of the process, which will lead to lower production costs and lower biomass requirements boosting the carbon balance of the process.

In addition to botryococcenes, *B. braunii* synthesises neutral lipids; triacylglycerides (TAG's), diacylglycerides (DAG's), monoacylglycerides (MAG'), free fatty acids (FFA's) and sterols. With the exception of 300 FLU, the total neutral lipid yield increased with irradiance. This result contradicts that for terpenes production determined by spectroscopy where production was growth associated, but may be due to differences in synthesis and storage

mechanisms. The increase may also be anomalous with variability attributed to the recycling of cells between runs and the natural aging of the culture. For a thorough analysis of extractable lipids by ASE measurements would need to been taken throughout each run. This was not possible in this study due to restriction with sampling volumes as a large quantity of algal cells would be required if reliable values were to be obtained. As such ASE extractions were only performed on harvested material.

Total extractable hydrocarbon yields as determined by ASE varied between 40 and 70 % of DCW. Further analysis of the extract revealed that approximately 40 % of this was identifiable as neutral lipid by GC giving 'oil' yields of between 35 % and 40 % dry weight which is considered the normal for *B. braunii* (Race B) (Banerjee *et al*, 2002). Irradiance and or lighting type did not have any effect on the distribution of intra- or inter-cellular oil which remained relatively constant between 70 – 80 % of the total extractable yield. There was also no measured effect on the composition of the extractable material with neutral lipid accounting for less than 10 % of identifiable components under all illumination conditions.

The accumulation of botryococcenes differs from those regarding the accumulation of FFA derivatives by microalgae such as *Chlorella* and *Chlamydomonas* species where synthesis is associated with nitrogen deficiency and conditions where growth is limited (Kojima & Zhang, 1999). *B. braunii* cells did not experience nitrogen limitation over the 14 day growth period which may correlates with the small quantity of neutral lipids identified in extracts for all illumination conditions. An increase in TAG may have been observed if experiments were run for greater that 14 days.

In order to exploit *B. braunii* for large scale biofuel production it is necessary to optimise productivity as means of obtaining higher rates of biomass and lipid accumulation and reducing the overall cost. As well as a potential biofuel feedstock other *B. braunii* metabolites may be extracted with applications in different industrial sectors such as fine chemicals and bulk products, nutrition

and food additives, high protein animal feed and pharmaceuticals (Mata *et al*, 2010), which will make an important contribution to cost reduction.

4.1.3 Nutritional Requirements

The nutritional requirements of *B. braunii* are not well studied, however in common with all plants both nitrate and phosphate are required for active growth. There was no significant difference in the uptake of either nitrate or phosphate for 300 FLU, 300 LED and 450 LED. Therefore, rate does not appear to be influenced by illumination type or irradiance in these conditions. Rates of nitrate and phosphate assimilation were reduced for *B. braunii* cultured at 600 LED, presumably due to the effects of photoinhibition.

Ruangsomboon (2011) found the total lipid yield of *B. braunii* to increases as the culture matured with cultures in stationary phase (cultivation time > 20 days) achieving a significantly higher biomass compared to day 10. The observed increase in biomass may be attributable to nitrogen limitation which inhibits protein synthesis and thus increases lipid or carbohydrate accumulation. Dayananda *et al* (2005) optimised conditions for growth and hydrocarbon production to show a N:P ratio of 1:4 favouring hydrocarbon production, while an N:P ratio of 1:0.5 favoured both biomass and hydrocarbon yield. These results indicate the possibility of using single stage or two-stage cultivation step for biomass and hydrocarbon production in *B. braunii*, however, further studies are required.

4.1.4 Increasing Productivity

The green microalgae *B. braunii* is considered a potential renewable resource for hydrocarbon production. In addition to increasing irradiance, lipid content in microalgae has shown to be improved by nitrogen, phosphate and silicon

limitation (Ruangsomboon, 2011). A number of algae such as *Chlamydomonas* (Lalibertè and de la Noüe, 1993), *Spirulina* (Andrade and Costa, 2007) and *Chlorella* (Abreu *et al*, 2012) have also been shown to grow both mixotrophically and heterotrophically in the presence of carbohydrates resulting in higher specific growth rates and final biomass and lipid yields than algae cultivated under photoautotrophic conditions (Abreu *et al*, 2012). Takako *et al* (2011) reports growth of *B. braunii* to be substantially enhanced by the addition of carbon compounds including glucose, mannose, fructose, galactose, sucrose or lactic acid under light conditions. Assimilation of inorganic carbon and acetate by *B. braunii* has been confirmed by Tenaud *et al* (1989).

Heterotrophic and mixotrophic production of microalgae can minimize the inhibitory effects of seasonal and diurnal light limitation on growth in outdoor cultures (Takako *et al*, 2011) and the impact of biomass loss during dark respiration (Brennan and Owende, 2009). As algae growth is independent of light energy it allows higher cell densities to be achieved. The higher density of biomass not only reduce the effect of photoinhibition, but provide for much simpler scale-up possibilities as smaller reactor surface to volume ratio's may be used thus lower harvesting costs (Brennan and Owende, 2009). The only drawback is an increased risk of bacterial contamination. Further studies are required to see if *B. braunii* can sustain heterotrophic growth for long periods of time in the dark.

Photoinhibition is an energy intensive. In order to exploit algae for large scale cultivation, Simionato *et al* (2011) recommends that cells are maintained in a state of active duplication to avoid reduced productivity brought about by the effects of photoinhibition (Simionato *et al*, 2011). The increased sensitivity of cells in the stationary phase is attributed to the absorption of excessive light energy as it is no longer used for increasing biomass, and nitrogen deficiency where reduced protein synthesis impairs the continuous repair of the D1 protein in PSII.

4.1.5 Colony sizing

The increase in colony size with irradiance observed in this set of experiments is consistent with work carried out by Zhang and Kojima (1998). Under identical hydrodynamic conditions, they found that the average colony size shifted to an equilibrium size depending on the average light intensity within the photobioreactors (PBR). These observations fell into two parts. When cell concentration was low and there was sufficient light for photosynthesis the average colony size increased with irradiance. However, as biomass accumulates over the course of a run the average light intensity within the photobioreactor falls due to the effect of self-shading, the extra competition for light resulting in a decrease in average colony size. The effect of self shading was not observed in this study as cells were grown to a maximum density of 2.5 g l^{-1} which was less than that achieved by Zhang and Kojima (1998) at 6 g l^{-1}. The low cell concentration minimised the effect of self-shading and therefore there was no substantial reduction in irradiance within the reactor.

Recovery of algal biomass contributes to 20 - 30% of the total production costs (Mata *et al*, 2011) with conventional drying procedure consuming as much as 90% of lipid energy. However, the formation of larger colonies by *B. braunii* under high irradiance would aid in their flocculation and facilitate biomass recovery through sedimentation, centrifugation or filtration, reducing the cost of harvesting and dewatering in an industrial process.

The mechanism behind colony size distributions of *B. braunii* is related to the production of extracellular polysaccharides which has been shown to increase when cells are exposed to high irradiances (Zhang and Kojima, 1998). An increase in extracellular polysaccharide enhances the mechanical strength of the colonies and therefore allows the formation of larger structures. The equilibrium size is determined by the dynamic balance between mechanical strength and the hydronamic stress due to turbulence in the PBR.

The relationship between colony size and extracellular polysaccharide production is supported by ASE extraction data, where an increase in the total extractable yield was observed with increasing irradiance. Compositionally the extracts remained constant with approximately 40 % identifiable as neutral lipid and 60 % unknown material which includes cellular components not removed during the clean-up procedure, phospholipids and polysaccharides. This observation could be confirmed by further analysis of the extracts.

4.1.6 Photosynthetic Pigment Composition

A change in chlorophyll content can be considered the first line of adaptive response to high light. Under high irradiance photosynthetic organisms respond by decreasing the size of the light harvesting antenna by down regulating the production of chlorophyll. This limits the excessive absorption of photons which would otherwise result in their eventual wasteful dissipation as heat energy or cause photoinhibition (Förster *et al*, 2005).

Cellular chlorophyll content of *B. braunii* was influenced by the illumination condition. When measured by spectroscopy cells grown at 300 µm m^{-2} s^{-1} accumulated more chlorophyll than cells cultured under 600 µm m^{-2} s^{-1}. However, there was no significant difference between chlorophyll a, chlorophyll b or total chlorophyll measurements of *B. braunii* grown at 300 FLU, 300 LED and 450 LED ($P > 0.05$), at any time points investigated. This may to due to an insufficient range in lighting conditions.

The lowest chlorophyll content was observed in cell grown under 600 LED where cells showed signs of photoinhibition. The largest difference in total chlorophyll content was observed between extremes of irradiance *i.e.* 300 and 600 µmol m^{-2} s^{-1} and after a growth period of 7 days ($P < 0.05$). In the aging culture you would expect chlorophyll levels fall due to senescence. This was not observed. In order to maintain cell viability and reduced the lag time, PBR

runs lasted for no more than 14 days. In previous experiments senescence and the recycling of chlorophyll occurred between days 12 and 14.

As a culture matured, a steady increase in chlorophyll content per dry cell mass may be expected due to the effect of self shading. Cells respond to the increased competition for light by up-regulating the production of chlorophylls thereby maximising their capacity for light harvesting. Cells were grown to a relatively low density of 1.5g l^{-1} therefore light was not limiting to growth, thus an increase in chlorophyll with run time was not observed during this set of experiment.

The increase in chlorophyll may only be observed when algae are grown in a dense culture (*i.e.* mass culture) where the surface layer cells prevent the penetration of light deeper into the culture (Stephenson *et al*, 2011). Here, there would be cells where the light-saturation effect of photosynthesis would be mitigated, and may even become light-limited due to the effects of self shading. However, light saturation and non-photochemical quenching would apply to surface layer cells directly facing the sun. Consequently sub-populations can potentially become simultaneously photo-inhibited and light limited, the combination of which is reported to limit energy conversion efficiency by as much as 95% (Stephenson *et al*, 2011).

The chlorophyll composition of *B. braunii* was determined using two different techniques: spectrophotometry to obtain a fast although coarse result and HPLC to obtain more accurate results. In both methods the Chl a:b ratio increased with irradiance achieving the highest ratio at 450 µmol m^{-2} s^{-1}. Differences in spectroscopic measurements were considered non-significant for all illumination conditions and at all time points investigated ($P > 0.05$). This implies that *B. braunii* has similar organisation of its photochemical apparatus regardless of differences in illumination condition. This result is consistent with studies by Beneragama & Goto (2011) who proposed that changes in Chl a:b ratio with environmental irradiance may be characteristic of a species. Contradictory to this, chlorophyll determined by HPLC showed *B. braunii* to

modify the composition of its photochemical apparatus as irradiance increased (300 µm m^{-2} s^{-1} to 450 µm m^{-2} s^{-1}) by reducing the amount of accessory pigment relative to Chl a within the light harvesting antenna ($P < 0.05$). When irradiance was increased to 600 µm m^{-2} s^{-2} no further drop in the Chl a:b ratio was observed. This was likely caused by the effect of accumulative photodamage to *B. braunii* cells which impairs normal function.

Lee (2008) states that the ratio of chlorophyll a to chlorophyll b varies from 2.1 to 3.1, whereas Lichtenthaler (1987) reports high-light exposed chloroplasts to exhibit chlorophyll a:b ratios of 3.2 to 4 and low-light chloroplasts ratios of 2.5 to 2.9. The typical differences between algae grown under 'high light' and' low light' with respect to the Chl a:b ratio is consistent with results obtained from spectroscopy, although results for all irradiances were within the high light range. This could be due to the what is perceived as low light or high light intensities; for growth of *B. braunii* low light is considered 40 - 87.5 µmol m^{-2} s^{-1} and high light anything over 500 µmol m^{-2} s^{-1} (Carnicas *et al*, 2010). Ruangsomboon (2011) reported high light intensities of 200 and 538 µmol m^{-2} s^{-1} to limit algal growth. In this experiment both 300 and 450 µmol m^{-2} s^{-1} may be considered high light.

Contradictory to this, Chl a:b ratios obtained from HPLC were approximately 2.5-fold lower than those determined by UV-VIS spectroscopy. The discrepancy in measured value could be explained by the matrix effect. Methanol does not selectively extract photosynthetic pigments, but a complex range of pigments and pigment degradation products found in natural samples that absorb in overlapping regions of the spectrum *i.e.* degradation products of chlorophyll a (chlorophyllides, allomers, pheopigments) have the same maximum absorption at the value 665 nm (Jodłowska and Latała, 2011) which could lead to overestimation of chlorophyll a. HPLC is not without its drawbacks. Chlorophyll and carotenoids are found bound to proteins within the thylakoid membrane of chloroplasts (Pocock *et al*, 2004). Incomplete disruption of the external and internal membranes would therefore reduce the efficiency of the extraction and result in lower yields. Photosynthetic pigments are also

susceptible to degradation by heat, light and oxygen. When these are considered in combination with a small sample size and complex extraction method involving several preparation steps it could account for the lower values which were obtained.

Jodłowska and Latała (2011) found that spectrophotometric methods gave comparable results to HPLC methods for quantification of pigments when there were no degradation products of chlorophyll a in sample. Even though there is a 2.5-fold difference in the results from UV-VIS spectroscopy and HPLC for pigment determination the trend for an increase in Chl a:b ratio under high light is consistent. Due to limitations with time and resources the reason for the difference could not be identified.

While Chlorophylls are essential for light harvesting, carotenoids play an essential role in protection of the photosynthetic apparatus. The results of this study show that *B. braunii* are capable of producing photoprotective carotenoids under high irradiance. Both β-carotene, the precursor of xanthophyll cycle pigments and zeaxanthin were identified in pigment extracts, however, neither antheraxanthin, violaxanthin, neoxanthin or lutein were found.

Pigment extracts obtained from *B. braunii* cultured at 300 LED Run 1 and 300 LED Run 2 were deficient in both β-carotene and zeaxanthin. The lack of these carotenoid may be due to their absence in the algal extracts. However, as these pigments were identified in 300 LED Run 3 and *B. braunii* cells were acclimated for 12 months at 300 µm m^{-2} s^{-1} prior to this study (fluorescent bulbs), it is unlikely that there was no requirement for their production. The absence of β-carotene and zeaxanthin in 300 LED Run 1 and Run 2 is more feasibly attributable to their inherent low concentration in the extracts, which in combination with the small sample size that was available for extraction, the complexity of the extraction procedure and the susceptibility of these pigments to heat, light and oxygen, may resulted in reduced values. Consequently, pigment concentrations could be below the limit detection when quantified by HPLC.

The increased accumulation of both β-carotene and zeaxanthin during growth of *B. braunii* under high irradiance (450 µm m^{-2} s^{-1}) is consistent with their role in photoprotection and is indicative of the acclimative response of *B. braunii* to increasing light intensities. The increase in cellular β-carotene under 450 µm m^{-2} s^{-1} irradiance was not consistent with an increase in the weight ratio of β-carotene to relative to chlorophyll a. Although not statistically significant, exposure to high irradiance caused a decrease in the chlorophyll content per cell when measured by spectroscopy. Consequently, the increase in cellular β-carotene content should have resulted in an increase in the Chl a:β-carotene ratio. The higher the irradiance, the lower the chlorophyll content and the higher the β-carotene content per cell, therefore the higher the Chl a:β-carotene:ratio which is achieved (Ben-Amotz and Avron, 1983). This erroneous result may be attributable to limitations of the HPLC method.

The accumulation of zeaxanthin in many species of green alga have shown them to be more tolerant towards excess light than those without. A substantial increase in the zeaxanthin content per cell was observed for *B. braunii* cultured at 450 µmol m^{-2} s^{-1} compared to that those grown at 300 LED, and coincided with cellular accumulation β-carotene. The increase in zeaxanthin is most likely attributed to the rapid conversion of antheraxanthin to zeaxanthin via the xanthophyll cycle under conditions of light stress. Accumulation of zeaxanthin did result in an increase in the Chl a:zeaxanthin ratio for *B. braunii* cultured at 450 µmol m^{-2} s^{-1} and also at 600 µmol m^{-2} s^{-1} despite showing no zeaxanthin accumulation within the cell. The ratio of zeaxanthin relative to β-carotene remained relatively constant throughout the growth period for each irradiance investigated. However the β-carotene:zeaxanthin ratio did increase with irradiance; zeaxanthin was approximately 40 % of the weight of β-carotene when *B. braunii* was cultured at 300 LED and 450 LED, but increased to 40 – 50 % of β-carotene in cells cultured at 600 LED. Unfortunately the significance of changes in the Chl a:zeaxanthin ratio and the β-carotene:zeaxanthin ratio were unable to be determined by ANOVA analysis.

An increase in the Chl a:carotenoid ratio has been observed in the thylakoid membranes of many photosynthetic species when grown at high irradiances. Schagerl & Müller (2006) reported total carotenoids of approximately 25% of Chl-a content in high light and 15% in low light in four freshwater cyanobacterial strains (*Anabaena cylindrica* Lemm, *Anabaenopsis elenkinii* var. Miller, *Anabaena torulosa* and *Nostoc* species) with an increase in the weight ratio of zeaxanthin to Chl-a observed after exposure to high irradiances over several days. Millie *et al* (1990) reported a 2.2-fold increase in the ratio of carotenoids to chlorophyll a in *Oscillatoria agardhii* when irradiance was increased from 50 - 230 µm m^{-2} s^{-1}, however when *Anabaena circinalis* was exposed to the same range of irradiance the Chl a:carotenoid ratio remained constant (Millie *et al*., 1992). In addition to playing a crucial role in photoprotection, some carotenoids serve as accessory light harvesting pigments (Schagerl and Müller, 2006). Enhanced carotenoid accumulation and a high chlorophyll a:carotenoids ratio has been reported improve PE (Jodłowska and Latała, 2011).

Adverse effect on photosynthesis are only observed when the rate of photodamage exceeded the rate of repair. In this study cells experienced photoinhibition during 300 LED Run 3 and when irradiance was increased to 600 µm m^{-2} s^{-1}, evident as a crash in SGR. This also resulted in a 20 % reduction in β-carotene and 2.7-fold decrease in cellular zeaxanthin and is connected with the inability of cells to maintain normal function after the first signs of photodamage became evident.

Beta-carotene and zeaxanthin levels may be lower than reported in previous studies as cultures were grown under artificial lighting systems free from ultraviolet radiation (UVR) radiation. Under natural conditions, plants are unavoidably exposed to UVR from sunlight that damages DNA, RNA and photosynthetic pigments and proteins which may act to exacerbate photoinhibition (Takahashi & Badger, 2011). Approximately 1/3 of photodamage is associated with UVR wavelengths, but the responses is species-specific due to varying effectiveness of photoprotective mechanisms (Takahashi & Badger, 2011; Fouqueray *et al*, 2007). UVR has been shown to

enhance the synthesis of specific carotenoids favouring dissipation of excess energy (Schagerl & Müller, 2006). In natural environments such as the open ocean, changes in the position of microalgae in the water column provide protection against UVR, whereas in artificial aquaculture ecosystems, such as oyster-ponds, the shallow depth and low water turbidity offer no protection against UV radiation (Fouqueray *et al*, 2007). Other species may enhance synthesis of UV-screening phenolics compounds under strong UV and visible light conditions thereby minimize the photodamage to PSII (Takahashi & Badger, 2011). As such, natural sunlight may yield differences in experimental results than artificial lighting in relation to growth rate, photosynthetic pigment composition and the accumulation of carotenoids and xanthophylls.

B. braunii was unable to sustain growth after prolonged exposure to irradiances over 450 µmol m^{-2} s^{-1}. The experimental light range was therefore limited due to the effects of photoinhibition and as a result no data was obtained for intensities between 300 µmol m^{-2} s^{-1} and that where the first signs of photoinhibition were observed (450 LED Run 3). The insufficient light range was due to limitations of the LED light shroud where 300 µmol m^{-2} s^{-1} was the lowest achievable intensity out of all available lighting configurations. For a better indication of changes in pigment composition during exposure to high light the initial light intensity should have been reduced to 40 - 87.5 µmol m^{-2} s^{-1} (Ruangsomboon, 2011; Carnicas *et al*, 2010; Li and Qin, 2005). Carnicas *et al* (1999) performed a two stage light experiment whereby the red alga *Gracilaria tenuistipitata* was acclimated to low irradiance (40 µmol m^{-2} s^{-1}) then transferred to high irradiance (500 µmol m^{-2} s^{-1}) to observed the short (55 hours) and long term (10 days) effects of acclimation to light stress. Ruangsomboon (2011) grew *B. braunii* KMITL 2 isolated from Thailand over a larger range of irradiances up to 538 µmol m^{-2} s^{-1} (0.3, 87.5, 200 and 538 µmol m^{-2} s^{-1}) under continuous illumination for a period of 24 hours. There was no gradual acclimation to high light in either method.

Acclimation to high light is complex and involves the accumulative effect of many photoprotective processes. Future experiments should focus on other

mechanisms of photoprotection including antioxidants and the repair of damaged D1 proteins in PSII.

5. Conclusion

The results presented in this investigation indicate that the alga *Botryococcus braunii* Guadeloupe was able to adjust the composition of light harvesting and photoprotective pigments within the antenna complex to accommodate an increase in irradiance. Higher rates of growth and biomass were observed as irradiance increased from 300 µmol m^{-2} s^{-1} to 450 µmol m^{-2} s^{-1}. Although not statistically significant, growth at 450 and 600 µmol m^{-2} s^{-1} caused a decrease in the chlorophyll content per cell thereby effectively minimising the absorption of excessive photons. Cells also increased the accumulation of both β-carotene and zeaxanthin during exposure to 450 µmol m^{-2} s^{-1} which is consistent with their role in photoprotection and the dissipation of excess light energy as heat through the process of NPQ. *B. braunii* was however unable to optimise the photosynthetic apparatus in order to sustain active growth in prolonged exposure to irradiances over 450 µmol m^{-2} s^{-1}. Investigations into illumination type (fluorescent or LED) showed that lighting method had no effect on the growth of *Botryococcus braunii* when cultured at 300 µmol m^{-2} s^{-1}.

The aim is to deploy open algal ponds within the equatorial region where conditions make it suitable for all year round cultivation. However, the light-saturation of *B. braunii* was identified between 450 and 600 µm m^{-2} s^{-1} (450 LED Run 3) where the first signs of photoinhibition became apparent. This is over 5 times lower than the intensity which sunlight can reach at the equator (2500 µm m^{-2} s^{-1}). For the purpose of growing *B. braunii* in the industrial production of biofuels it will be necessary to enhance its ability to survive under high illumination through the up-regulation of photoprotective mechanisms, especially if harnessing the power of sunlight. This can be achieved through strain selection, acclimation or the development of microalgal strains with permanent mutations (GM). Another significant goal in *B. braunii* research is to understand how and where the hydrocarbons are produced and retained within the colony, and the mechanism by which they are segregated into globules and eventually into the extracellular space, which thus far is still unknown.

6. Appendices

6.1 Raw Data Optical Density (680 nm)

Day	300 FLU					300 LED			450 LED			600 LED	
	Run 1	Run 2	Run 3	Run 4	Run 5	Run 1	Run 2	Run 3	Run 1	Run 2	Run 3	Run 1	Run 2
0	0.215	0.259	0.199	0.230	0.200	0.196	0.213	0.212	0.230	0.197	0.171	0.221	0.217
2	0.262	0.370	0.306	0.317	0.347	0.271	0.357	0.401	0.492	0.324	0.295	0.353	0.308
5	0.314	0.557	0.562	0.560	0.511	0.439	0.534	0.567	0.614	0.445	0.542	0.458	0.516
7	0.481	0.690	0.581	0.655	0.702	0.615	0.609	0.649	0.766	0.600	0.632	0.504	0.533
9	0.656	1.072	0.745	0.783	1.049	0.756	0.818	0.736	1.008	0.752	0.758	0.558	0.565
12	0.793	1.279	0.931	1.076	1.302	0.867	-	0.921	1.309	0.947	0.699	0.569	0.554

6.2 Raw Data Biomass (DCW) (g l^{-1} d^{-1})

Day	300 FLU					300 LED			450 LED			600 LED	
	Run 1	Run 2	Run 3	Run 4	Run 5	Run 1	Run 2	Run 3	Run 1	Run 2	Run 3	Run 1	Run 2
0	0.3700	0.5200	0.3500	0.5000	0.3100	0.3800	0.4600	0.5400	0.4600	0.4700	0.4300	0.6000	0.7900
2	0.5600	0.8700	0.6300	0.5900	0.5700	0.5600	0.7400	0.7300	1.3500	0.8200	0.7300	0.8000	0.7500
5	0.8300	1.4100	1.6000	1.1400	0.8600	1.0100	1.4100	1.2700	1.6100	1.0800	1.5200	1.1000	1.2300
7	1.0200	1.4400	1.2900	1.3900	1.1000	1.0700	1.6500	1.5200	1.6900	1.4900	1.4700	1.2200	1.2700
9	1.5500	1.7400	1.5900	1.3500	1.7800	1.2800	1.6700	1.6500	2.7000	1.8200	1.6400	1.2600	1.3000
12	1.7500	2.5458	1.8000	1.9700	2.0900	1.6500	-	2.2700	2.9500	2.3300	1.8100	1.5900	1.6200

6.3 Terpene Production (mg l^{-1})

Day	300 FLU					300 LED			450 LED			600 LED	
	Run 1	Run 2	Run 3	Run 4	Run 5	Run 1	Run 2	Run 3	Run 1	Run 2	Run 3	Run 1	Run 2
0	-	-	175	204	148	159	190	150	275	220	180	280	265
2	-	-	225	217	207	168	275	190	390	270	225	315	290
5	-	475	563	970	267	235	380	307	460	390	-	405	430
7	-	458	425	422	383	308	540	375	620	578	515	450	435
9	-	660	525	532	640	428	650	458	1930	680	553	525	475
12	-	800	670	766	791	460	900	610	2110	840	718	525	495

6.4 Terpene Production normalised to DCW (µg mg^{-1})

Day	300 FLU					300 LED			450 LED			600 LED	
	Run 1	Run 2	Run 3	Run 4	Run 5	Run 1	Run 2	Run 3	Run 1	Run 2	Run 3	Run 1	Run 2
0	-	-	175	204	148	159	190	150	275	220	180	280	265
2	-	-	225	217	207	168	275	190	390	270	225	315	290
5	-	475	563	970	267	235	380	307	460	390		405	430
7	-	458	425	422	383	308	540	375	620	578	515	450	435
9	-	660	525	532	640	428	650	458	1930	680	553	525	475
12	-	800	670	766	791	460	900	610	2110	840	718	525	495

6.5 ASE Extractions

300 FLU Run 1		FFA (%)	Terpenes / MAGs (%)	Sterols (%)	DAG (%)	TAG (%)	Identifiable Components (%)	Grav. Yield (% of DW)	Of which are Identified lipids (%)
Repeat 1	Extracellular Oil	0.4	87.2	0.5	0.1	0.1	88.3	32.60	28.79
	Intracellular Oil	11	8.6	5.2	12.8	16.9	54.5	27.62	15.05
Repeat 2	Extracellular Oil	0.6	92.1	0.4	0.1	0.1	93.3	25.56	23.85
	Intracellular Oil	18.4	8.2	4.9	11.5	14.4	57.4	38.69	22.21

300 FLU Run 2		FFA (%)	Terpenes / MAGs (%)	Sterols (%)	DAG (%)	TAG (%)	Identifiable Components (%)	Grav. Yield (% of DW)	Of which are Identified lipids (%)
Repeat 1	Extracellular Oil	0.40	87.20	0.50	0.10	0.10	88.30	32.60	28.79
	Intracellular Oil	11.00	8.60	5.20	12.80	16.90	54.50	27.62	15.05
Repeat 2	Extracellular Oil	0.60	92.10	0.40	0.10	0.10	93.30	25.56	23.85
	Intracellular Oil	18.40	8.20	4.90	11.50	14.40	57.40	38.69	22.21

300 FLU Run 3		FFA (%)	Terpenes / MAGs (%)	Sterols (%)	DAG (%)	TAG (%)	Identifiable Components (%)	Grav. Yield (% of DW)	Of which are Identified lipids (%)
Repeat 1	**Extracellular Oil**	2.50	63.75	3.90	1.10	0.20	71.45	48.16	34.41
	Intracellular Oil	14.80	17.00	7.80	5.00	3.80	48.40	18.45	8.93
Repeat 2	**Extracellular Oil**	0.10	81.39	4.10	0.70	0.10	86.39	42.12	36.39
	Intracellular Oil	16.20	22.05	5.80	3.80	1.70	49.55	12.08	5.99

300 LED Run 2		FFA (%)	Terpenes / MAGs (%)	Sterols (%)	DAG (%)	TAG (%)	Identifiable Components (%)	Grav. Yield (% of DW)	Of which are Identified lipids (%)
Repeat 1	**Extracellular Oil**	0.88	45.40	-	0.20	0.11	46.59	31.50	14.68
	Intracellular Oil	2.24	2.66	-	2.98	15.32	23.20	4.98	1.15
Repeat 2	**Extracellular Oil**	0.18	40.35	-	0.10	0.10	40.73	28.50	11.61
	Intracellular Oil	4.82	3.84	-	5.19	6.00	19.85	7.02	1.39
Repeat 3	**Extracellular Oil**	0.31	22.50	-	0.12	0.10	23.03	28.84	6.64
	Intracellular Oil	3.27	2.79	-	2.80	6.00	14.86	7.77	1.16

300 LED Run 3		FFA (%)	Terpenes / MAGs (%)	Sterols (%)	DAG (%)	TAG (%)	Identifiable Components (%)	Grav. Yield (% of DW)	Of which are Identified lipids (%)
Repeat 1	**Extracellular Oil**	-	39.15	-	-	-	39.15	33.12	12.97
	Intracellular Oil	10.09	11.74	0.00	8.60	10.10	40.53	7.98	3.24
Repeat 2	**Extracellular Oil**	-	33.25	-	-	-	33.25	34.78	11.56
	Intracellular Oil	8.70	15.51	0.00	7.90	11.80	43.91	7.36	3.23

450 LED Run 1		FFA (%)	Terpenes / MAGs (%)	Sterols (%)	DAG (%)	TAG (%)	Identifiable Components (%)	Grav. Yield (% of DW)	Of which are Identified lipids (%)
Repeat 1	**Extracellular Oil**	-	41.00	-	-	-	41.00	37.67	15.44
	Intracellular Oil	7.10	12.57	-	3.60	3.90	27.17	10.49	2.85
Repeat 2	**Extracellular Oil**	-	37.30	-	-	-	37.30	39.94	14.90
	Intracellular Oil	9.80	13.11	-	8.30	13.60	44.81	9.51	4.26

450 LED Run 2		FFA (%)	Terpenes / MAGs (%)	Sterols (%)	DAG (%)	TAG (%)	Identifiable Components (%)	Grav. Yield (% of DW)	Of which are Identified lipids (%)
Repeat 1	**Extracellular Oil**	-	43.70	-	-	-	43.70	55.59	24.29
	Intracellular Oil	7.90	12.61	8.00	6.80	10.36	45.67	23.63	10.79
Repeat 2	**Extracellular Oil**	-	39.85	-	-	-	39.85	58.65	23.37
	Intracellular Oil	6.90	16.49	9.60	7.50	11.10	51.59	16.46	8.49

600 LED Run 1		FFA (%)	Terpenes / MAGs (%)	Sterols (%)	DAG (%)	TAG (%)	Identifiable Components (%)	Grav. Yield (% of DW)	Of which are Identified lipids (%)
Repeat 1	**Extracellular Oil**	0.32	47.10	4.30	1.30	0.65	53.67	37.71	20.24
	Intracellular Oil	8.50	8.69	12.30	1.07	6.22	36.78	9.93	3.65
Repeat 2	**Extracellular Oil**	1.42	39.55	2.61	0.74	2.36	46.68	50.93	23.77
	Intracellular Oil	4.37	6.71	6.86	7.72	10.30	35.96	13.55	4.87

600 LED Run2		FFA (%)	Terpenes / MAGs (%)	Sterols (%)	DAG (%)	TAG (%)	Identifiable Components (%)	Grav. Yield (% of DW)	Of which are Identified lipids (%)
Repeat 1	**Extracellular Oil**	3.00	40.30	3.01	0.62	1.99	48.92	55.54	27.17
	Intracellular Oil	2.95	3.32	0.70	2.81	1.09	10.87	20.39	2.22
Repeat 2	**Extracellular Oil**	2.18	40.60	3.09	0.66	2.76	49.29	51.76	25.51
	Intracellular Oil	2.64	1.16	0.42	2.26	2.38	8.86	28.10	2.49

6.6 Cation and Anion Analysis

300 FLU Run 1	Days From Inoculation	Sodium (mg l^{-1})	Potassium (mg l^{-1})	Magnesium (mg l^{-1})	Calcium (mg l^{-1})	Sulphate (mg l^{-1})	Nitrate (mg l^{-1})	Phosphate (mg l^{-1})
	0	89	211	17	65	98	251	45
	2	88	180	15	53	78	172	29
	5	94	221	18	63	94	182	32
	7	102	217	18	63	92	150	32
	9	73	187	15	56	81	77	27
	12	103	207	17	62	89	44	28
	14	96	179	15	56	82	10	21

300 FLU Run 2	Days From Inoculation	Sodium (mg l^{-1})	Potassium (mg l^{-1})	Magnesium (mg l^{-1})	Calcium (mg l^{-1})	Sulphate (mg l^{-1})	Nitrate (mg l^{-1})	Phosphate (mg l^{-1})
	0	5	228	18	55	96	226	59
	2	4	236	18	56	96	159	55
	5	20	228	17	55	93	108	52
	7	53	232	18	59	111	67	49
	9	19	226	17	59	93	6	45
	12	20	239	18	63	97	6	46
	14	4	227	17	63	99	No Data	43

300 FLU Run 3	Days From Inoculation	Sodium (mg l^{-1})	Potassium (mg l^{-1})	Magnesium (mg l^{-1})	Calcium (mg l^{-1})	Sulphate (mg l^{-1})	Nitrate (mg l^{-1})	Phosphate (mg l^{-1})
	0	90	236	20	60	100	237	67
	2	89	234	19	62	102	171	56
	5	102	231	19	74	94	126	51
	7	106	238	20	62	103	75	50
	9	91	239	19	62	109	24	45
	12	105	233	19	64	101	8	42
	14	99	233	18	64	98	12	39

300 LED Run 1	Days From Inoculation	Sodium (mg l^{-1})	Potassium (mg l^{-1})	Magnesium (mg l^{-1})	Calcium (mg l^{-1})	Sulphate (mg l^{-1})	Nitrate (mg l^{-1})	Phosphate (mg l^{-1})
	0	98	215	18	56	102	243	44
	2	111	243	20	63	107	224	35
	5	122	183	18	69	114	206	41
	7	101	232	19	60	101	146	36
	9	115	260	21	69	108	70	34
	12	139	331	27	87	129	15	39
	14	127	237	20	71	110	7	23

300 LED Run 2	Days From Inoculation	Sodium (mg l^{-1})	Potassium (mg l^{-1})	Magnesium (mg l^{-1})	Calcium (mg l^{-1})	Sulphate (mg l^{-1})	Nitrate (mg l^{-1})	Phosphate (mg l^{-1})
	0	107	237	20	61	106	189	59
	2	No Data	No Data	No Data	No Data	No Data	No Data	No Data
	5	106	235	19	82	103	83	51
	7	91	223	19	58	104	27	46
	9	106	229	18	62	104	7	44
	12	119	252	20	66	106	0	51
	14	114	251	21	169	115	5	44

300 LED Run 3	Days From Inoculation	Sodium (mg l^{-1})	Potassium (mg l^{-1})	Magnesium (mg l^{-1})	Calcium (mg l^{-1})	Sulphate (mg l^{-1})	Nitrate (mg l^{-1})	Phosphate (mg l^{-1})
	0	87	230	19	57	100	236	70
	2	94	237	20	63	110	180	67
	5	89	240	20	66	101	124	55
	7	104	230	19	57	94	70	55
	9	102	224	18	55	95	11	48
	12	107	237	18	58	94	2	47
	14	113	239	19	66	108	7	42

450 LED Run 1	Days From Inoculation	Sodium (mg l^{-1})	Potassium (mg l^{-1})	Magnesium (mg l^{-1})	Calcium (mg l^{-1})	Sulphate (mg l^{-1})	Nitrate (mg l^{-1})	Phosphate (mg l^{-1})
	0	10	780	20	40	80	230	No Data
	2	<10	720	10	30	70	180	No Data
	5	10	810	10	30	80	170	No Data
	7	<10	800	20	40	70	140	No Data
	9	<10	920	20	40	80	50	No Data
	12	<10	870	20	40	70	10	No Data
	14	<10	770	10	30	60	<10	No Data

450 LED Run 2	Days From Inoculation	Sodium (mg l^{-1})	Potassium (mg l^{-1})	Magnesium (mg l^{-1})	Calcium (mg l^{-1})	Sulphate (mg l^{-1})	Nitrate (mg l^{-1})	Phosphate (mg l^{-1})
	0	20	790	20	30	80	230	No Data
	2	<10	740	10	30	70	170	No Data
	5	<10	800	10	30	80	160	No Data
	7	10	830	10	30	70	100	No Data
	9	10	850	10	30	70	20	No Data
	12	10	850	10	30	60	<10	No Data
	14	<10	780	10	30	60	<10	No Data

600 LED Run 1	Days From Inoculation	Sodium (mg l^{-1})	Potassium (mg l^{-1})	Magnesium (mg l^{-1})	Calcium (mg l^{-1})	Sulphate (mg l^{-1})	Nitrate (mg l^{-1})	Phosphate (mg l^{-1})
	0	10	780	20	40	80	230	No Data
	2	<10	720	10	30	70	180	No Data
	5	10	810	10	30	80	170	No Data
	7	<10	800	20	40	70	140	No Data
	9	<10	920	20	40	80	50	No Data
	12	<10	870	20	40	70	10	No Data
	14	<10	770	10	30	60	<10	No Data

600 LED Run 2	Days From Inoculation	Sodium (mg l^{-1})	Potassium (mg l^{-1})	Magnesium (mg l^{-1})	Calcium (mg l^{-1})	Sulphate (mg l^{-1})	Nitrate (mg l^{-1})	Phosphate (mg l^{-1})
	0	20	790	20	30	80	230	No Data
	2	<10	740	10	30	70	170	No Data
	5	<10	800	10	30	80	160	No Data
	7	10	830	10	30	70	100	No Data
	9	10	850	10	30	70	20	No Data
	12	10	850	10	30	60	<10	No Data
	14	<10	780	10	30	60	<10	No Data

6.7 Colony Size Analysis (All measurements in µm)

	300 FLU				300 LED		450 LED			600 LED	
	Run 1	**Run 2**	**Run 3**	**Run 4**	**Run 1**	**Run 2**	**Run 1**	**Run 2**	**Run 3**	**Run 1**	**Run 2**
Max	887.2724	562.511	777.6838	636.0906	120.4252	88.65101	646.9001	387.1184	337.3474	387.64	436.8905
75%	26.05795	27.60116	52.211	38.73579	22.89468	26.01616	90.6336	87.54776	87.38682	110.7827	82.93335
Median	16.07351	16.17622	25.80248	18.47064	17.92518	20.4659	29.03401	43.02979	46.95011	66.6714	20.90982
25%	12.20871	12.34361	14.89707	12.34361	13.68232	14.21886	15.11778	20.67084	18.84782	16.65537	13.97943
Min	10.13314	10.13314	10.13314	10.13314	10.02829	10.02829	10.13314	10.13314	10.13314	10.13314	10.06981

	300 FLU				300 LED		450 LED			600 LED	
	Run 1	**Run 2**	**Run 3**	**Run 4**	**Run 1**	**Run 2**	**Run 1**	**Run 2**	**Run 3**	**Run 1**	**Run 2**
Mean	30.4048	31.1654	43.5709	33.5164	20.6059	22.1999	59.1195	65.8111	62.7730	78.5483	52.2692
SD	45.5895	44.9258	52.8589	39.6200	10.6464	10.5196	61.2227	61.9331	55.3596	68.1546	56.2601
Count	7159	5033	2051	3353	754	794	1624	1064	1070	700	1047

6.8 Chlorophyll UV-VIS Spectroscopy

Chlorophyll a (µg mg^{-1})

Day	300 FLU					300 LED			450 LED			600 LED	
	Run 1	Run 2	Run 3	Run 4	Run 5	Run 1	Run 2	Run 3	Run 1	Run 2	Run 3	Run 1	Run 2
0	10.989	11.559	11.997	7.704	11.520	13.213	14.425	15.248	14.890	13.135	9.918	12.350	6.127
2	8.467	11.583	8.259	7.812	9.993	10.996	10.236	11.099	8.710	9.017	5.076	9.036	5.906
5	7.975	11.750	8.849	10.460	11.777	7.662	9.716	9.622	10.086	9.133	No Data	8.683	8.902
7	10.590	13.560	10.874	12.830	12.978	11.189	3.571	11.463	12.649	13.683	10.509	7.586	7.171
9	12.215	14.346	11.764	12.866	13.989	12.158	13.017	12.217	4.818	13.174	12.099	8.639	7.575
12	12.891	11.280	12.075	12.857	13.143	12.516	No Data	11.426	10.350	10.446	12.873	6.597	5.722

Chlorophyll b (µg mg^{-1})

Day	300 FLU					300 LED			450 LED			600 LED	
	Run 1	Run 2	Run 3	Run 4	Run 5	Run 1	Run 2	Run 3	Run 1	Run 2	Run 3	Run 1	Run 2
0	5.803	3.835	4.589	4.288	7.780	6.932	5.938	4.752	6.423	6.557	3.619	4.400	2.881
2	4.001	4.634	3.001	4.154	4.979	4.836	3.696	3.501	2.695	3.168	1.506	3.403	2.202
5	2.841	3.430	4.026	2.695	3.427	3.348	3.722	2.762	2.954	3.424	No Data	2.726	3.500
7	3.953	5.776	4.558	4.333	4.824	3.299	2.364	3.262	3.636	4.036	3.261	2.552	2.236
9	5.585	5.576	4.654	5.700	4.117	3.556	3.977	3.551	1.689	4.169	3.860	3.019	2.642
12	4.572	4.120	4.547	4.114	4.049	3.858	No Data	3.779	3.239	3.375	4.272	2.512	2.152

Total Chlorophyll (µg mg^{-1})

Day	300 FLU					300 LED			450 LED			600 LED	
	Run 1	Run 2	Run 3	Run 4	Run 5	Run 1	Run 2	Run 3	Run 1	Run 2	Run 3	Run 1	Run 2
0	16.792	15.394	16.586	11.992	19.300	20.145	20.363	20.000	21.313	19.691	13.537	16.750	9.008
2	12.468	16.216	11.260	11.966	14.972	15.832	13.932	14.600	11.404	12.184	6.582	12.439	8.108
5	10.817	15.180	12.875	13.154	15.203	11.010	13.438	12.384	13.040	12.556	13.770	11.409	12.402
7	14.543	19.336	15.433	17.163	17.803	14.489	5.935	14.725	16.285	17.719	15.959	10.138	9.407
9	17.800	19.922	16.418	18.567	18.106	15.715	16.994	15.767	6.507	17.343	17.145	11.658	10.217
12	17.463	15.400	16.622	16.971	17.192	16.373	No Data	15.205	13.588	13.821	14.555	9.109	7.875

Chlorophyll a:b Ratio

Day	300 FLU					300 LED			450 LED			600 LED	
	Run 1	Run 2	Run 3	Run 4	Run 5	Run 1	Run 2	Run 3	Run 1	Run 2	Run 3	Run 1	Run 2
0	1.894	3.014	2.614	1.796	1.481	1.906	2.429	3.209	2.318	2.003	2.741	2.807	2.127
2	2.116	2.500	2.752	1.881	2.007	2.274	2.769	3.170	3.232	2.847	3.370	2.655	2.682
5	2.807	3.425	2.198	3.882	3.437	2.288	2.610	3.483	3.414	2.667	No Data	3.185	2.543
7	2.679	2.348	2.386	2.961	2.690	3.391	1.511	3.514	3.478	3.390	3.223	2.973	3.206
9	2.187	2.573	2.528	2.257	3.398	3.419	3.273	3.441	2.852	3.160	3.134	2.861	2.867
12	2.820	2.738	2.656	3.125	3.246	3.244	No Data	3.023	3.196	3.095	3.013	2.626	2.659

6.9 Photosynthetic Pigments measured by HPLC

300 LED Run 1

Run Time (Days)	Repeat	Sample Weight (mg)	Raw HPLC Data				Normalised HPLC Data			
			Zeaxanthin (μg ml^{-1})	Chlorophyll a (μg ml^{-1})	Chlorophyll b (μg ml^{-1})	β-Carotene (μg ml^{-1})	Zeaxanthin (μg mg^{-1})	Chlorophyll a (μg mg^{-1})	Chlorophyll b (μg mg^{-1})	β-Carotene (μg mg^{-1})
0	1	6.5000	0.0000	2.1000	1.8000	0.0000	0.0000	0.3231	0.2769	0.0000
0	2	6.2000	0.0000	1.6000	1.3000	0.0000	0.0000	0.2581	0.2097	0.0000
2	1	7.2000	0.0000	1.6000	1.2000	0.0000	0.0000	0.2222	0.1667	0.0000
2	2	7.4000	0.0000	1.8000	1.5000	0.0000	0.0000	0.2432	0.2027	0.0000
5	1	9.4000	0.0000	4.6000	4.5000	1.5000	0.0000	0.4894	0.4787	0.1596
5	2	9.2000	0.0000	0.0000	0.0000	0.0000	0.0000	0.0000	0.0000	0.0000
7	1	11.7000	0.0000	6.3000	6.6000	2.6000	0.0000	0.5385	0.5641	0.2222
7	2	12.1000	0.0000	1.7000	1.7000	0.0000	0.0000	0.1405	0.1405	0.0000
9	1	13.1000	0.0000	6.0000	6.0000	2.5000	0.0000	0.4580	0.4580	0.1908
9	2	13.5000	0.0000	2.5000	2.4000	1.1000	0.0000	0.1852	0.1778	0.0815
14	1	19.3000	0.0000	11.5000	10.5000	5.3000	0.0000	0.5959	0.5440	0.2746
14	2	18.7000	0.0000	8.0000	8.0000	3.9000	0.0000	0.4278	0.4278	0.2086

300 LED Run 2

Run Time (Days)	Repeat	Sample Weight (mg)	Raw HPLC Data				Normalised HPLC Data			
			Zeaxanthin (μg ml^{-1})	Chlorophyll a (μg ml^{-1})	Chlorophyll b (μg ml^{-1})	β-Carotene (μg ml^{-1})	Zeaxanthin (μg mg^{-1})	Chlorophyll a (μg mg^{-1})	Chlorophyll b (μg mg^{-1})	β-Carotene (μg mg^{-1})
0	1	6.9000	0.0000	1.7000	1.4000	0.0000	0.0000	0.2464	0.2029	0.0000
0	2	7.2000	0.0000	0.0000	0.0000	0.0000	0.0000	0.0000	0.0000	0.0000
2	1	9.2000	0.0000	2.3000	2.2000	1.0000	0.0000	0.2500	0.2391	0.1087
2	2	9.3000	0.0000	5.3000	5.1000	1.7000	0.0000	0.5699	0.5484	0.1828
5	1	11.9000	0.0000	9.3000	9.2000	3.9000	0.0000	0.7815	0.7731	0.3277
5	2	12.0000	0.0000	0.0000	0.0000	0.0000	0.0000	0.0000	0.0000	0.0000
7	1	13.7000	0.0000	4.1000	4.1000	1.9000	0.0000	0.2993	0.2993	0.1387
7	2	13.3000	0.0000	1.3000	1.2000	1.0000	0.0000	0.0977	0.0902	0.0752
9	1	15.8000	0.0000	4.7000	4.5000	2.2000	0.0000	0.2975	0.2848	0.1392
9	2	13.9000	0.0000	0.0000	0.0000	0.0000	0.0000	0.0000	0.0000	0.0000
14	1	18.6000	0.0000	3.8000	3.4000	1.7000	0.0000	0.2043	0.1828	0.0914
14	2	19.0000	0.0000	1.5000	1.3000	1.0000	0.0000	0.0789	0.0684	0.0526

300 LED Run 3

Run Time (Days)	Repeat	Sample Weight (mg)	Raw HPLC Data				Normalised HPLC Data			
			Zeaxanthin (μg ml^{-1})	Chlorophyll a (μg ml^{-1})	Chlorophyll b (μg ml^{-1})	β-Carotene (μg ml^{-1})	Zeaxanthin (μg mg^{-1})	Chlorophyll a (μg mg^{-1})	Chlorophyll b (μg mg^{-1})	β-Carotene (μg mg^{-1})
0	1	7.4000	0.6000	9.0000	7.1000	1.6000	0.0811	1.2162	0.9595	0.2162
0	2	8.1000	0.5000	9.1000	7.4000	1.6000	0.0617	1.1235	0.9136	0.1975
2	1	9.8000	0.0000	12.6000	10.8000	2.7000	0.0000	1.2857	1.1020	0.2755
2	2	9.6000	0.9000	11.2000	9.6000	2.5000	0.0938	1.1667	1.0000	0.2604
5	1	12.2000	1.3000	15.6000	13.6000	4.1000	0.1066	1.2787	1.1148	0.3361
5	2	12.6000	1.5000	17.1000	15.3000	4.6000	0.1190	1.3571	1.2143	0.3651
7	1	13.9000	0.0000	12.3000	11.1000	3.6000	0.0000	0.8849	0.7986	0.2590
7	2	13.9000	0.6000	8.7000	7.9000	2.5000	0.0432	0.6259	0.5683	0.1799
9	1	15.3000	1.1000	13.8000	13.3000	4.2000	0.0719	0.9020	0.8693	0.2745
9	2	15.3000	1.6000	15.6000	14.9000	4.5000	0.1046	1.0196	0.9739	0.2941
12	1	18.8000	1.4000	14.8000	14.3000	4.2000	0.0745	0.7872	0.7606	0.2234
12	2	18.5000	1.3000	13.0000	13.3000	4.0000	0.0703	0.7027	0.7189	0.2162
14	1	20.0000	1.6000	16.7000	17.4000	4.8000	0.0800	0.8350	0.8700	0.2400
14	2	21.1000	0.0000	11.5000	12.0000	3.3000	0.0000	0.5450	0.5687	0.1564

450 LED Run 1

Run Time (Days)	Repeat	Sample Weight (mg)	Raw HPLC Data				Normalised HPLC Data			
			Zeaxanthin (μg ml^{-1})	Chlorophyll a (μg ml^{-1})	Chlorophyll b (μg ml^{-1})	β-Carotene (μg ml^{-1})	Zeaxanthin (μg mg^{-1})	Chlorophyll a (μg mg^{-1})	Chlorophyll b (μg mg^{-1})	β-Carotene (μg mg^{-1})
0	1	7.1000	0.6000	8.9000	6.9000	1.6000	0.0845	1.2535	0.9718	0.2254
0	2	7.6000	0.6000	9.3000	7.3000	1.7000	0.0789	1.2237	0.9605	0.2237
2	1	10.9000	0.0000	10.6000	9.8000	2.8000	0.0000	0.9725	0.8991	0.2569
2	2	10.6000	1.5000	14.5000	14.4000	4.0000	0.1415	1.3679	1.3585	0.3774
5	1	13.3000	1.5000	14.5000	13.8000	4.1000	0.1128	1.0902	1.0376	0.3083
5	2	12.9000	1.5000	14.3000	12.6000	4.0000	0.1163	1.1085	0.9767	0.3101
7	1	14.8000	1.2000	14.5000	12.5000	4.2000	0.0811	0.9797	0.8446	0.2838
7	2	15.3000	1.8000	19.2000	17.2000	5.7000	0.1176	1.2549	1.1242	0.3725
9	1	17.4000	1.8000	20.5000	18.0000	5.5000	0.1034	1.1782	1.0345	0.3161
9	2	16.9000	1.2000	15.2000	13.2000	4.1000	0.0710	0.8994	0.7811	0.2426
12	1	18.3000	1.7000	20.0000	17.4000	5.0000	0.0929	1.0929	0.9508	0.2732
12	2	15.1000	0.7000	12.5000	10.8000	3.0000	0.0464	0.8278	0.7152	0.1987
14	1	21.8000	1.4000	16.3000	13.6000	4.0000	0.0642	0.7477	0.6239	0.1835
14	2	23.9000	1.9000	20.9000	17.6000	5.4000	0.0795	0.8745	0.7364	0.2259

450 LED Run 2

Run Time (Days)	Repeat	Sample Weight (mg)	Raw HPLC Data				Normalised HPLC Data			
			Zeaxanthin (μg ml^{-1})	Chlorophyll a (μg ml^{-1})	Chlorophyll b (μg ml^{-1})	β-Carotene (μg ml^{-1})	Zeaxanthin (μg mg^{-1})	Chlorophyll a (μg mg^{-1})	Chlorophyll b (μg mg^{-1})	β-Carotene (μg mg^{-1})
0	1	6.7000	0.3000	7.3000	4.7000	0.9000	0.0448	1.0896	0.7015	0.1343
0	2	5.9000	0.2000	6.5000	4.1000	0.8000	0.0339	1.1017	0.6949	0.1356
2	1	7.2000	0.7000	7.2000	6.0000	1.7000	0.0972	1.0000	0.8333	0.2361
2	2	8.0000	0.7000	7.6000	6.5000	1.8000	0.0875	0.9500	0.8125	0.2250
5	1	10.2000	1.3000	12.7000	10.2000	3.7000	0.1275	1.2451	1.0000	0.3627
5	2	6.8000	0.8000	8.8000	7.2000	2.1000	0.1176	1.2941	1.0588	0.3088
7	1	11.4000	2.1000	19.5000	15.7000	5.8000	0.1842	1.7105	1.3772	0.5088
7	2	9.2000	1.5000	14.6000	11.9000	4.1000	0.1630	1.5870	1.2935	0.4457
9	1	14.0000	3.1000	28.0000	20.8000	8.2000	0.2214	2.0000	1.4857	0.5857
9	2	11.5000	1.9000	20.0000	14.3000	5.7000	0.1652	1.7391	1.2435	0.4957
12	1	15.5000	3.0000	28.1000	20.4000	7.6000	0.1935	1.8129	1.3161	0.4903
12	2	14.9000	2.7000	26.0000	18.8000	7.0000	0.1812	1.7450	1.2617	0.4698
14	1	17.0000	3.8000	30.8000	21.0000	7.7000	0.2235	1.8118	1.2353	0.4529
14	2	23.5000	3.9000	32.7000	21.6000	8.5000	0.1660	1.3915	0.9191	0.3617

450 LED Run 3

Run Time (Days)	Repeat	Sample Weight (mg)	Raw HPLC Data				Normalised HPLC Data			
			Zeaxanthin (μg ml^{-1})	Chlorophyll a (μg ml^{-1})	Chlorophyll b (μg ml^{-1})	β-Carotene (μg ml^{-1})	Zeaxanthin (μg mg^{-1})	Chlorophyll a (μg mg^{-1})	Chlorophyll b (μg mg^{-1})	β-Carotene (μg mg^{-1})
0	1	4.8000	0.2000	4.2000	2.2000	0.4000	0.0417	0.8750	0.4583	0.0833
0	2	5.8000	0.3000	5.5000	3.3000	0.6000	0.0517	0.9483	0.5690	0.1034
2	1	8.5000	0.7000	7.2000	6.0000	1.7000	0.0824	0.8471	0.7059	0.2000
2	2	8.4000	0.6000	6.9000	5.6000	1.5000	0.0714	0.8214	0.6667	0.1786
7	1	14.5000	2.3000	20.0000	14.3000	5.5000	0.1586	1.3793	0.9862	0.3793
7	2	12.2000	1.7000	18.3000	13.6000	5.0000	0.1393	1.5000	1.1148	0.4098
9	1	13.3000	1.8000	19.4000	14.0000	5.2000	0.1353	1.4586	1.0526	0.3910
9	2	10.8000	1.8000	17.1000	12.5000	4.5000	0.1667	1.5833	1.1574	0.4167
12	1	14.5000	2.4000	23.7000	17.1000	5.8000	0.1655	1.6345	1.1793	0.4000
12	2	14.6000	2.7000	22.7000	16.1000	5.5000	0.1849	1.5548	1.1027	0.3767
14	1	13.6000	2.4000	20.3000	14.2000	4.3000	0.1765	1.4926	1.0441	0.3162
14	2	13.8000	2.0000	22.0000	15.2000	4.5000	0.1449	1.5942	1.1014	0.3261

600 LED Run 1

Run Time (Days)	Repeat	Sample Weight (mg)	Raw HPLC Data				Normalised HPLC Data			
			Zeaxanthin (μg ml^{-1})	Chlorophyll a (μg ml^{-1})	Chlorophyll b (μg ml^{-1})	β-Carotene (μg ml^{-1})	Zeaxanthin (μg mg^{-1})	Chlorophyll a (μg mg^{-1})	Chlorophyll b (μg mg^{-1})	β-Carotene (μg mg^{-1})
0	1	7.7000	0.4000	6.4000	4.5000	0.8000	0.0519	0.8312	0.5844	0.1039
0	2	7.8000	0.4000	6.8000	4.8000	0.9000	0.0513	0.8718	0.6154	0.1154
2	1	11.3000	0.7000	6.5000	6.8000	1.5000	0.0619	0.5752	0.6018	0.1327
2	2	10.1000	0.9000	6.4000	6.8000	1.4000	0.0891	0.6337	0.6733	0.1386
5	1	12.9000	1.1000	10.4000	11.4000	3.1000	0.0853	0.8062	0.8837	0.2403
5	2	11.6000	0.0000	9.7000	10.3000	2.8000	0.0000	0.8362	0.8879	0.2414
7	1	11.8000	0.0000	9.9000	10.6000	2.5000	0.0000	0.8390	0.8983	0.2119
7	2	12.7000	0.0000	9.9000	10.5000	2.8000	0.0000	0.7795	0.8268	0.2205
9	1	14.8000	0.8000	8.3000	8.3000	2.0000	0.0541	0.5608	0.5608	0.1351
9	2	13.8000	0.8000	8.1000	8.1000	1.9000	0.0580	0.5870	0.5870	0.1377
12	1	13.2000	0.8000	7.6000	7.6000	1.6000	0.0606	0.5758	0.5758	0.1212
12	2	14.6000	0.8000	6.9000	6.8000	1.7000	0.0548	0.4726	0.4658	0.1164
14	1	16.6000	0.5000	4.3000	4.2000	1.1000	0.0301	0.2590	0.2530	0.0663
14	2	16.9000	0.9000	6.4000	6.3000	1.7000	0.0533	0.3787	0.3728	0.1006

600 LED Run 2

Run Time (Days)	Repeat	Sample Weight (mg)	Raw HPLC Data				Normalised HPLC Data			
			Zeaxanthin (μg ml^{-1})	Chlorophyll a (μg ml^{-1})	Chlorophyll b (μg ml^{-1})	β-Carotene (μg ml^{-1})	Zeaxanthin (μg mg^{-1})	Chlorophyll a (μg mg^{-1})	Chlorophyll b (μg mg^{-1})	β-Carotene (μg mg^{-1})
0	1	8.0000	0.5000	5.5000	3.8000	0.7000	0.0625	0.6875	0.4750	0.0875
0	2	7.1000	0.2000	3.2000	2.0000	0.4000	0.0282	0.4507	0.2817	0.0563
2	1	7.9000	0.6000	3.6000	3.7000	0.9000	0.0759	0.4557	0.4684	0.1139
2	2	7.5000	0.5000	3.4000	3.4000	0.7000	0.0667	0.4533	0.4533	0.0933
5	1	13.1000	0.0000	9.4000	10.0000	2.6000	0.0000	0.7176	0.7634	0.1985
5	2	9.7000	0.8000	7.7000	8.5000	2.1000	0.0825	0.7938	0.8763	0.2165
7	1	14.1000	0.0000	9.3000	10.1000	2.7000	0.0000	0.6596	0.7163	0.1915
7	2	14.3000	0.0000	10.1000	10.9000	3.0000	0.0000	0.7063	0.7622	0.2098
9	1	14.5000	0.7000	6.2000	6.4000	1.8000	0.0483	0.4276	0.4414	0.1241
9	2	14.2000	0.8000	7.3000	7.6000	2.1000	0.0563	0.5141	0.5352	0.1479
12	1	14.7000	0.0000	7.9000	8.0000	2.0000	0.0000	0.5374	0.5442	0.1361
12	2	16.7000	1.3000	10.3000	9.9000	2.6000	0.0778	0.6168	0.5928	0.1557
14	1	16.7000	0.9000	6.8000	6.6000	2.0000	0.0539	0.4072	0.3952	0.1198
14	2	17.3000	0.6000	7.6000	7.3000	2.0000	0.0347	0.4393	0.4220	0.1156

7. Bibliography

Abreu, A. P., Fernandes, B., Vicente, A. A., Teixeira, J., Dragone, G. (2012). Mixotrophic cultivation of Chlorella vulgaris using industrial dairy waste as organic carbon source. *Bioresource technology*. 118, 61-66.

Andrade, M. R., Costa, J. A. V. (2007). Mixotrophic cultivation of microalga *Spirulina platensis* using molasses as organic substrate. *Journal of Aquaculture*. 264, 130-134.

Banerjee, A., Sharma, R., Chisti, Y., and Banerjee, U. C. (2002). *Botryococcus braunii*: A Renewable Source of Hydrocarbons and Other Chemicals. *Critical Reviews in Biotechnology*. 22, 245 - 279.

Barber, J. (2008). Photosynthetic energy conversion: natural and artificial. *Chemical society Reviews*. 38, 185 - 196.

Barnes, D., Cohen, A., Bruick, R. K., Kantardjieff, K., Fowler, S., Efuet, E., Mayfield, S. P. (2004). Identification and characterization of a novel RNA binding protein that associates with the 5'-untranslated region of the chloroplast psbA mRNA. *Journal of Biochemistry*. 26, 8541 - 50.

Beadle, C. L. and Long, S. P. (1985). Photosynthesis - is it Limiting to Biomass Production? Biomass. 8, 119 - 168.

Becker, E. W. (1994). Microalgae Biotechnology and microbiology. Cambridge University Press.

Ben-Amotz, A., Avron, M. (1983). On the Factors Which Determine Massive beta-Carotene Accumulation in the Halotolerant Alga *Dunaliella bardawil*. *Journal of Plant Physiology*. 72, 593 - 7.

Beneragama, C. K., Goto, K. (2010). Chlorophyll a:b Ration Increase Under Low-light in 'Shade-tolerant' *Euglena gracilis*. *Tropical Agricultural Research*. 22, 12 - 25.

Blazina, D. (2011). Analysis Report 24760 - Microscopy of BBG Algae Grown in Flasks and Wash Samples. Internal Report. Shell Global Solutions, Thornton.

Bligh, E. J., Dyer, W. J. (1959). A rapid method of total lipid extraction and purification. *Canadian Journal of Biochemistry and Physiology*. 37, 911 - 917.

Boyer, R. F. (1990). Isolation and Spectrophotometric Characterisation of Photosynthetic Pigments. *Biochemical Education*. 18, 203 - 206.

Brennan, L., Owende, P. (2010). Biofuels from microalgae - A review of technologies for production, processing, and extractions of biofuels and co-products. *Renewable and Sustainable Energy Reviews*. 14, 557 - 577.

Carnicas, E., Jiménez, C., Niell, F. X. (1999). Effects of changes of irradiance on the pigment composition of *Gracilaria tenuistipitata* var. *liui* Zhang et Xia. *Journal of Photochemisty and Photobiology*. 50, 149-158.

Casadeval, E., Dif, D., Largeau, C., Gudin, C., Chaumont, D., Desant, O. (1985). Studies on Batch and Continuous Cultures of *Botryococcus braunii*: Hydrocarbon Production in Relation to Physiological State, Cell Ultrastructure, and Phosphate Nutrition. *Biotechnology and Bioengineering*. 27, 286 - 295.

Chlamydomonas Resource Centre. (no date of publication). *CC-3389 psbA (A251L*) mt+* | *Chlamydomonas Centre*, [online], Available: http://chlamycollection.org/strain/cc-3389-psba-a251l-mt/ [16 February 2013].

Chojnacka, K., Noworyta, A. (2004). Evaluation of *Spirulina* sp. growth in photoautotrophic, heterotrophic and mixotrophic cultures. *Enzyme and Microbial Technology*. 3, 461 - 465.

Darzins, A., Pienkos, P., and Edye, L. (2010). Current Status and Potential for algal biofuels production. IEA Bioenergy, Task 39.

Dayananda, C., R. S., Bhattacharya, S. and Ravishankar, G.A. (2005). Effect of media and culture conditions on growth and hydrocarbon production by *Botryococcus braunii*. *Process Biochemistry*. 40, 3125 - 3131.

Dayananda, C., R. Sarada., Kumar, V., Ravishankar, G.A. (2007). Isolation and characterization of hydrocarbon producing green alga *Botryococcus braunii* from Indian freshwater bodies. *Electronic Journal of Biotechnology*. 10, **pages unknown**.

Demmig-Adams, B., Adams, W. W. (1996). The role of Xanthophyll Cycle Carotenoids in the Protection of Photosynthesis. *Trends in Plant Science: Reviews*. 1, 21-26.

Dreuw, A., Fleming, G. R., Head-Gordon, M. (2003). Chlorophyll fluorescence quenching by xanthophylls. *Physical Chemistry Chemical Physics*. 5, 3247–3256.

Dring, M.J. (1998). The biology of marine plants (Contemporary Biology). *Cambridge University Press*. Cambridge. 199.

Dunn, J. L, Turnbull, J. D, Robinson, S. A. (2004). Comparison of solvent regimes for the extraction of photosynthetic pigments from leaves of higher plants. *Functional Plant Biology*. 31, 195-202.

Eroglu, E., Melis, A. (2010). Extracellular terpenoid hydrocarbon extraction and quantitation from the green microalgae *Botryococcus braunii* var. Showa. *Bioresource Technology*. 101, 2359 - 2366.

Falkowski, P.G., LaRoche, J. (1991). Acclimation to spectral irradiance in algae. *Journal of Phycology*. 27, 8-14.

Ferrell, J., Sarisky-Reed, V. (2010). National Algal Biofuels Technology Roadmap. U.S. Department of Energy: Energy Efficiency and Renewable Energy.

Formaggio, E., Cinque, G., Bassi, R. (2001). Functional Architecture of the Major Light-harvesting Complex from Higher Plants. *Journal of Molecular Biology*. 314, 1157-1166.

Förster, B., Osmond, C. B., Boynton, J. E., Gillham, N. W. (1999). Mutants of Chlamydomonas reinhardtii resistance to very high light. *Journal of Photochemistry and Photobiology B: Biology*. 48, 127-135.

Förster, B., Osmond, C. B., Boynton, J. E. (2001). Very high light resistant mutants of Chlamydomonas reinhardtii: Responses of Photosystem II, non-photochemical quenching and xanthophyll pigments to light and CO2. Journal of Photosynthetic Research. (67), 5 - 15.

Förster, B., Osmond, C. B., Pogson, B. J. (2005). Improved survival of very high light and oxidative stress is conferred by spontaneous gain-of-function mutations in *Chlamydomonas*. *Biochimica et Biophysica Acta*. 1709, 45-57.

Förster, B., Mathesius, U., Pogson, B. J. (2006). Comparative proteomics of high light stress in the model alga Chlamydomonas reinhardtii. *Journal of Proteomics*. 15, 4309 - 20.

Fouqueray, F., Mouget, J. L., Morant-Manceau, A., Tremblin, G. (2007). Dynamics of short-term acclimation to UV radiation in marine diatoms. Journal *of Photochemistry and Photobiology*. 89, 1 - 8.

Foyer, C. H., P. Descourviéres, P., Kunert, K. J. (1994). Protection against oxygen radicals: an important defence mechanism studied in transgenic plants. *Plant, Cell & Environment*. 17, 507-523.

Frenz, J., Largeau, C., Casadevall, E., Kollerup, F., Daugulis, A. J. (1999). Hydrocarbon recovery and biocompatibility of solvents for extraction from cultures of *Botryococcus braunii*. *Biotechnology and Bioengineering*. 6, 755 - 62.

Ge, Y., Liu, J., Tian, G. (2011). Growth characteristics of *Botryococcus braunii* 765 under high CO_2 concentration in photobioreactor. *Bioresource Technology*. 102, 130 - 134.

Hall, D. O., Rao, K. (1999). Photosynthesis, 6th Edition, Cambridge: Cambridge University Press.

Hannoufa, A., Hossain, Z. (2011). Plant Lipid Biochemistry – Carotenoid Biosynthesis and Regulation in Plants, [Online], Available: http://lipidlibrary.aocs.org/plantbio/carotenoids/index.htm [18 March 2013]

Harrison, M. A., Melis, A., Allen, J. F. (1992). Restoration of irradiance-stressed *Dunaliella salina* (green alga) to physiological growth conditions: changes in antenna size and composition of Photosystem II. *Biochimica et Biophysica Acta*. 1100, 83-91.

Hejazi, M. Amin., Wijffels R. H. (2004). Milking of Microalgae. *TRENDS in Biotechnology*. 22, 189-194.

Hill, Walter. (1996). 5 - Effects of Light. *Algal Ecology*. 121-148.

Huner, N. P. A., Őquist, G., Sarhan, F. (1998). Energy balance and acclimation to light and cold. *Trends in Plant Science: Reviews*. 3, 224-230.

Ishikawa, T., Dowdle, J., Smirnoff, N. (2006). Progress in manipulating ascorbic acid biosynthesis and accumulation in plants. *Physiologia Plantarum*. 126, 343 – 355.

Jahns, P. Holzwarth, A. R. (2012). The role of the xanthophyll cycle and of lutein in photoprotection of photosystem II. *Biochimica et Biophysica Acta*. 1817, 182–193.

Jin, E., Polle, J. E. W., Melis, A. (2001). Involvement of zeaxanthin and of the Cbr protein in the repair of photosystem II from photoinhibition the green alga *Dunaliella salina*. *Biochimica et Biophysica Acta*. 1506, 244-259.

Jodłowska, S., Latała, A. (2011). The Comparison of Spectrophotometric Method and High-Performance Liquid Chromatography in Photosynthetic Pigments Analysis. *On Line Journal of Biological Sciences*. 11, 63 - 69.

Jodłowska, S., Latała, A. (2012). 'Mechanisms of Photoacclimation on Photosynthesis Level in Cyanobacteria' in Najafpour, M. M. (ed.). *Advances in Photosynthesis - Fundamental Aspects*. Open Access: InTech. Available from: http://www.intechopen.com/books/advances-in-photosynthesisfundamental-aspects/mechanisms-of-photoacclimation-on-photosynthesis-level-in-cyanobacteria

Johnson, M. P., Ruban, A. V. (2011). Restoration of rapidly reversible photoprotective energy dissipation in the absence of PsbS protein by enhanced DeltapH. *The journal of Biological Chemistry*. 286, 19973-19981.

Kim, J. H., Glick, R. E., Melis, A. (1993). Dynamics of Photosystem Stoichiometry Adjustment by Light Quality in Chloroplasts. *Journal of Plant Physiology*. 102, 181-190.

Kitajima, K. Hogan, K. P. (2003). Increases of chlorophyll a/b ratios during acclimation of tropical woody seedlings to nitrogen limitation and high light. *Plant, Cell and Environment*. 26, 857-865.

Kojima, E., Zhang, K. (1999). Growth and hydrocarbon production of microalga *Botryococcus braunii* in bubble column photobioreactors. *Journal of Bioscience and Engineering*. 87, 811 - 815.

Krause, G.H. (1988). Photoinhibition of photosynthesis: an evaluation of damaging and protective mechanisms. *Physiologia Plantarum*. 74, 566–574.

Lalibertè, G., de la Noüe, J. (1993). Auto-, hetero-, and mixotrophic growth of *Chlamydomonas humicola* (Chlorophyceae) on acetate. *Journal of Phycology*. 29, 612 - 620.

Largeau, C., Casadevall, E., Berkaloff, C., Dhamelincourt, P. (1980). Sites of accumulation and composition of hydrocarbons in *Botryococcus braunii*. *Phytochemistry*. 19, 1043 - 1051.

Lee, R. E. (2008). Phycology. Fourth Edition. Cambridge University Press.

Li, Y., Qin, J. G. (2005). Comparison of growth and lipid content in three *Botryococcus braunii* strains. *Journal of Applied Phycology*. 17, 551 - 556.

Lichtenthaler, H. K. (1987). Chlorophylls and carotenoids: Pigments of Photosynthetic Biomembranes. *Methods in Enzymology*. 148, 350-382.

Lichtenthaler, H. K., Burkart, S. (1999). Photosynthesis and High Light Stress. *Bulgarian Journal of Plant Physiology*. 25, 3-16.

Lichtenthaler, H. K., Ač, A., Marek. M. V., Kalina, J., Urban, O. (2007). Differences in pigment composition, photosynthetic rates and chlorophyll fluorescence images of sun and shade leaves of four tree species. *Plant Physiology and Biochemistry*. 45, 577-588.

Liu, Z. Y., Wang, G. C., Zhou, B. C. (2008). Effect of iron on growth and lipid accumulation in *Chlorella vulgaris*. *Bioresourse Technology* . 11, 4717 - 4722.

Masamoto, K., Furukawa, K. (1996). Accumulation of Zeaxanthin in Cells of the Cyanobacterium, *Synechococcus* sp. Strain PCC 7942 Grown under High Irradiance. *Journal of Plant Physiology*. 155, 257-261.

Mata, T. M., Martins, A. A., Caetano, N. S. (2010). Microalgae for biodiesel production and other applications: A review. *Renewable and Sustainable Energy Reviews*. 14, 217-232.

Mayfield, S. P., Bennoun, P., Rochaix, J. D. (1987). Expression of the nuclear encoded OEE1 protein is required for oxygen evolution and stability of photosystem II particles in Chlamydomonas reinhardtii. *The EMBO Journal*. 6, 313-318.

Melis, A. (1990). Dynamics of photosynthetic membrane composition and function. *Biochimica et Biophysica Acta*. 1058, 87-106.

Melis, A. (2009). Solar energy conversion efficiencies in photosynthesis: Minimizing the chlorophyll antennae to maximize efficiency. *Plant Science*. 177, 272-280.

Melis, A., Harvey, G. W. (1981). Regulation of photosystem stoichiometry, chlorophyll a and chlorophyll b content and relation to the chloroplast ultrastructure. *Biochimica et Biophysica Acta*. 637, 138-145.

Meisinger, J. (2009). Algae for Energy, Security, and Development – Conference Proceedings, The Project on International Peace and Security (PIPS), Virginia, pp. 1 - 6.

Metzger, P., Villarreal-Rosales, E., Casadevall, E., Coute, A. (1989). Hydrocarbons, aldehydes and triacylglycerols in some strains of the race of the green alga *Botryococcus braunii*. *Phytochemistry*. 28, 2349 - 2353.

Millie, D. F., Ingram, D. A., Dionigi, C. P. (1990). Pigment and photosynthetic responses of *Oscillatoria agardhii* (Cyanophyta) to photon flux density and spectral quality. *Journal of Phycology*. 26, 660 - 6.

Millie, D. F., Hersh, C. M., Dionigi, C. P. (1992). Simazine-induced inhibition in photoacclimated populations of *Anabaena circinalis* (Cyanophyta). *Journal of Phycology*. 28, 19 – 26.

Moore, C. M., Suggett, D. J., Hickman, A. E., K. Young-Nam., Sharples, J., Geider, R. J., Holligan, P. M. (2006). Phytoplankton photo-acclimation and photo-adaptation in response to environmental gradients in a shelf sea. *The American Society of Limnology and Oceanography*. 51, 936–949.

Mosier, N., Wyman, C., Dale, B. E., Elander, R., Lee, Y. Y., Holtzapple, M., Ladisch, M. (2005). Features of promising technologies for pretreatment of lignocellulosic biomass. *Bioresource Technology*. 96, 673-686.

Mussgnug, J. H., Wobbe, L., Elles, I., Claus, C., Hamilton, M., Fink, A., Kahmann, U., Kapazoglou, A., Mullineaux, C. W., Hippler, M., Nickelsen, J., Nixon, P. J., Krusea, O. (2005). NAB1 Is an RNA Binding Protein Involved in the Light-Regulated Differential Expression of the Light-Harvesting Antenna of Chlamydomonas reinhardtii. *The Plant Cell*. 17, 3409 – 3421.

Niyogi, K. K. (1999). Photoprotection Revisited: Genetic and Molecular Approaches. *Annual Review of Plant Physiology and Plant Molecular Biology*. 50, 333-359.

Niyogi, K. K. (2000). Safety valves for photosynthesis. *Current Opinion in Plant Biology*. 3, 455-460.

Niyogi, K. K., Bjorkman, O., Grossman, A. R. (1997a). *Chlamydomonas* Xanthophyll Cycle Mutants identified by Video Imaging of Chlorophyll Fluorescence Quenching. *The Plant Cell*. 9, 1369-1380.

Niyogi, K. K., Grossman, A. R., Björkman, O. (1998). *Arabidopsis* Mutants Define a Central Role for the Xanthophyll Cycle in the Regulation of Photosynthetic Energy Conversion. *The Plant Cell*. 10, 1121-1134.

Niyogi, K. K., Rkman, O. B., Grossman, A. R. (1997b). The roles of specific xanthophylls in photoprotection. *Plant Biology*. 94, 14162-14167.

Noctor, G., Foyer, C. H. (1998). Ascorbate and Glutathione: Keeping Active Oxygen Under Control. *Annual Review of Plant Physiology and Plant Molecular Biology*. 49, 249-279.

Page, M., Sultana, N., Paszkiewicz, K., Florance, H., Smirnoff, N. (2012). The influence of ascorbate on anthocyanin accumulation during high light acclimation in *Arabidopsis thaliana*: further evidence for redox control of anthocyanin synthesis. *Plant, Cell & Environment*. 35, 388 - 404.

Pallardy, S. G. (2008). Physiology of Woody Plants. Third Edition. Academic press. Elsevier.

Pisal, D. S., Lele, S. S. (2004). Carotenoid production from microalga, *Dunaliella salina*. *Indian Journal of Biotechnology*. 4, 476-483.

Pocock, T., Król, M., Huner, N. P. (2004). The Determination and Quantification of Photosynthetic Pigments by Reverse Phase High-Performance Liquid Chromatography, Thin-Layer Chromatography, and Spectrophotometry. *Methods in Molecular Biology*. 274, 137 - 148.

Roberts, M., Reiss, M., Monger, G. (2000). Advanced Biology. Cheltenham. Nelson Thornes Ltd (UK).

Ruangsomboon, S. (2011). Effect of light, nutrient, cultivation time and salinity on lipid production of newly isolated strain of the green microalga, *Botryococcus braunii* KMITL 2. *Bioresource Technology*. Article in Press.

Ruban, A. V., Johnson, M.P. (2009). Dynamics of higher plant photosystem cross-section associated with state transitions. *Photosynthesis Research*. 99, 173-183.

Schagerl, M., Müller, B. (2006). Acclimation of chlorophyll a and carotenoid levels to different irradiances in four freshwater cyanobacteria. *Journal of Plant Physiology*. 163, 709-716.

Scott, S. A., Davey, M. P., Dennis, J. S., Horst, I., Howe, C. J., Lea-Smith, D. J., Smith, A. G. (2010). Biodiesel from algae: challenges and prospects. *Current Opinion in Biotechnology*. 21, 277–286.

Simionato, D., Sforza, E., Carpinelli, E. C., Bertucco, A., Giacometti, G. M., Morosinotto, T. (2011). Acclimation of *Nanochloropsis gaditana* to different illumination regimes: Effect on lipid accumulation. *Bioresourse Technology*. 102, 6026-6032.

Smirnoff, N. (1996). The Function and Metabolism of Ascorbic Acid in Plants. *Annals of Botany*. 78, 661 – 669.

Spencer, Christopher., Spiering, W. (2011). Downstream process development for secreting organisms. Internal Report. Shell Global Solutions, Thornton.

Steiger, S., Schäfer, L., Sandmann, G. (1999). High-light-dependent up-regulation of carotenoids and their antioxidative properties in the cyanobacterium *Synechocystis* PCC 6803. *Journal of Photochemistry and Photobiology B: Biology*. 52, 14-18.

Stephenson, P. G., Moore, M., Terry, M. J., Zubkov, M. V. and Bibby, T. S. (2011). Improving photosynthesis for algal biofuels: towards a green revolution. *Trends in Biotechnology*. 12, 615-623.

Takahashi, S., Badger, M. R. (2011). Photoprotection in plants: a new light on photosystem II damage. *Trends in Plant Science*. 16, 53-60.

Takako, T., Kawachi, M., Watanabe, M. M. (2011). Effects of carbon source on growth and morphology of *Botryococcus braunii*. *Journal of Applied Phycology*. 23, 25 - 33.

Tenaud, M., Ohmori, M., Miyachi, S. (1989). Inorganic carbon and acetate assimilation in *Botryococcus braunii* (Chlorophyta). *Journal of Phycology*. 25, 662–667.

Val, J., Monge, E., Baker, N. R. (1994). An improved HPLC method for the rapid analysis of the Xanthophyll pigments. *Journal of Chromatographic Science*. 32, 286 - 289.

Vasilikiotis, C., Melis, A. (1994). Photosystem II reaction centre damage and repair cycle: Chloroplast acclimation strategy to irradiance stress. *Biochemistry*. 91, 7222-7226.

Wang, B., Lan, C. Q., Horsman, M. (2012). Closed photobioreactors for production of microalgal biomasses. *Biotechnology Advances*. 30, 904 - 912.

Warner, M. E., Madden, M. L. (2006). The impact of shifts to elevated irradiance on the growth and photochemical activity of the harmful algae *Chattonella subsalsa* and *Prorocentrum minimum* from Delaware. *Harmful Algae*. 6, 332-342.

Weiss, T. L., Roth, R., Goodson, C., Vitha, S., Black,I., Azadi, P., Rusch, J., Holzenburg, A., Devarenne, T. P., Goodenoughc, U. (2012). Colony Organization in the Green Alga *Botryococcus braunii* (Race B) is Specified by a Complex Extracellular Matrix. *Eukaryotic Cell*. 12, 1424-1440.

Williams, P. J. B., Laurens, L. M. L. (2010). Microalgae as biodiesel and biomass feedstocks: Review and analysis of the biochemistry, energetics and economics. *Energy and Environmental Science*. 3, 554-590.

Jarmoskaite, I., Russell, R. (2011). DEAD-box proteins as RNA helicases and chaperones. *Wiley interdisciplinary reviews: RNA*. 2, 135-52.

Wolf, F. R., Nonomura, A. M., Bassham, J. A. (1985). Growth and Branched Hydrocarbon Production in a Strain of *Botryococcus braunii* (Chlorophyta). *Journal of Phycology*. 21, 388 - 396.

Yakovleva, I.M., Titlyanov, E. A. (2001). Effect of high visible and UV irradiance on subtidal *Chondrus crispus*: stress, photoinhibition and protective mechanisms. *Aquatic Botany*. 71, 47-61.

Yuan, J. S., Tiller, K, H., Al-Ahmad, H., Stewart, N. R., Stewart, C. N. (2008). Plants to power: bioenergy to fuel the future. *Trends in Plant Science*. 13, 421-429.

Zhang, K. and Kojima, E. (1998). Effect of light intensity on colony size of microalga *Botryococcus braunii* in bubble column photobioreactors. *Journal of Fermentation and Bioengineering*. 86, 573 - 576.

Zhu, X. G., Long, S. P and Ort, D. R. (2008). What is the maximum efficiency with which photosynthesis can convert solar energy into biomass? *Current Opinion in Biotechnology*. 19, 153-159.

Zhu, J. Y., Pan, X. J. (2010). Woody biomass pretreatment for cellulosic ethanol production: Technology and energy consumption evaluation. *Bioresource Technology*. 101, 4992-5002.

Zigman, M., Dubinsky., Iluz, D. (2012). 'The Xanthophyll Cycle in Aquatic Phototrophs and its Role in the Mitigation of Photoinhibition and Photodynamic Damage' in Najafpour, M. M. (Ed.). *Applied Photosynthesis*. Open Access: InTech. Available from: http://www.intechopen.com/books/applied-photosynthesis/the-xanthophyll-cycle-in-aquatic-phototrophs-and-its-role-in-the-mitigation-of-photoinhibition-and-p